



**Politecnico
di Torino**

MSc degree in Energy and Nuclear Engineering

A.Y. 2022/2023

**Techno-economic assessment of a Hybrid Energy Storage
System for the production of green hydrogen using Particle
Swarm Optimization**

Supervisors:

Prof. Dr. Andrea Lanzini
Dr. Francesco Minuto

Candidate:

Marcel Stolte

October 2023

Abstract

In a future energy system, the large share of volatile renewable energy will increase flexibility needs to resolve the temporal mismatch between demand and supply. A central enabler for this flexibility needs is energy storage. While short duration storage applications recently are getting widely adopted, in a renewable based future energy system there will be an increasing need for longer storage durations. Stand-alone long duration energy storage technologies, however, face economic challenges due to their high capital costs and limited revenue streams. To overcome these challenges, Hybrid Energy Storage Systems (HESS) that combine long duration storage with short duration storage have gained significant attention in scientific literature. By integrating different storage technologies, HESS can enhance the overall performance and economic viability of energy storage systems, benefitting from the strength of both technologies.

This master's thesis project focuses on conducting a techno economic analysis of an energy system to produce green hydrogen in combination with a Li-ion battery storage and a hydrogen storage. The hydrogen is produced to substitute the methane consumption of a final heavy industry user on an hourly basis. The hydrogen string consists of an electrolyzer and a storage system for storing hydrogen if it is not directly consumed by the final user. The battery, on the other hand, is integrated into the electricity system to reduce curtailment of renewable electricity and potentially decrease the size of the electrolyzer. It is connected only to renewable electricity production to provide electricity to the electrolyzer. The renewable energy plants are connected to the electrolyzer and to the grid, to have the possibility feeding in excess electricity in case of full storages and thereby avoiding curtailment.

By utilizing Particle Swarm Optimization (PSO), the research aims to optimize contemporary the sizing of the components. A rule-based control system determines the control strategy, considering the specific requirements of heavy industry applications. Through the development of a rule-based energy management strategy, the system takes the generation and demand profile and is able to compute the hourly state for each component. From the component states and electricity consumption the operational costs are obtained. This cost is summed to the annualized cost of components and allows the optimization algorithm to choose the next iterations component sizes. After each simulation the optimal component sizes and cost are determined, based on the given assumptions. The whole system is developed in python.

The results highlight that the high capital cost of battery storage cannot be recovered through a better exploitation of solar energy. To make the Li-ion battery storage interesting the electricity acquisition price must be increased substantially, or other revenue sources for the battery storage must be included. Hydrogen storage on the other side allows to transform a higher share of PV into hydrogen and with the comparably low capital cost reduce the levelized cost of hydrogen. Consequently, the optimal solution is not represented by a HESS, but rather by a single storage solution with hydrogen.

A sensitivity analysis on the electricity prices shows that if grid injection is remunerated at a price close to the levelized cost of electricity of PV or higher, it is convenient to maximize the installed capacity. For these grid injection prices the PV grid injection subsidizes the hydrogen production. On the other side lower electricity acquisition prices lower the installed PV capacity and consequently also the installed electrolyzer and hydrogen storage capacity.

The analysis of a 2030 future scenario shows significant cost reductions compared to today, being in line with recent studies on green hydrogen production. However, none of the solutions is able to economically compete with the cost of conventional natural gas supply, even if carbon taxes are considered. These results highlight further need for technological improvement as well as policy adaptations to generate interesting investment cases and foster the substitution of natural gas.

Acknowledgements

First and foremost, I would like to express my profound gratitude to prof. Andrea Lanzini and Dr. Francesco Minuto for supervising and guidance during this thesis and I am looking forward to the upcoming three years of the PhD. The work at the energy center provided many learning opportunities for which I am very thankful. Also, I would like to thank Alessandro Perol for the mentorship, dedication, and not overlooking the cases of real-world projects.

I would like to deeply thank my parents, who have always been there despite the distance and are a strong anchor for me. Thank you for your support and for making all this possible, and for standing by me in all decisions. Also, I'm immensely grateful for my 1 brother, Alex, and his invaluable support. I want to give a special shoutout to Simba, whose guidance and presence have been invaluable.

Thanks to the many people I crossed paths with during my studies. To Fabian, Leon and JP in Germany, to my fellows during the master's degree and of course to my colleagues at energy center to create such a positive working environment. Last but not least, thank you to my friends, from Crauxel, triathlon and university, both old and new, for the wonderful moments together.

To all those mentioned above and to everyone else who has played a role in my personal and professional growth, I offer my heartfelt thanks. I feel privileged to have had the opportunity to learn from such incredible individuals.

Für Lore, mit der ich jeden Moment teilen will.

Table of Contents

Abstract.....	I
Acknowledgements.....	III
Table of Contents	IV
List of Figures.....	VI
List of Tables.....	VIII
Main Acronyms.....	IX
1. Introduction	1
1.1 Relevance of energy storage to future energy systems	1
1.2 Long Duration Energy Storage	2
1.3 Hybrid Energy Storage.....	2
1.4 Green Hydrogen	3
1.5 Legislative Background.....	4
1.6 Objective and structure of the thesis	6
2. Methodology.....	8
2.1 Definition of the case study.....	8
2.1.1 Choice of Location.....	9
2.1.2 Photovoltaic plant	9
2.1.3 Electrolyzer	14
2.1.4 Hydrogen storage	17
2.1.5 Battery storage	20
2.1.6 Grid	23
2.1.7 Industrial user.....	24
2.2 Cost methodology	26
2.3 Control logic.....	27
2.4 Particle Swarm optimization	35
2.4.1 Setting the PSO algorithm	36
2.4.2 Improvements and variations to the standard algorithm.....	38
2.5 Global modelling strategy	39
2.6 Scenario definition	40
2.6.1 Base scenarios.....	40

2.6.2	Case studies.....	41
3.	Results.....	44
3.1	Base scenario 2023.....	44
3.1.1	Sensitivity analysis electricity acquisition prices	53
3.1.2	Sensitivity analysis electricity injection prices	55
3.2	Base scenario 2030.....	56
3.2.1	Sensitivity analysis electricity acquisition prices	58
3.2.2	Sensitivity analysis electricity injection prices	59
3.3	Case studies	61
3.3.1	Blending without constraints	61
3.3.2	Blending and area constraints	61
3.3.3	Cases including battery storage	63
4.	Discussion	67
4.1	Comparison to Methane	67
4.2	Context of green hydrogen production.....	68
4.3	Limitations	68
5.	Conclusions and future research potentials	71
	Bibliography	73

List of Figures

Figure 1.1: Global installed energy storage capacity estimation: BloombergNEF [3].....	1
Figure 1.2: Long Duration Energy Storage technologies, based on data from LDES council [5] .	2
Figure 2.1: Overview of the system structure and energy flows	8
Figure 2.2: PV generation data for Catania, fix mounted, 35° inclination, 180° solar azimuth angle, Polysun.....	10
Figure 2.3: PV generation data for Catania, vertical monoaxial tracking, Polysun.....	11
Figure 2.4: PV generation data for Catania, biaxial tracking, Polysun.....	12
Figure 2.5: Monthly energy production of different tracking system 1 kWp.....	12
Figure 2.6: Commodity and freight price indexes PV Source: IEA Renewable Energy Market Update June 2023 [25].....	13
Figure 2.7: Electrolyzer efficiency curve 2023, based on HHV [35], [36].....	15
Figure 2.8: Hydrogen storage technology overview, based on Andersson and Grönkvist [39]....	18
Figure 2.9: Utility scale Li-ion battery cost, data from [44].....	22
Figure 2.10: Industrial user consumption profile.....	25
Figure 2.11: Control strategy overview	29
Figure 2.12: Control strategy upper part U1	30
Figure 2.13: Control strategy upper part U2.....	31
Figure 2.14: Control strategy, connection of upper and lower part	32
Figure 2.15: Control strategy lower part L1	33
Figure 2.16: Control strategy lower part L2	33
Figure 2.17: Example of preventive charging strategy to reduce supply loss probability.	35
Figure 2.18: Global modelling strategy	39
Figure 3.1: LCOH and PV sizes of all particles for every iteration.....	45
Figure 3.2: LCOH and Electrolyzer sizes of all particles for every iteration	45
Figure 3.3: LCOH and Battery capacity of all particles for every iteration	46
Figure 3.4: LCOH and Battery power of all particles for every iteration.....	47
Figure 3.5: LCOH and hydrogen storage sizes of all particles for every iteration	47
Figure 3.6: Development of the best global LCOH in function of the iteration.....	48
Figure 3.7: Overview on the total cost of the optimal solution of base scenario 2023.....	49
Figure 3.8: Sankey diagram of the energy flows in the optimal solution of base scenario 2023 [GWh] [64].....	49
Figure 3.9: PV production, grid injection and grid withdrawal, week in January	50
Figure 3.10: Hydrogen demand, production and storage, week in January.....	50
Figure 3.11: PV production, grid injection and grid withdrawal, week in July	51
Figure 3.12: Hydrogen demand, production and storage, week in July	51
Figure 3.13: Electrolyzer operation profile, ordered by size	52
Figure 3.14: Sensitivity analysis electricity price of base scenario 2023	53
Figure 3.15: Cost overview of simulations with different electricity acquisition prices 2023	54
Figure 3.16: Cost overview of different electricity acquisition prices 2023.....	56
Figure 3.17: Optimal component sizes for the base scenario 2023 and 2030.....	56

Figure 3.18: Sankey diagram of the energy flows in the optimal solution of base scenario 2030 [GWh] [62].....	57
Figure 3.19: Sensitivity analysis electricity price base scenario 2030.....	58
Figure 3.20: Cost overview of different electricity acquisition prices 2030.....	59
Figure 3.21: Cost overview of simulations with different grid injection prices 2030	60
Figure 3.22: Cost overview for different PV constraints	62
Figure 3.23: Analysis on the required area for the different PV-constraints.....	63
Figure 3.24: Sankey diagram of the energy flows in 4-hour LIB case [MWh] [63]	64
Figure 3.25: Hydrogen demand, production and SOC of the storages during a typical day in July	65
Figure 3.26: Hydrogen demand, production and SOC of the storages during a sunny day in January	66

List of Tables

Table 1.1: Overview on recent legislation on green hydrogen in the EU and Italy [14]	6
Table 2.1: Main technical parameters for PV systems.....	10
Table 2.2: Main techno-economical parameters for PV systems.....	14
Table 2.3: Main techno-economic parameters for Electrolyzers	17
Table 2.4: Technical parameters of the hydrogen storage.....	19
Table 2.5: Main techno-economic parameters for hydrogen storage.....	20
Table 2.6: Technical parameters of Li-ion batteries.....	21
Table 2.7: Main techno-economic parameters for Li-ion battery storage.....	23
Table 2.8: Electricity price assumptions main scenario.....	24
Table 2.9: Italian gas imports and HHV in 2022	26
Table 2.10: Advantages and disadvantages of main control strategies [7],[56],[57].....	28
Table 2.11: Hydrogen blending cases	42
Table 2.12: Sensitivity analysis limited PV-size.....	42
Table 3.1: Optimal sizes for the base scenario 2023.....	44
Table 3.2: Sensitivity analysis of the optimal component sizes for different electricity acquisition prices 2023	54
Table 3.3: Sensitivity analysis of the optimal component sizes for different grid injection prices 2023.....	55
Table 3.4: Sensitivity analysis of the optimal component sizes for different electricity acquisition prices 2030.....	58
Table 3.5: Sensitivity analysis of the optimal component sizes for different grid injection prices 2030.....	60
Table 3.6: Case analysis H ₂ -blending, no size constraints on components	61
Table 3.7: Case analysis 20 % H ₂ -blending, limited PV-size	62
Table 3.8: Case analysis, 20 % H ₂ blending, 2023 cost, battery size forced	64

Main Acronyms

ARERA	Autorità di regolazione per energia reti e ambiente
CAPEX	Capital Expenditures
CCS	Carbon Capture and Storage
H2	Hydrogen
HESS	Hybrid Energy Storage System
IEA	International Energy Agency
GHG	Greenhouse Gas
GWP	Global Warming Potential
HHV	Higher Heating Value
LDES	Long Duration Energy Storage
LIB	Lithium-Ion Battery
LHV	Lower Heating Value
MILP	Mixed Integer Linear Programming
NREL	National Renewable Energy Laboratory
OPEX	Operating expense
PPA	Power Purchase Agreement
PEMEC	Proton Exchange Membrane Electrolyzer Cell
PSO	Particle Swarm Optimization
PUN	Prezzo Unico Nazionale
RFNBO	Renewable Fuel of Non-Biological Origin
SMR	Steam Methane Reforming
SOEC	Solid Oxide Electrolyzer Cell
SOC	State of Charge
STC	Standard Test Conditions
TRL	Technology Readiness Level

1. Introduction

1.1 Relevance of energy storage to future energy systems

The urgency to address climate change necessitates radical changes in power systems. As today energy production is the most responsible emitter, the introduction of renewable energy sources (RES) is inevitable. Today renewables passed fossil power supply as cheapest electricity sources and consequently the diffusion of wind and solar energy is surging rapidly.[1] However, the intermittent nature of RES and the inherent mismatch between energy demand and production pose significant challenges. To resolve these issues and enable a sustainable energy future, the deployment of energy storage technologies, specifically Long Duration Energy Storage (LDES), becomes imperative.

The current penetration of RES in both Italy and worldwide is still far from a 100 % renewable energy system. Therefore, the characteristics of a future energy system will be different to the present situation. However, even for the current power composition the intermittent nature of solar and wind power generation introduces variability in energy production. Consequently, instances arise where energy demand exceeds the available renewable energy supply. To mitigate the volatility and mismatch in energy demand and production, short duration energy storage solutions have been implemented worldwide. Energy Storage contributes to grid stability, facilitates RES integration, and optimizes energy supply and demand. With these characteristics and different potential revenue sources short duration storages like Li-ion batteries (LIB) represent a feasible business model today and become widely adopted. LIB are experiencing a boom with their application from portable electronics to electric cars and stationary electricity storage.[2] Generally, the trend of increasing installations of energy storages is observed worldwide (Figure 1.1), with large capacity additions in the future.

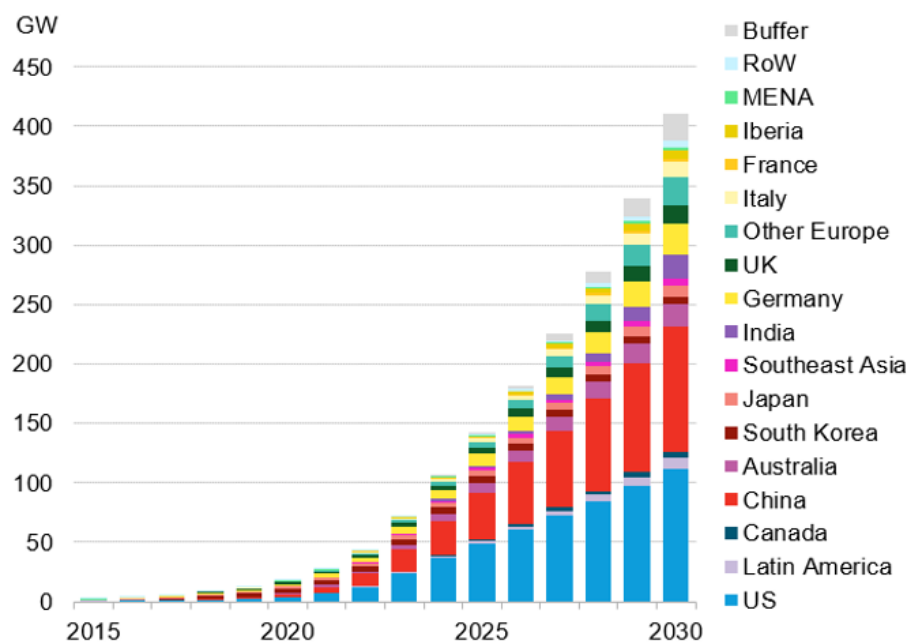


Figure 1.1: Global installed energy storage capacity estimation: BloombergNEF [3]

1.2 Long Duration Energy Storage

As the proportion of renewable energy increases, longer periods will occur where electricity demand exceeds renewable energy production. This necessitates the development and deployment of LDES solutions capable of storing excess energy during periods of high generation and releasing it during periods of scarcity. LDES systems ensure the reliability and resilience of the power grid, bridging the gaps in energy supply and demand.

The economic viability of LDES technologies currently faces challenges, primarily due to the need for significant capital investment and the uncertainty surrounding revenue streams. Additionally, regulatory uncertainties add to the complexities. To facilitate the rapid integration of LDES solutions, cost reduction is imperative to enhance their competitiveness in comparison to conventional fossil fuel-based approaches.[4] Unlike the well-established dominance of specific technologies in short-term energy storage, the landscape for LDES is characterized by a wide range of technologies competing for prominence. The choice of the most suitable storage method heavily depends on specific application requirements, with an expectation that multiple technologies will coexist simultaneously in the future. For a comprehensive overview of Long Duration Energy Storage technologies, refer to Figure 1.2.

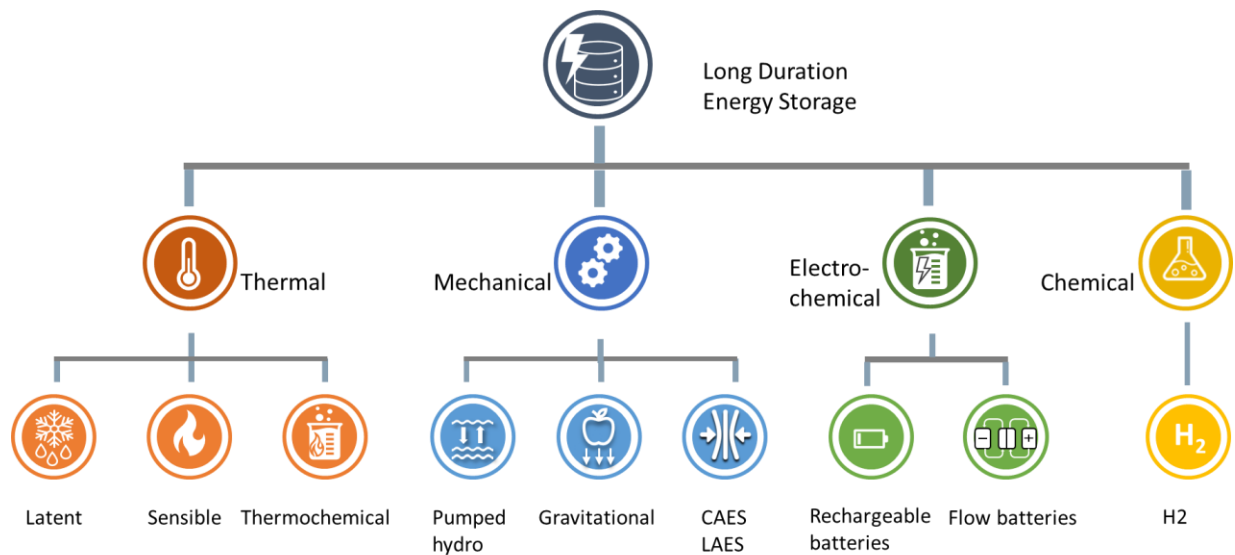


Figure 1.2: Long Duration Energy Storage technologies, based on data from LDES council [5]

1.3 Hybrid Energy Storage

The current landscape of energy storage solutions is characterized by a certain immaturity across various aspects, limiting their widespread adoption. The different energy storage technologies exhibit divergent cost structures and technical attributes. The prospect of a singular, impeccable energy storage system technology that adeptly addresses limitations from all dimensions is unlikely to develop in the immediate future. The idea of hybrid energy storage is to combine two heterogeneous storages and take advantage of the strengths of each individual technology and at

the same time hide their drawbacks. This typically involves the combination of a high-power density storage system with a high energy density counterpart.[6] The control logic governing HESS constitutes a subject of substantial research interest, with different control schemes and power electronic layouts. A common categorization is the distinction into active, semiactive, and passive control, which describe where the power electronic converters are placed and how flexible each storage can be controlled.[7]

Usually, these control schemes focus on regulation in a timeframe of few seconds or below. However, in this thesis, a macro-level optimization is undertaken, utilizing an hourly demand profile as a basis. As a result, the influence of rapid dynamics becomes relatively minor, rendering the need for intricate control logic modelling less significant. Furthermore, the arrangement involves situating one storage unit upstream for electricity and the other downstream for hydrogen. This configuration distinguishes the proposed system from conventional HESS setups, wherein both storage elements are interconnected to a shared bus. Notably, this configuration eliminates the presence of independent control challenges.

Numerous articles focus on the application and Sizing of Hybrid energy storage, particularly concerning transportation applications and microgrids. Hajiaghasi et al. offer a comprehensive overview of hybrid storage applications, sizing methodologies, and associated control strategies in microgrid contexts. Given the multifaceted nature of optimization problems and the distinct requirements of various systems, there is no universally applicable design procedure. System design is inherently case-specific and tailored to the unique demands of each application.[8]

Marocco et al. undertake a sizing analysis employing Mixed Integer Linear Programming (MILP) for a hydrogen-battery Hybrid Energy Storage System designed to meet the requirements of a remote off-grid island. This approach is subsequently compared to a meta-heuristic methodology employing Particle Swarm Optimization alongside a rule-based control strategy. The MILP-based approach yields lower minimum levelized cost of energy outcomes; however, it comes at the expense of greater computational overhead.[9] In remote off-grid regions, the expense of fossil fuel procurement is substantially higher due to the necessity of imports, resulting in escalated costs. Consequently, fully renewable energy systems, characterized by their competitive edge, emerge as compelling alternatives. Such remote areas, challenged by high fossil fuel costs, represent noteworthy study subjects for the evaluation of future energy systems reliant solely on renewable sources and practical applications of hybrid energy storage systems.

1.4 Green Hydrogen

The necessity for decarbonization extends beyond the power sector to cover other sectors like heat as well. Especially the decarbonization of high-temperature processes poses significant challenges, due to the difficulty to substitute fossil fuels in cost effective way. Industries requiring elevated temperatures often encounter limitations in terms of electrifying such demanding processes, thereby necessitating the adoption of alternative energy carriers, such as hydrogen. However, the cost of hydrogen is typically higher than a conventional natural gas supply.

Hydrogen has several **advantages** and will serve a central role in a future renewable energy system, acting as a Long Duration Energy storage. It is a highly versatile fuel and can be used in hydrogen ready turbines, as well as fuel cells. Hence, hydrogen can substitute natural gas without the need of building a new infrastructure as long as certain technical differences are taken into consideration. Moreover, hydrogen is essential in numerous chemical processes, further highlighting its importance.[10]

However, the adoption of hydrogen is not without challenges. The main **drawbacks** include the necessary conversion processes which entail energy losses, reducing overall efficiency. Additionally, hydrogen possesses a lower volumetric energy density when compared to conventional fuels, which presents complexities in terms of both transportation and storage. Furthermore, conventional hydrogen production pathways, often reliant on fossil fuels, contribute to emissions, counteracting the clean energy objective. Finally, the production, transport, and storage of hydrogen come with significant costs, making it an expensive energy source that will not be suitable for all energy needs.[10]

Generally different production pathways for hydrogen exist, which are frequently associated with colours. The most common production pathways are shortly described here: **Green Hydrogen** is produced by water electrolysis, using renewable electricity. This method yields minimal CO₂ emissions and aligns with the thesis's commitment to sustainable practices. **Grey hydrogen** is usually generated through steam methane reforming (SMR) from natural gas and therefore no carbon-neutral alternative to methane and even more impacting than the direct use of methane. **Blue hydrogen** uses the same production pathway as grey hydrogen but with subsequent carbon capture and storage (CCS) technologies in place to mitigate emissions. Also, other colour codes for hydrogen exist like pink, black and turquoise. In some cases, a different colour coding is used in other sources.[11] For this thesis green hydrogen is used for further considerations, due to the potential to produce it locally by water electrolysis from renewable electricity and thereby causing very little CO₂ emissions.

1.5 Legislative Background

In early market stages, having a clearly defined regulatory environment and removing legislative barriers is essential to facilitate investments in energy storage and hydrogen production. In recent years, the legislative landscape evolved rapidly. Now, there is a specific definition that determines when hydrogen production is considered 100 % renewable and which incentives apply. An overview on this development on European as well as Italian level is given in this chapter.

On a European basis **RED II** defines the general outlook for the policy on green hydrogen production and targets[12]. However, the specific technical requirements are not provided within RED II but are instead defined by two additional Delegated Regulations. Delegated Regulation **EU 2023/1185** establishes minimum threshold for greenhouse gas emissions savings for the production of renewable fuels of non-biological origins RFNBO. **EU 2023/1184** defines detailed rules for energy used to produce RFNBO. The requirements to classify hydrogen as green are outlined in the following articles:

Article 3 specifies that in the case of a direct physical connection between the electrolyzer and the RES plant, the production can be considered as 100 % renewable if both of the following conditions are met:

- The RES plant must not be installed prior to 3 years before the electrolyzer
- It is ensured that the electricity is not drawn from the grid

Article 4 defines that if the electricity is taken from the grid, one of the following rules must be satisfied to classify the hydrogen as 100 % renewable:

- The electrolyzer is placed in the bidding zone where the share of renewable energy is higher than 90 % and the electrolyzer operational hours are limited to the share of renewable electricity in the bidding zone.
- The emission intensity of electricity in the bidding zone is less than 18 g_{CO₂eq}/MJ and a PPA is concluded, which covers at least the amount of electricity used for green hydrogen production and satisfies the temporal and geographical correlation requirements (see next paragraph)
- The electricity is used during imbalanced grid conditions where RES plants are curtailed, and the hydrogen production reduces the curtailment need by the corresponding amount.

If none of the above rules regarding electricity in the bidding zone are met, the requirements of the following three articles must be respected:

- Article 5, Additionality assures that the electricity is taken from additionally installed renewable energy capacity. It's important to note that the rules regarding additionality do not apply until 2038 for electrolyzers installed prior to 2028, which significantly relaxes the requirements for currently installed electrolyzers. [13]
- Article 6, Temporal correlation requires that renewable production (e.g., through a PPA) and consumption occur during the same period. The requirement for temporal correlation is set to one calendar month until the end of 2029 and then tightened to one hour.
- Article 7, Geographical correlation regulates that the renewable plants are located in the same bidding zone or, under certain conditions, in interconnected bidding zones with respect to the electrolyzer[13]

New legislation related to green hydrogen is being introduced not only at the European level but also within member states. In Italy **DL 36/2022** exempts electricity from renewables used in electrolysis from general network fees. It also exempts resulting green hydrogen from excise duty when it is not directly used as fuel in combustion engines. Additionally new legislation was introduced regulating authorization processes and the definition of areas with special national interest. **DM 21/09/2022** further defines the exemption from general system charges for green hydrogen, using GHG reduction thresholds similar to those defined in RED II on the European level.[14] Table 1.1 provides an overview on recently enacted legislation related to green hydrogen.

Under this new legislative environment, it is important to understand to which extent the production of green hydrogen can be accelerated. However, the precise implementation of

financial incentives, such as those related to capital expenditures or operational costs, is yet to be determined. Further national or regional subsidies may exist which further influence the project costs.

Table 1.1: Overview on recent legislation on green hydrogen in the EU and Italy [14]

Legislation	Content
EU RED II[12]	RFNBOs have to obtain a lifecycle GHG emission reduction of at least 70 % compared to a fossil fuel with a reference emission factor of 94 gCO ₂ /MJ. The threshold is increased to 80 % for plants for electricity generation, heating or cooling installed after 2025.
EU Gas Hydrogen Package [14]	Defines regulating fee exemptions which should be applied until 2030. Currently in revision
EU Delegated Acts RED II (EU) 2023/1184 [13] (EU) 2023/1185 [15]	Supplementing RED II Defines under which conditions hydrogen, hydrogen-based fuels or other energy carriers can be considered as a renewable fuel of non-biological origin (RFNBO). EU 2023/1185 defines minimum greenhouse gas savings.
Law Decree 36/2022[16]	Electricity from renewables used in electrolysis is exempt from general network charges. The resulting green hydrogen is exempt from excise duty when not used directly as fuel in combustion engines.
Legislative Decree 199/2021 [17]	Referring to RED II Facilitating authorization processes for electrolyzers. The guarantee of origin is defined and expanded for green hydrogen.
DL 115/2022 [14]	Define how areas of strategic interest for large scale investments can be established, and how these benefit from facilitated regional authorization processes if a strategic national interest is applicable.
DM 21/09/2022[14]	Defines the condition under which green hydrogen is exempt from the variable part of general system charges. The conditions are in line with the GHG reductions required by RED II. The exemption request procedure is defined by ARERA.
Delibera ARERA 557/2022/R/EEL [14]	Defines the request modality of the network fee exemption.
DL 13/2023[14]	Regulates authorization processes for green hydrogen production plants and adds them to a group of prioritized projects to accelerate the environmental impact assessment procedures.

1.6 Objective and structure of the thesis

In the realm of green hydrogen production and energy storage systems, this thesis aims to evaluate the potential of simulating a real industrial consumer use case. To achieve this goal, a hybrid energy storage system is modelled, comprising a photovoltaic plant, an electric grid, Li-ion battery

storage, an electrolyzer, and hydrogen storage. The simulations are conducted based on a one-year hydrogen demand profile. The model is governed by a rule-based operational logic designed to maximize hydrogen production from renewable energy sources, minimize grid power consumption, and ensure fulfilment of the end user's hydrogen demand. The optimization of component sizes is executed using the particle swarm optimization (PSO) algorithm, chosen for its ability to reduce computational time and effectively handle multi-objective optimization. To authenticate the outcomes and explore potential future developments, sensitivity analyses are performed.

This thesis is organized as follows: **Chapter 2** explains the methodology used in this study. It covers a detailed description of the model's components, including their techno-economic aspects. The chapter provides insights into the functioning of the control logic and the particle swarm optimization (PSO) algorithm and concludes by outlining the various scenarios examined. **Chapter 3** provides a detailed analysis of the results from both the base case and the sensitivity analysis. The outcomes are presented in depth, offering insights into the system's performance across different scenarios. **Chapter 4** discusses the results comprehensively, placing them within the context of green hydrogen production. The findings are also compared with a conventional fossil fuel-based energy supply. **Chapter 5** concludes the thesis, summarizing the key points, which are drawn from the results. A look ahead is presented, suggesting potential avenues for future research in this field.

2. Methodology

Chapter 2 provides an overview of the methodology employed in this thesis. First the system is described, defining its components, specific system boundaries, and outlining the underlying assumptions. The section on cost methodology, outlines economic modelling approach and the associated challenges. The chapter further introduces particle swarm optimization and explains its function in the global modelling strategy. In the end the scenarios which are simulated are summarized.

2.1 Definition of the case study

The energy system under analysis comprises a combination of hydrogen production, hydrogen storage and a Li-ion battery to meet the electricity demand of a heavy industry user. The hydrogen string includes an electrolyzer, which converts excess electricity into hydrogen through electrolysis, and a storage system for hydrogen when it is not directly consumed by the end user. The Li-ion battery is integrated into the system to reduce curtailment of renewable electricity and decrease the necessary size of the electrolyzer. It is connected only to renewable production to be able to store excess renewable electricity. The renewable energy plants are also connected to the electrolyzer and the grid, allowing them to feed surplus electricity into the grid, in case of full storages and thereby avoid curtailment. The modeling process begins with a simplified approach for each component to facilitate result tracking and validation, gradually increasing complexity as needed. Once the energy system's framework is defined, the assumptions regarding prices, efficiencies and operational strategies must be established.

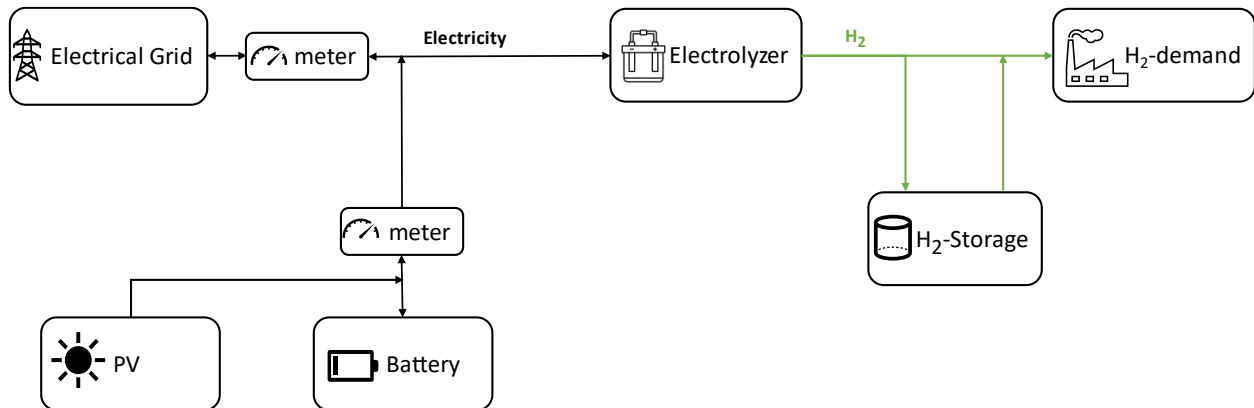


Figure 2.1: Overview of the system structure and energy flows

The physical system boundaries extend from the renewable plants to the entry point of the final customer. Little is known to the location and geographical details of the industrial user's site. Hence, the objective is to satisfy the clients energy demand without modelling downstream processes. The components are treated as black boxes in the simulations, and system efficiencies are used for modelling.

2.1.1 Choice of Location

To test whether a system with two storages can be economically viable a location with large renewable availability has to be chosen. Thereby a comparably low LCOH can be obtained and set into context. For this study, the city of Catania in Sicily was chosen as the study site due to two key advantages for renewable hydrogen production. Firstly, Catania receives an average global horizontal irradiation of approximately 1.800 kWh/m²/y, which is one of the highest values in Europe and therefore ideal for PV power generation[18]. Secondly, Catania has a large existing steel industry that is looking to decarbonize its operations. Given that the steel industry is anticipated to become a major consumer of hydrogen in the future, it is likely to foster an economy centred around the production of green hydrogen. This, combined with its proximity to the sea, makes Catania a favourable site for this study.

2.1.2 Photovoltaic plant

To obtain the power production values, radiation data for the selected location is needed. PVGIS is a reliable source where the location can be imported and it can calculate hourly electricity production based on past meteorological data.[19] The problem is that the user profile is given for 2021 while PVGIS has radiation data from until 2020. Although PV production tends to have less annual variability compared to wind or hydropower generation, there are still notable fluctuations, ranging between 93 % and 106 % of the average over the past 30 years. Hence selecting the right year is important.

To solve this problem by the calculating the average production for each day poses the problem of unrealistically smooth profiles. A more suitable approach is to select a reference meteorological year and calculate the power production based on this input data. For this task the modelling software Polysun is used. The meteorological reference year is generated by Polysun using the software Meteonorm, which provides the necessary meteorological data.[20]

The main technical parameters can be seen in Table 2.2. The plant is placed in Catania, Sicily. To achieve an optimal power output the slope is set at 35°[21]. The selection whether solar trackers are used to follow the suns position is a trade-off between capital cost and power output. Both fixed-mount and tracking systems are available on a utility scale. The decision which tracking system to use is more precisely discussed in the following section.

In recent years modules increased in size as well as in efficiency. For this study a module with a peak power of 585 W and an efficiency of 20.85 % at STC is chosen, which represents the current state of the art of utility scale PV.[22] The simulation of the power output uses the preset values by Polysun of 2 % cable loss and 4 % mismatching loss due to the interconnection of the cells with different operation properties under certain conditions. The overall inverter efficiency in the simulation exceeds 95 %.[21]

Table 2.1: Main technical parameters for PV systems

Location	Catania, Sicily
PV-surface slope	35° [21]
Tracking	Monoaxial tracking system on the vertical axis
Efficiency at STC	20,85 %
Module Power	585 W
Cable loss	2 %

Polysun then generates a one-year PV-production profile from the reference meteorological year, incorporating the selected components and assumptions. To investigate the impact of a tracking system, three simulations are carried out.

In the case of fixed mounting, a low variation in productive hours can be observed throughout the year and a total production of 1.547 kWh/kWp is reached.

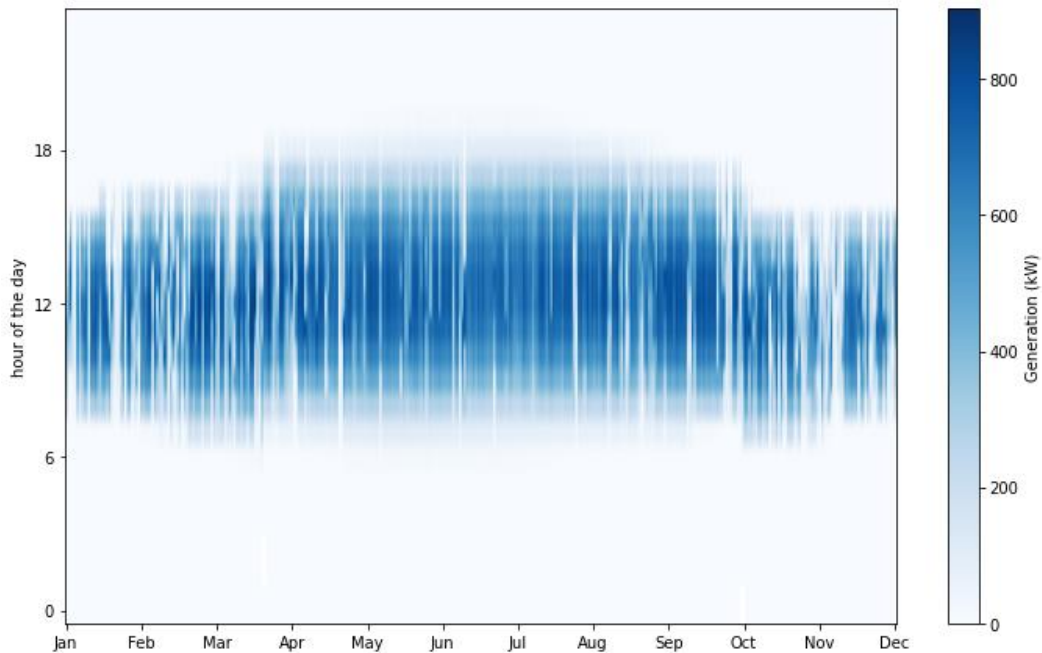


Figure 2.2: PV generation data for Catania, fix mounted, 35° inclination, 180° solar azimuth angle, Polysun

Monoaxial tracking is commonly employed in modern plants. While it involves slightly higher capital expenditure, it significantly improves the power output. The power output is also made more constant over the day, with a higher productivity especially during summer. As a result of the tracking system, the AC power output reaches 1.985 kWh/kWp, marking a substantial 28% increase.[23]

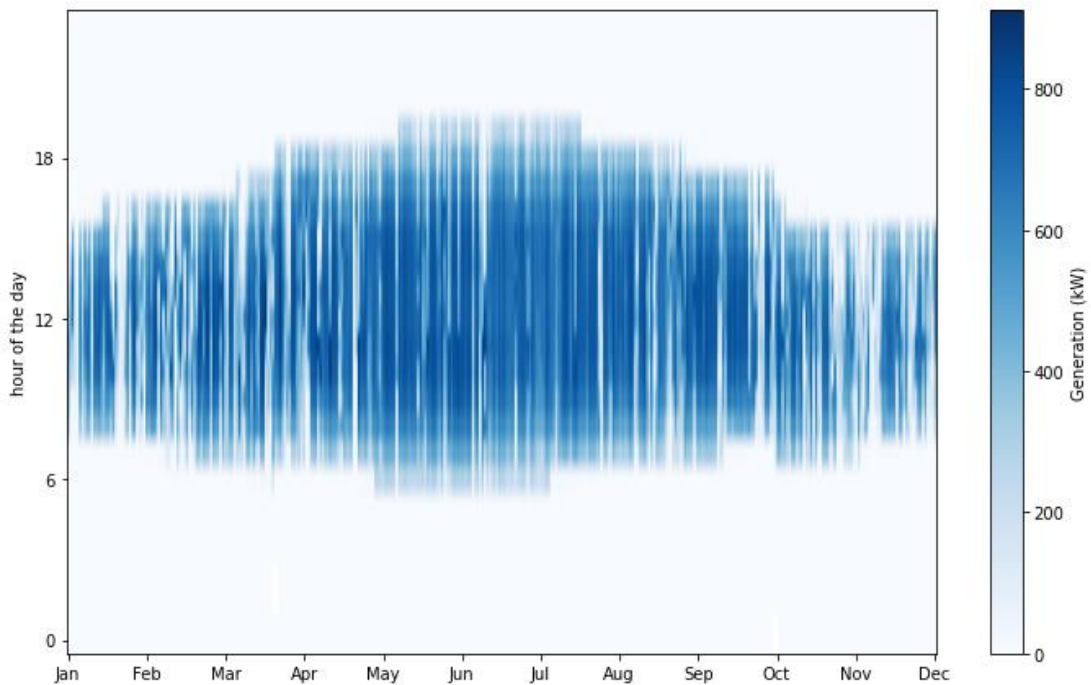


Figure 2.3: PV generation data for Catania, vertical monoaxial tracking, Polysun

In addition to monoaxial tracking systems, biaxial trackers are available, optimizing both the azimuth angle as well as the slope. Thereby the daily Energy Curves are flattened as the sun always is at the right angle and the yearly production. Overall, the yearly production increases to 2.163 kWh/kW, which is a nearly 40 % improvement compared to the fixed-mounted cases.

However, it is important to note the drawbacks of biaxial trackers, including increased CAPEX and maintenance cost due to greater complexity of the system. Additionally, systems with biaxial trackers run into shading issues in off-peak hours and require a larger space demand.[23]

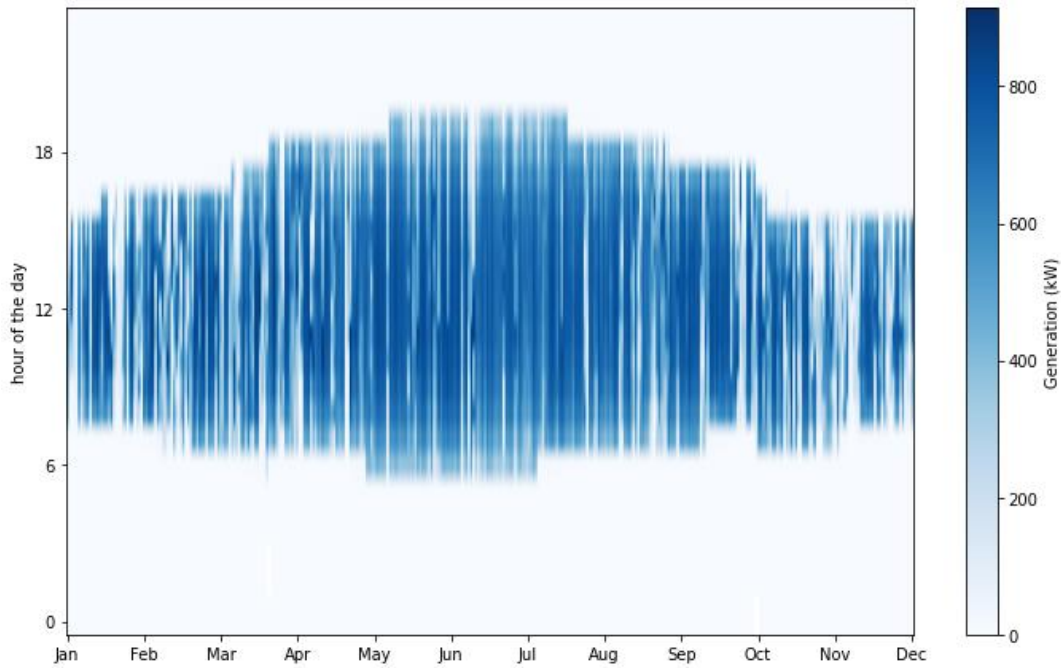


Figure 2.4: PV generation data for Catania, biaxial tracking, Polysun

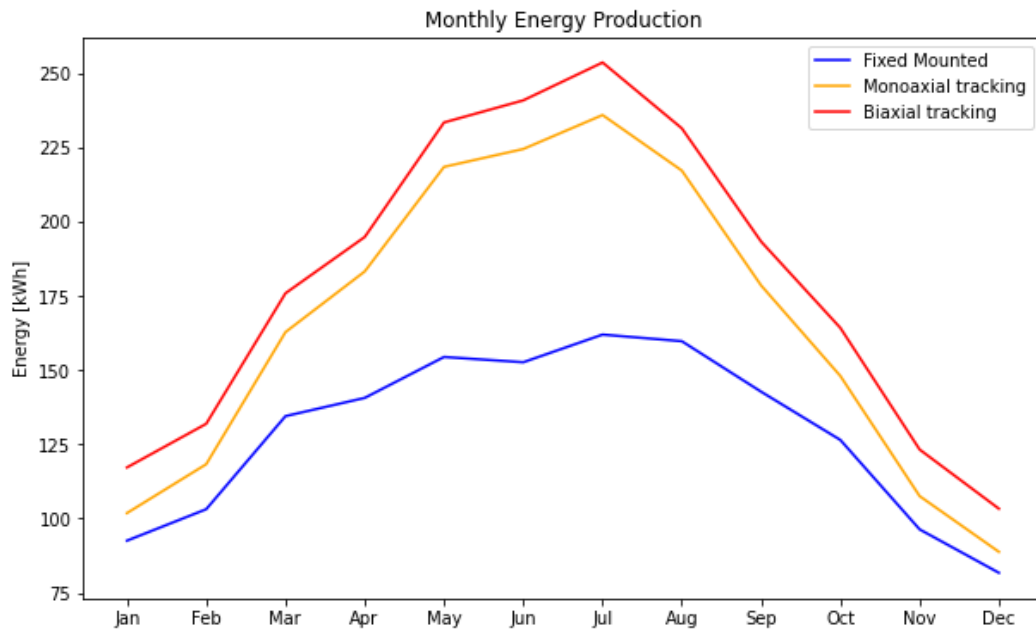


Figure 2.5: Monthly energy production of different tracking system 1 kWp

For this thesis, a vertical axis tracking system is selected, as it strikes a favourable balance between high electricity generation and extended production hours throughout the day. Figure 2.5 shows that the monoaxial tracking the vertical axis achieves this objective very well

already capturing most of the advantage relative to a biaxial tracking system. In the context of this study, the demand profile of the final user remains relatively constant throughout on a daily, weekly and seasonal basis. Therefore, achieving high-power generation during morning and evening hours is crucial to prevent over-sizing of the plant. The central goal of the energetic system is to consistently satisfy the users demand profile, and demand side management is not considered possible. Hence monoaxial tracking is considered a convenient option in this case.

The size of the PV-plant is treated as an optimization parameter. To calculate the power output the plant's size is multiplied for each hour by the specific production profile for 1 kWp.

Apart from the technical considerations also **economic assumptions** must be made. The selection of realistic component prices has become increasingly difficult over the last years. Whilst previously the specific cost for solar panels wind turbines, electrolysers and storages constantly went down with improvement of the technologies and their high learning rates, this behaviour changed. The Pandemic and later the energy crisis inflation led to a high volatility in prices. In late 2021 and 2022 a general upward trend in prices occurred, which also reflects on PV component cost. While the IEA in the 2022 World Energy Outlook uses a price of 704 €/kWp based on 2021 assumptions, this price increased after this[1]. In another report on the Electricity generation cost the IEA reports cost of 735 €/kWp specifically for Italian utility scale plants in 2020.[24]

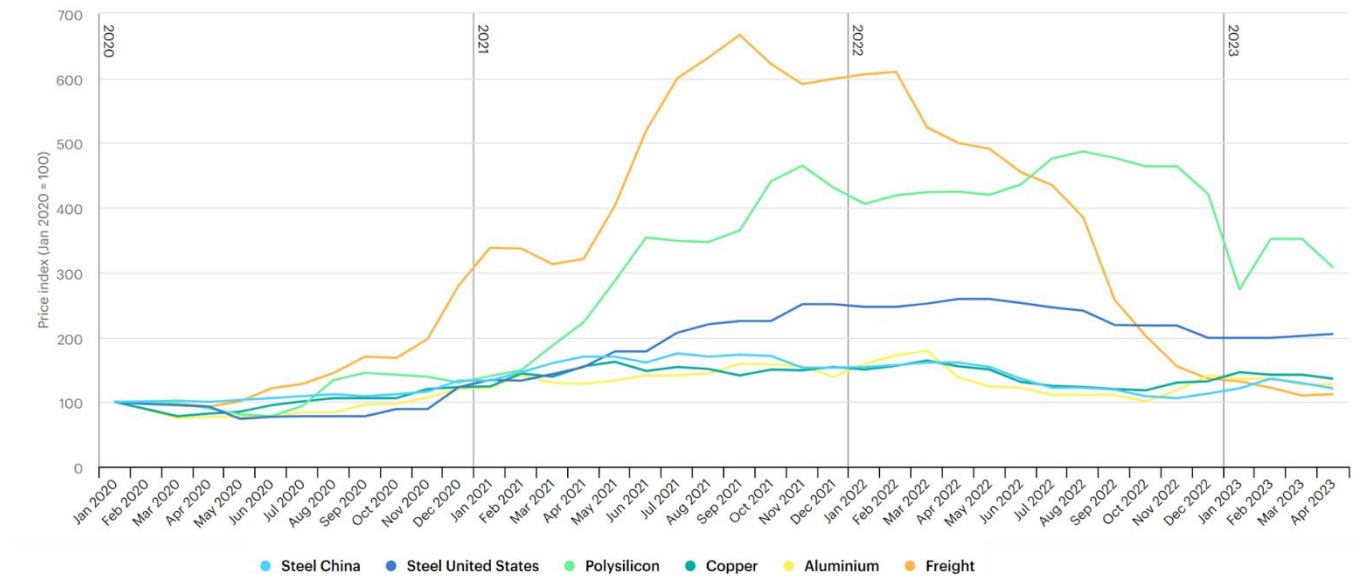


Figure 2.6: Commodity and freight price indexes PV Source: IEA Renewable Energy Market Update June 2023 [25]

The impacts of these on developments on PV- price components can be seen in Figure 2.6. In 2022, main commodities and transportation costs made up around 30-35 % of overall capital expenditure (CAPEX) for utility-scale and wind projects, doubling from 2020. The combined impact of higher prices and annual cost reductions due to technological innovation led to an estimated 15-20 % increase in the Levelized Cost of Electricity (LCOE) for these technologies in 2022. In 2023, commodity prices have significantly fallen from their peaks but remain higher compared to 2020.

For instance, average prices in Q1 2023 were over 200 % higher for polysilicon, 100 % for steel in the United States and Europe, and 20-40 % for aluminium, copper, and freight.[25]

In the midterm future a new decline in prices is expected together with new production capacities coming online. Taking into account the IEA technology costs from 2020 and 2021 and the recent price increases of 10-20 % together with the increased cost due to the tracking, the baseline scenario consists of a PV-system cost of 900 €/kWp.[26]

In the analysis of future scenarios, the projected costs for utility-scale solar PV in 2030 are examined. The U.S. Department of Energy has set a target for the LCOE for utility-scale solar at 20 €/MWh for single-axis tracking ground-mounted PV plants. This target entails more than halving the cost, primarily driven by reductions in module prices.[27] The Fraunhofer Institute for Solar Energy Systems projects a more conservative learning rate of about 30 % in the PV cost from 2021 to 2030. In their 2040 projections system cost for utility scale PV plants are expected to be lower than 350 €/kWp.[28] presents a wide range of installation cost estimates for 2030, ranging from 340 to 840 \$/kW. This variation underscores the high degree of uncertainty and the specificity of individual cases.[29] From these estimates, a price of 550 €/kWp is selected for 2030, representing one of the more conservative values.

Table 2.2: Main techno-economical parameters for PV systems

	2023	2030
Investment cost	900 €/kWp [1], [24], [26]	600 €/kWp [1],[28]
Operation and maintenance cost	20 €/kWp/year [30]	20 €/kWp/year [30]
Lifetime	25 Years [1]	25 Years [1]
Discount rate	6 % [31]	6 % [31]

2.1.3 Electrolyzer

The electrolyzer converts electricity from the PV plant or the grid into hydrogen through water electrolysis. Three main types of electrolyzer cells exist: Alkaline electrolyzer cells, proton exchange membrane (PEM) electrolyzer cells, and solid oxide electrolyzer cells. In comparison to alkaline electrolysis, PEM electrolyzers represent a more recent technology with a history of rapid advancements and a promising trajectory for future improvements. Although alkaline electrolysis comes with slightly lower initial investment costs, PEM electrolyzers offer superior efficiencies. Another advantage of PEM electrolyzers is their higher power density relative to the space they require, making them particularly advantageous when available area for installation is limited.[10] [32] A disadvantage of PEM electrolyzers is their reliance on precious catalyst like platinum and iridium, which represent a significant cost factor and source of price volatility.

Solid oxide electrolyzer cells have the potential for higher efficiencies but operate at high temperatures, typically between 500 °C and 900 °C. They are considered a less mature technology,

with a Technology Readiness Level (TRL) of around 7, and due to the high temperatures do have drawbacks regarding fluctuation operation conditions.[33] For this study, where the primary input for the electrolyzer is renewable energy with highly variable input, the PEM electrolyzer is considered the most suitable choice due to its favourable dynamic behaviour, and it is selected for further modelling.

Electrolyzer efficiency model

The efficiency of an electrolyzer depends on activation, ohmic, and concentration losses, along with auxiliary consumption. These factors, combined with auxiliary consumption, compose the characteristic efficiency curve, with peak efficiency occurring during part-load operation.

The electrolyzer is modelled as a Blackbox, with only its efficiency curve considered. This efficiency curve given to transform electricity to hydrogen. The electrolyzer's efficiency is represented by a curve that varies based on the load, employing four fixed points and spline interpolation. These points are chosen to match the efficiency curve observed in a real system of a PEM electrolyzer.[34] The efficiency curve is not modelled as a function of the size. In all observed scenarios, the optimal electrolyzer size falls within the utility-scale range, and it is assumed that the electrolyzer's efficiency remains relatively consistent within these dimensions. All efficiency values are based on the HHV of hydrogen.

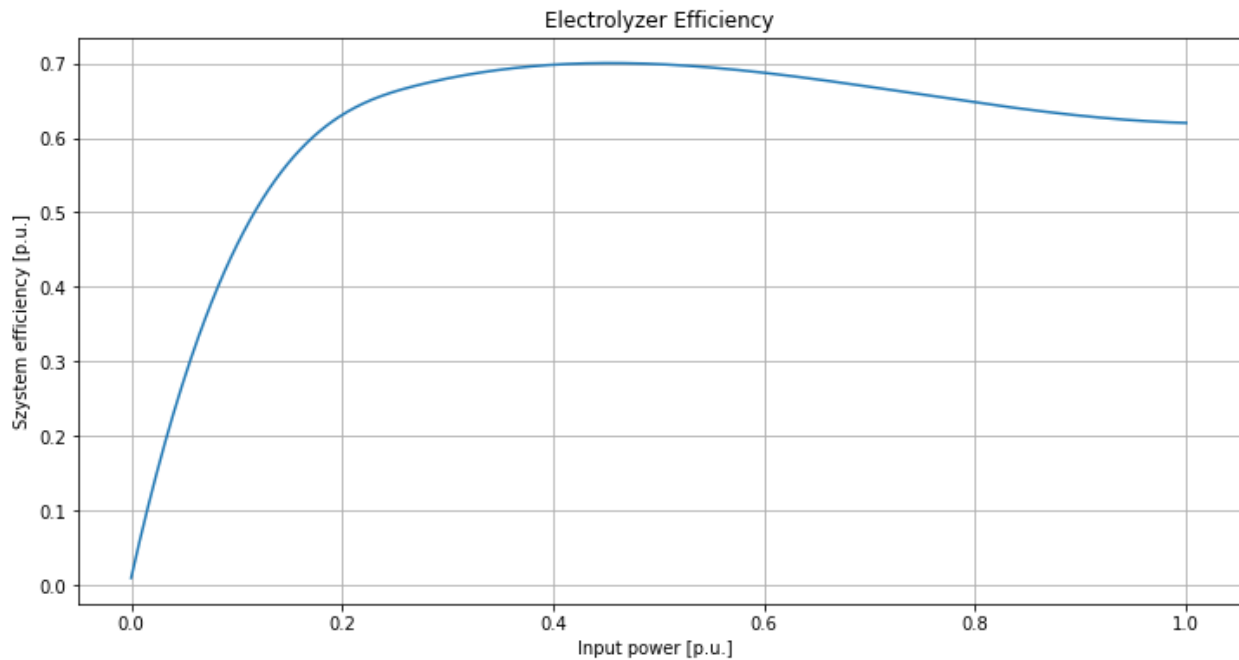


Figure 2.7: Electrolyzer efficiency curve 2023, based on HHV [35], [36]

To follow the control logic of the system and align with the objectives of the operational strategy, there are situations where it is imperative to achieve a precise system output while simultaneously determining the electricity input. This is particularly relevant during periods of low-res production and low storage SOC. The critical scenario arises when the hydrogen demand from end-users exceeds the production capacity of RES. In these cases, it is essential to determine the correct grid

withdrawal, knowing the total electrolyzer output and the efficiency curve. The solution is achieved through the application of the bisection method, which eliminates the need for calculating derivatives on a spline. The bisection iteratively calculates the correct electrolyzer input and efficiency by halving the search space with every iteration and checking whether the computed hydrogen production is larger or smaller than the desired value.

$$P'_{el} * \eta_{sy}(P'_{el}) = P_{H_2}' \quad 2.1$$

The electrolyzer output of the iteration P_{H_2}' is calculated considering the electrolyzer input power P'_{el} and the corresponding efficiency η_{sy} . The Bisection method stops when the difference to the desired electrolyzer output P_{H_2} drops below a predefined threshold tolerance Δ_{tol} .

$$\Delta_{tol} > abs(P'_{H_2} - P_{H_2}) \quad 2.2$$

If the difference is larger than the threshold value, the interval boundaries are update, and a new input power is tested. Establishing the appropriate tolerance level involves finding a balance between obtaining precise values and minimizing computational expenses. As the available computational resources represents already a bottleneck the tolerance is set to 1 kW. This error is negligible as it can be positive as well as negative, and on a simulation basis of a whole year, it is probable that the error balances out.

Economic inputs

For PEMEC systems, at current R&D funding levels in 2020, experts estimate the lifetime to fall within the range of 41.000-60.000 hours (median values). Looking ahead to 2030, if current R&D funding remains constant, experts project a similar or slightly extended lifespan range of approximately 50.000 to 60.000 hours for PEMEC systems. It is anticipated that increased R&D funding is expected to improve PEMEC lifetimes further, with estimates of up to 85.000 hours by 2030 with a tenfold increase in funding. Overall, the expert elicitations indicate that PEMEC lifetimes may improve moderately by 2030 but are not expected to increase drastically compared to current levels of around 40.000-60.000 hours. Significant R&D funding could improve lifetimes further to 60.000-85.000 hours. Considering the typical operational hours, a lifetime of 10 years is chosen.[2]

In the future, advancements in technology are expected to significantly reduce stack costs, primarily through the reduction in the required catalyst, such as platinum According to an in-depth study by the Fraunhofer ISE on electrolyzer costs, these stack advancements are projected to diminish the overall significance of the stack in terms of cost, reducing it to approximately 40 %. At the same time cost for the power supply won't increase to the same extent. In comparison to 2020, a substantial cost reduction of about 30 % for the entire system can be expected.[32] The IEA, in its Global Hydrogen Review 2022, assumes a learning rate of 18 % for stack improvements, while other components are expected to progress at a lesser rate, ranging from 7 % to 13 %. Their cost estimates in 2022 range from 1.400 to 1.770 \$/kW. Overall, the IEA expects significantly higher cost reductions. Depending on the scenario 500-220 €/kWe are projected for PEM electrolysis in 2030. Simultaneously the average system efficiency increases from 60 % in

2020 to 70 % in 2030. In the World Energy Outlook, three scenarios are presented, each with varying degrees of optimism. These scenarios include a conservative stated policy scenario, a more optimistic announced pledge scenario with increased investments and research and development efforts in renewable technologies, and a net-zero emissions case by 2050.[1], [24], [33] Another study of Schmidt et al. estimates the cost and efficiency of electrolyzers based on expert interviews. On average the experts predict a price of 850 to 1.650 €/kWe for 2030 which is significantly higher compared to other studies. Regarding the efficiency an increase to 70 % is expected on average.[35]

To take into considerations not only the IEA predictions, but also the more conservative findings of the Fraunhofer ISE and Schmidt et al., for 2030 an electrolyzer cost of 600 €/kWe is selected. For the average system efficiency relative to the HHV of hydrogen of 70 % is chosen for 2030.

Another cost factor for electrolysis is the water supply. In regions with water scarcity, the water supply for electrolysis must be thoroughly planned and considered from the beginning. If not, enough freshwater resources are available, desalination plants can be a solution to overcome water related constraints and conflicts. The cost of desalination via reverse osmosis are in the range of 1 USD/m³, contributing to approximately 0.5 % of the total electrolysis cost and electricity consumption during desalination makes up of for less than 0.1 % of the electrolysis consumption. Hence, the cost of water is neglected in the tecno-economic analysis.[33], [37]

Table 2.3: Main techno-economic parameters for Electrolyzers

	2023	2030
Investment Cost	1.500 €/kWe [1],[2] [16] [32]	600 €/kWe [1],[2] [16] [32]
Operation and Maintenance cost	3 % of investment cost [38]	3 % of investment cost [38]
Lifetime	10 Years [2]	10 Years [2]
Discount rate	7 % [24]	7 % [24]

2.1.4 Hydrogen storage

Hydrogen storage is confronted by the challenge of its notably low density, measuring at 0.899 kg/m³ under standard conditions. This inherent limitation restricts its practicality for various applications, necessitating the exploration of methods to enhance its energy density. One of the options to increase energetic density is compression, which is associated to high energy consumption. The pressure levels range from lower pressures for utility scale storages to applications in fuel cell vehicles that require pressures of 350 or even 700 bar.[39]

Liquefaction represents another strategy for augmenting hydrogen's energy density. This process requires cooling hydrogen to cryogenic temperatures, resulting in the transition from a gaseous to a liquid state, thereby substantially reducing its volume. However, the challenges lie in maintaining

the low temperatures, requiring effective insulation, and addressing the auxiliary energy consumption associated with the cooling process.

Furthermore, exploring storage within metal hydrides or chemical hydrides, such as ammonia, offers intriguing prospects. Metal hydrides form through the reaction of hydrogen with specific metals, providing a mechanism for reversible hydrogen storage. Similarly, chemical hydrides form stable compounds with hydrogen, which can be released under suitable conditions. These approaches enable compact storage, although challenges involving reaction kinetics, material stability, and energy requirements for hydrogen release must be considered.[10],[39]

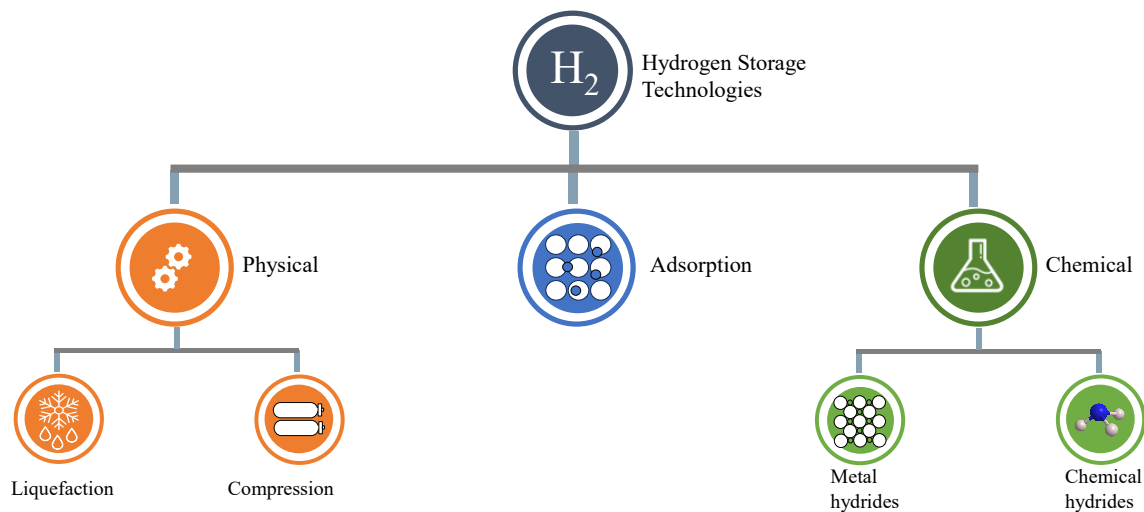


Figure 2.8: Hydrogen storage technology overview, based on Andersson and Grönkvist [39]

To address energy-intensive processes and operational complexities, opting for compressed storage proves pragmatic. This choice offers the advantage of avoiding additional components and costs. While salt caverns are the most economical for gaseous storage, their application is limited by the presence of geological conditions and therefore they cannot provide the solution in many circumstances. An alternative is aboveground storage within pressure vessels, usually at lower storage pressures usually below 100 bar which is selected for this work.

Strategic pressure selection often aligns with electrolyzer output, typically at 25-35 bar. This decision eliminates the need for supplementary compression, thus bypassing compressor requirements and compression work. Nevertheless, lower pressure leads to higher capital expenses due to the need for larger vessels resulting from hydrogen's lower density and increased space demand. The initial SOC is set at 0 and the during operation it can vary from 0 to 100 %.

Table 2.4: Technical parameters of the hydrogen storage

	2023	2030
Operation pressure	30 bar	30 bar
Charging efficiency	100 %	100 %
Discharge efficiency	100 %	100 %

Economic inputs

Hydrogen storage in pressure tanks is a well-established and widely adopted technology. Numerous manufacturers offer a variety of tank sizes, plant configurations, and pressure options. For example, Baglioni S.p.A. provides vertical and horizontal storage solutions at 35 or 70 bar in different sizes, up to 570 kg of Hydrogen.[40] Using this manufacturer data, an estimation of the needed area can be made, to respect constraints regarding the available land. The hydrogen storage itself is modelled as a black box with an associated charging and discharging efficiency.

Regarding the cost estimation literature values diverge highly. On mobility applications precise estimates exist but the structure of stationary storages is typically different with lower pressures and larger storage volumes. Hence, the applicability of the mobility hydrogen storage costs is not necessarily given.

For stationary storage Vera et al. estimate 850 €/kg studies cost per kg range from 850 €/kg [41]. Other studies suggest a cost of approximately 470 €/kg_{H2} for a 50-bar storage system in 2017 and predict similar values for 2025. When operating at 30 bar, the lower volumetric energy density necessitates about 60 % more storage volume, but it also entails fewer structural requirements due to lower pressure forces. Therefore, the capital expenditures are not expected to change significantly for a 30-bar storage system [38]. Urs et al. provide an overview over the hydrogen tank cost used in literature. The costs vary broadly in a range from 1 €/kg_{H2} up to approximately 1.300 €/kg_{H2}. [42] Taking into consideration all the different sources, and the recent component cost inflations one of the higher estimates is selected. In this thesis a cost of 700 €/kg_{H2} is selected, corresponding to 18 €/kWh on base of the HHV of hydrogen. For the future scenarios no huge cost improvements can be expected as pressurized steel cylinders are a mature technology. Cost reductions could be mostly reached due to economy of scale and standardization with increased manufacturing due higher demands. However, to take a conservative approach and follow the literature values for 2030 the storage cost is kept constant. The techno-economic modelling assumptions can be seen in Table 2.5.

Table 2.5: Main techno-economic parameters for hydrogen storage

	2023	2030
Specific storage cost	18 €/kWh [42]	18 €/kWh [42]
Lifetime	25 Years [41]	25 Years [41]
Operation and maintenance cost	2 % of investment cost [43]	2 % of investment cost [43]
Discount rate	7 % [16]	7 % [16]

2.1.5 Battery storage

In this study not only a hydrogen storage is simulated, but also the combination with a Li-ion battery (LIB) storage. Several types of Li-Ion batteries exist, which are distinguished mainly by the cathode chemistry. For utility scale battery storage nickel manganese cobalt (NMC) and lithium iron phosphate (LFP) chemistries are frequently used. LFP has the advantage of slightly lower cost and a good stability, increasing the safety. Further it allows a high cyclability, increasing the lifetime. LFP batteries achieve lower gravimetric energy densities compared to chemistries including cobalt. However, this characteristic is less important for stationary applications, unlike for electric mobility. Due to these characteristics LFP is expected to become the dominant chemistry on the battery storage market by 2030 and is the one considered in this study.[44]

The idea of the additional battery storage is to increase the self-consumption of renewable energy and allow to reduce the size of the electrolyzer. Thereby the time where the electrolyzer is operated at a higher load is increased too. However, the main drawback of using batteries is the added upfront cost. Further, the battery produces additional losses due to charging and discharging efficiencies as well as auxiliaries for cooling. Grimaldi et al. studied the roundtrip efficiency of a utility-scale grid connected Li-ion battery in various use cases. Due to auxiliary consumptions, limited operational hours and conversion loss the effective round-trip efficiency decreases to 65 - 85 %, especially for operations at lower power rates.[45] In this study, achieving economic viability for battery operation poses challenges due to the absence of opportunities to directly utilize low-cost renewable electricity from the battery. Therefore, an optimistic scenario of 85 % system round trip efficiency is considered. For simplicity this loss is equally shared between discharging and charging, assuming the efficiency to be constant for all power ranges. As the efficiency of the battery itself is typically higher than 95 % only minor improvements can be generated in the future. The efficiency reductions on a system level are related for example to the electric system, standby loss or operation outside optimal voltage ranges.[46] Here potential for improvement is given. Hence, in a 2030 scenario the system roundtrip efficiency is increased to 90 %.

Further, constraints regarding the charging power and the state of charge are implemented. These constraints are also useful for error catching, given that the control logic is built to stay inside the constraints and outliers can be identified easily.

$$0 \leq \text{abs}(P_{LIB,ch}) \leq P_{LIB,nom} \quad 2.3$$

$$0 \leq SOC_{LIB} \leq 1 \quad 2.4$$

During charging the SOC is updated, where η_{ch} is the charging efficiency, Cap_{LIB} the capacity in kWh, $P_{LIB,ch}$ the charging power and $P_{LIB,nom}$ the nominal battery power.

$$SOC_t = SOC_{t-1} + \frac{P_{LIB,ch} * \eta_{ch}}{Cap_{LIB}} \quad 2.5$$

An overview of the Battery system efficiencies is given in Table 2.6.

Table 2.6: Technical parameters of Li-ion batteries

	2023	2030
Charging efficiency	$\sqrt{0.85} * 100 \%$ [45]	$\sqrt{0.9} * 100 \%$
Discharging efficiency	$\sqrt{0.85} * 100 \%$ [45]	$\sqrt{0.9} * 100 \%$

Similar to PV-plants, the cost of battery storage is subject to fluctuations due to external factors and has increased during energy crises. Modelling battery storage presents an additional challenge because the final cost depends not only on the installed power but also on the capacity. Typically, in a typical 4-hour battery storage system, most of the cost is attributed to the installed capacity. However, certain components, particularly power electronics such as inverters, scale with power rather than energy. To realistically model costs, both power-related and energy-related costs must be taken into account and combined into a single cost function.

$$Capex_{tot,\epsilon} = cost_{sp,P} * P_{kW} + cost_{sp,E} * E_{kWh} \quad 2.6$$

Equation 2.6 combines the two cost factors for power and energy and calculates the total system capital expenditures $Capex_{tot,\epsilon}$. This specific battery cost then depends on the ratio between energy and power of the battery. The term $cost_{sp,P}$ are the specific power cost in €/kW, P_{kW} the total system installed power in kW, $cost_{sp,E}$ the specific capacity cost in €/kWh, E_{kWh} the total system installed capacity in kWh. The cost function in Figure 2.9 is then benchmarked with 2021 utility battery storage cost provided by NREL.[44],[47]. All costs in USD are transformed into EUR using the yearly average exchange rate of the corresponding year. The results show that the cost function in this thesis follows well the data used by NREL if the factors $cost_{sp,P} = 260$ €/kW and $cost_{sp,E} = 260$ €/kWh are selected.

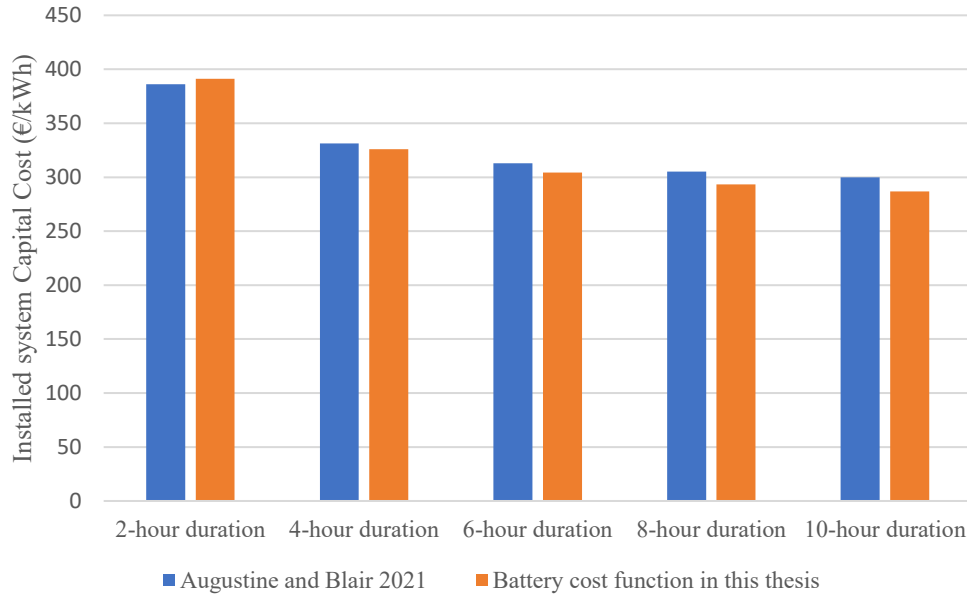


Figure 2.9: Utility scale Li-ion battery cost, data from [44]

In the future significant cost reductions on battery storage are to be expected. The NREL forecasts a reduction in costs ranging from 16 % to 47 %, with the extent depending on the particular scenario. [47] The IEA estimates even larger cost reductions to reach 161 €/kWh in 2030, based on a starting point of 248 €/kWh in 2021.[48] Future cost reductions are more significant on the energy component than on the power cost component. The most substantial cost reductions are expected to occur in the domain of battery production itself, whereas other cost factors such as power electronics and inverters are projected to remain relatively stable. +To be in line with the 2023 scenario the mid cost projections from the NREL are taken. For the 2030 scenario cost factors of $cost_{sp,P} = 226$ €/kW and $cost_{sp,E} = 174$ €/kWh is selected in line with the learning rate of 30 %. Using equation 2.6 for a 4-hour storage system this leads to a cost of 269 €/kWh, which is lower than the latest NREL scenario but significantly higher than the 161 €/kWh used by the IEA.[48]

The Battery lifetime depends on the technical specifications of the battery and on the operational characteristics. Especially the depth of discharge and number of cycles, and the battery temperature determine when failure occurs. A high depth of discharge significantly reduces the number of cycles to failure and reduces the lifetime. To estimate the lifetime of a battery approaches like the lifetime throughput exist, which estimate the energy a battery can deliver or store during its operational lifetime.[43],[49] However, these concepts require previous knowledge on the operational behaviour. In this study the sizes of the battery and the other components are determined by the PSO algorithm and vary greatly, completely changing the depth of discharge and operational behaviour of the battery storage. Since the LIB storage is mainly used as short-term storage to bridge short periods without sufficient PV production, a high depth of discharge can be expected. The IEA uses an estimate of 10 years of battery life, whereas Marocco et al. obtain a lifetime of 13 years in a microgrid application, using the lifetime throughput to estimate the lifetime. In this thesis the more conservative estimate of 10 years is used, further motivated by the

fact that degradation is not incorporated into the model.[24],[43] An overview on the techno-economic battery parameters is provided in Table 2.7.

Table 2.7: Main techno-economic parameters for Li-ion battery storage

	2023	2030
Cost factor power $cost_{sp,P}$	260 €/kW [47]	226 €/kW [47]
Cost factor energy $cost_{sp,E}$	260 €/kWh [47]	174 €/kWh [47]
Specific CAPEX final 4h storage	325 €/kWh [47]	230 €/kWh
Operation and maintenance cost	7 €/kWh/y [43]	7 €/kWh/y [43]
Lifetime	10 years [43]	10 years [43]
Discount rate	7 % [1]	7 % [1]

2.1.6 Grid

The goal is to provide the electricity predominantly from renewable energy generation on site. However, due to the fluctuations in generation and the demand profile which has to be satisfied also during periods of low-res availability also the electrical grid is included into the model. Various approaches exist to establish realistic prices. Looking at consumer statistics of industrial users Arera reports a price of 139 €/MWh in 2021 for users with a consumption of 20.000-70.000 MWh/year.[50] The price has to consider that electricity is taken from the grid usually when there is no PV-generation on-site, resulting in on average lower availability of renewable energy at the grid level, which causes higher prices. The code is implemented in a way that allows the input of an hourly energy price profile in future work. In this thesis the price is chosen to be fixed.

As discussed in chapter 1.5 there are different subsidies and tax breaks set by the European Union as well as the Italian government. However, accessing these incentives requires meeting certain sustainability criteria for the produced hydrogen. Given that Italy's current electricity mix is not entirely based on renewables and causes emissions of 250 g/kWh in 2021, satisfying the EU requirements for green hydrogen can be challenging[51]. To keep the assumption of a low emission grid withdrawal, other market mechanisms like Power Purchase Agreements need to be evaluated.

The grid connection serves not only for withdrawing electricity but also for injecting excess electricity into the grid when the storage systems are fully charged. Determining the price of electricity purchase involves considering various factors and available remuneration schemes. On a utility scale electricity can be typically sold at the zonal price. The zonal price is related closely to the PUN, but differences can occur depending on the electricity availability within a bidding zone. The high renewable electricity availability during the peak hours and no PV generation during the night has an effect on the zonal prices and PUN.[52] This causes higher electricity

acquisition prices and lower injection revenue for the client, as the PV based system usually sells electricity during the day and buys it during the night. For the 2030 scenario, this effect will have a large impact on the prices and is considered in a sensitivity analysis. Other possible remuneration schemes include example PPAs and contracts for difference. However, their applicability in combination with incentives for green hydrogen production must be carefully considered.

Additionally, when selecting the electricity injection price, it's important to note that a price above the LCOE of photovoltaic generation pushes the algorithm to maximize the PV-size. In fact, the PV subsidizes the hydrogen production as it sells electricity over the generation cost and generates additional revenue. The subsidization effect is investigated more in detail in chapter 3.1. The indirect subsidisation is a non-desired effect, as the goal of this study is not to investigate the economics of utility scale PV plants. Hence, for the optimization of the sizes in the main scenarios the price for electricity injection is set at 0 €/MWh. Furthermore, a sensitivity analysis investigates the effect of remuneration for grid-feed, using the fixed sizes obtained from the 2023 base scenario. An overview of the selected prices for the main scenarios is given in Table 2.8.

Table 2.8: Electricity price assumptions main scenario

	2023	2030
Cost electricity acquisition	120 €/MWh [53]	120 €/MWh [54]
Revenue grid injection	0 €/MWh	0 €/MWh

2.1.7 Industrial user

The goal of this this study is to satisfy the demand of an industrial user and substitute natural gas with hydrogen. The methane consumption profile of the user is shown in the following diagram. The industrial user acquires methane and employs it in a gas turbine. Specific information regarding the electricity and heat generation process or any further utilization by the end user is currently unavailable.

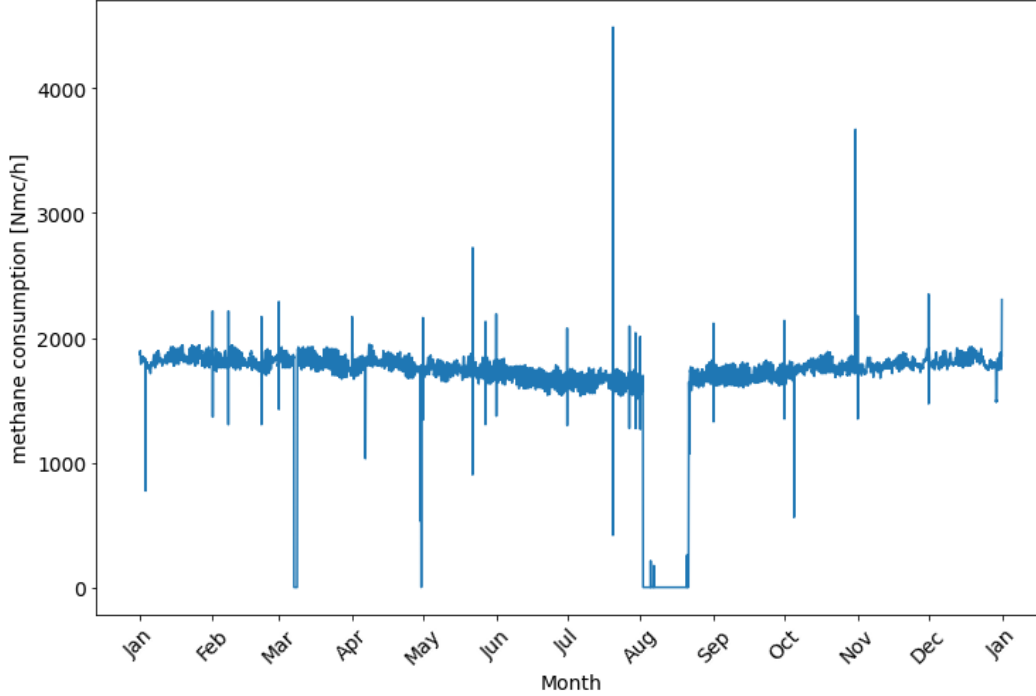


Figure 2.10: Industrial user consumption profile

The profile is characterized by an almost constant methane consumption over the duration of the whole year. A slight seasonality and higher consumption values are present during winter and a period of about two weeks without consumption during August. Some outliers exist in the profile, often followed by a lower consumption in the following hour. The cause of these outliers is unknown and could be apart from technical motives also attributed to measurement errors or data acquisition issues. Due to the infrequent occurrence of the outliers and a lack of in-depth knowledge on the industrial processes in the company as well as the reasons for the outliers the data is not modified or filtered.

The profile of the final user is given in normal cubic meters of natural gas. To determine the equivalent hydrogen energy content, the energy content of the natural gas is calculated, and it is assumed that the energy content needed is the same independently if the energy carrier is hydrogen on a HHV basis. To simplify calculations in later modelling stages, the energy content is expressed in kWh. The calculation for the energy content of the supplied methane in kWh is as follows, using the HHV of the fuels.

$$Energy [kWh] = NG [Nm^3] * \frac{1}{1.0549} \left[\frac{Sm^3}{Nm^3} \right] * HHV_{NG} \left[\frac{MJ}{Sm^3} \right] * \frac{1}{3.6} \left[\frac{kWh}{MJ} \right] \quad 2.7$$

Natural gas can have different compositions and energy contents, depending on its origin. Previously to the energetic crisis a large share of the European gas mix was imported from Russia. The import shares drastically changed in 2022. This is also valid for Italy. For the calculations a

weighted average HHV based on the 2022 import shares for Italy is used, calculated in the following table.

Table 2.9: Italian gas imports and HHV in 2022

Country	Import share in 2022 [%] [17]	HHV _{NG} [MJ/Sm ³] [16], [17]
Algeria	38	39.6
LNG	22	40.0
Azerbaijan	16	40.0
Russia	13	38.7
Northern Europe	6	39.0
Libya	4	39.5
Weighted average	100	39.6

2.2 Cost methodology

To evaluate the economic performance of the system the LCOH are used. LCOH is a financial metric employed to evaluate the comprehensive economic feasibility of hydrogen production across its complete lifecycle. Analogous to the widely utilized concept of Levelized Cost of Electricity

LCOH incorporates the entirety of costs entailed in generating, storing, and disseminating hydrogen. This encompasses initial capital investments, ongoing operational expenditures, and pertinent financial considerations. The primary goal of the optimization is to satisfy the user's request with the lowest LCOH possible.

Calculating the LCOH it is essential to thoroughly aggregate all costs involved. Nevertheless, a notable challenge arises due to limited data availability, as data for a single year of user demand is present. To prevent making speculative assumptions about future demand, which can be influenced by various external factors, the simulation is restricted to a one-year timeframe. A significant complexity arises when dealing with Capital Expenditures (CAPEX), as the entire lifespan of each component must be considered, even though the investment cost occurs only once at the beginning. In contrast, Operational Expenditures (OPEX) entail annual costs, and therefore do not undergo annualization. The OPEX consist of the cost of the electricity acquired, subtracting the revenues of grid injection, as well as operation and maintenance of the components.

The solution allowing to consider both OPEX and CAPEX in the results of a one-year simulation is the annualization of CAPEX. This is done calculating the equivalent annual cost EAC for each component i ,

$$EAC_i = \frac{NPC_i}{A_{r,i}} \quad 2.8$$

where NPC_i are the net present cost. The annuity factor $A_{r,i}$ can be calculated like the following:

$$A_{r,i} = \frac{1 - \frac{1}{(1+r)^t}}{r} \quad 2.9$$

The higher the discount rate r and the lower the lifetime of the component i , the lower will be the annualization factor and correspondingly causing higher equivalent annual cost.[55] Selecting an appropriate discount rate is not straightforward due to factors like inflation and the unpredictable regulatory and market environment. Based on historical trends and considering the increasing maturity of renewable energy technologies and decreasing investment risk, a discount rate in the range of 5-7 % appears reasonable. However, it's important to note that during times of energy crises and increased inflation, current discount rates may vary considerably.[31],[1]

Finally, the levelized cost of hydrogen can be obtained, summing the CAPEX of every component i and the OPEX from every contribution j for every time instance t in one year, dividing it by the sum of the hydrogen demand in one year.

$$LCOH = \frac{\sum_{i=1}^I CAPEX_i + \sum_{j=1}^J \sum_{t=0}^{8759} OPEX_{tot,t,j}}{\sum_{t=0}^{8759} P_{H2,Enduser,t}} \quad 2.10$$

As is the case with other economic comparison methods, the discount rate must be selected in advance for each project. If this forecast is inaccurate or changes occur during the project's lifetime, these alterations cannot be considered, significantly affecting the results. All costs in the model are denominated in EUR. Since some sources report costs in USD, the dollar-euro exchange rate of the year of the specific data is used. If no date is provided, the year of publication is utilized to determine the exchange rate. It's worth mentioning that in all calculations of component prices, conservative estimates have been applied.

2.3 Control logic

To manage the different components and decide how to operate the system a control logic is needed. Various types of control logics exist, and they are broadly divided into rule based and optimization-based strategies.

A rule-based control strategy offers several **advantages** in various applications. The logic behind rule-based systems is transparent and interpretable, enabling straightforward troubleshooting and adjustments. Moreover, rule-based systems tend to exhibit stability due to their deterministic nature, making them reliable for well-defined scenarios. Due to their simplicity, they also ensure low computational demand and work well together in combination with optimization algorithms.

However, rule-based control strategies come with **limitations**. They may struggle to adapt to unforeseen or complex situations that were not explicitly considered during rule formulation, leading to degraded performance in novel scenarios. This has to be especially taken into account when conducting a sensitivity analysis with different assumptions regarding efficiencies and costs of the components. Managing a large number of rules can become cumbersome, affecting scalability and maintainability. Defining rules can also be subjective, relying on expert knowledge to ensure their effectiveness. Moreover, handling trade-offs between conflicting objectives can be challenging for rule-based systems, potentially resulting in suboptimal decisions.[7],[56],[57]

Considering these characteristics, a rule-based control is used to reduce computational demand and create a solid base as an input for the PSO algorithm. Having an optimization-based control strategy in an inner loop and the PSO algorithm on the outer loop would significantly increase the computational demand and programming complexity.

Table 2.10: Advantages and disadvantages of main control strategies [7],[56],[57]

	Advantages	Drawbacks
Rule-based	<ul style="list-style-type: none"> • Low computational demand • Transparent and predictable behavior 	<ul style="list-style-type: none"> • Require expert knowledge. • Low adaptability to new conditions
Optimization-based	<ul style="list-style-type: none"> • High flexibility in variable modelling conditions • Less knowledge on the system behavior required 	<ul style="list-style-type: none"> • Difficult to implement. • High computational demand

The main scope in the design of the system control logic is to be in line with the predefined objectives of the system and establish a structured and efficient decision-making process. Hereby a central control logic is advantageous. From a programming perspective the decision to establish a central control logic is taken with the scope to follow an object-oriented programming approach. This central logic oversees power flows, state of charge, and user demand, and it determines the appropriate actions to be taken, which are then communicated to the individual components. Thereby the control system optimizes the utilization of renewable power, minimizes reliance on grid power, and ensures the fulfillment of the end user's hydrogen demand.

Practical implementation of the control strategy

In the following the rule-based control strategy is presented. Due to the complexity of the decisions to control, the modelling strategy is complicated and for clarity broken into pieces. The control system has two main parts. The upper part determines the general system state on the electricity side, while the lower part determines the situation downstream and if necessary, corrects the electrolyzer and battery storage operation.

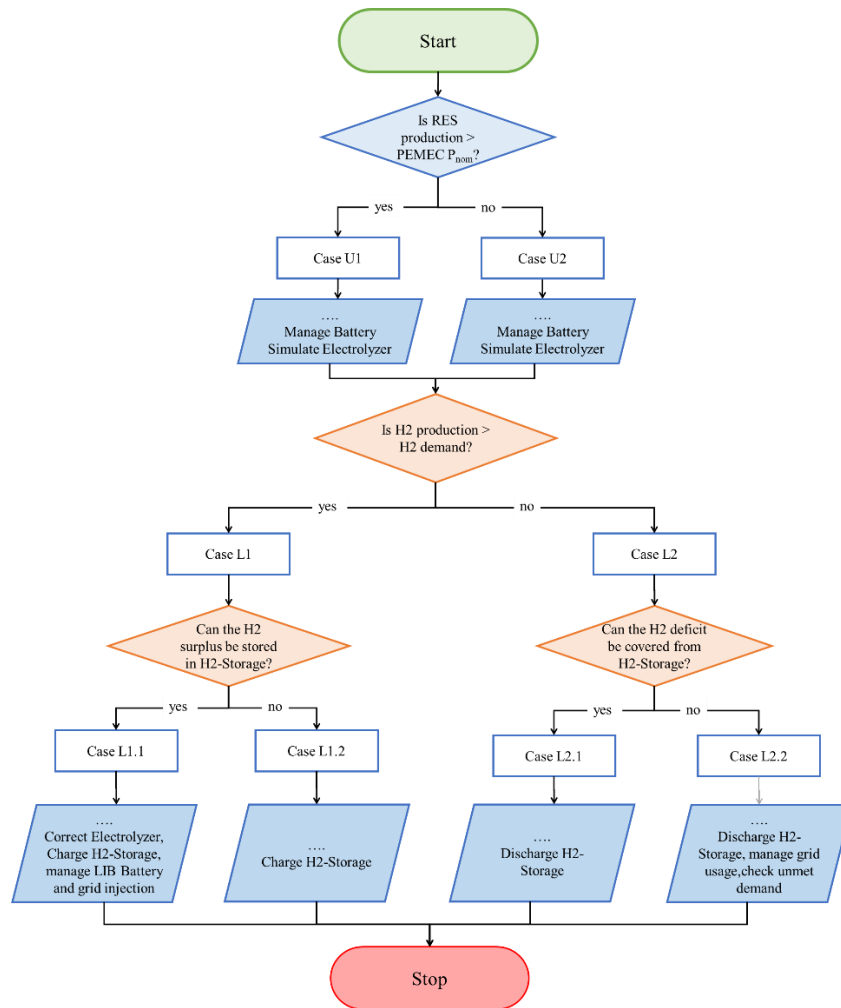


Figure 2.11: Control strategy overview

The logic of the **Upper Part** can be summarized as follows: In a first step the logic checks whether there is excess renewable power available. At this point the optimal hydrogen production according to the end users demand is not known and the system tries to transform all the renewable power available into hydrogen in a first guess. Thereby two cases can occur:

- Case U1: A larger RES power is available than the electrolyzer can convert.
- Case U2: The electrolyzer works below the nominal load as not enough RES power is available.

Case U1 occurs if the available RES electricity is more than the electrolyzers nominal power. Then the electrolyzer runs at its maximum power. It is then checked whether the battery has enough power and free capacity to be charged and to take in the surplus RES power. If the battery is not able to handle all the surplus the remaining excess power is injected into the grid. Possible congestion of the grid is neglected at this modelling stage.

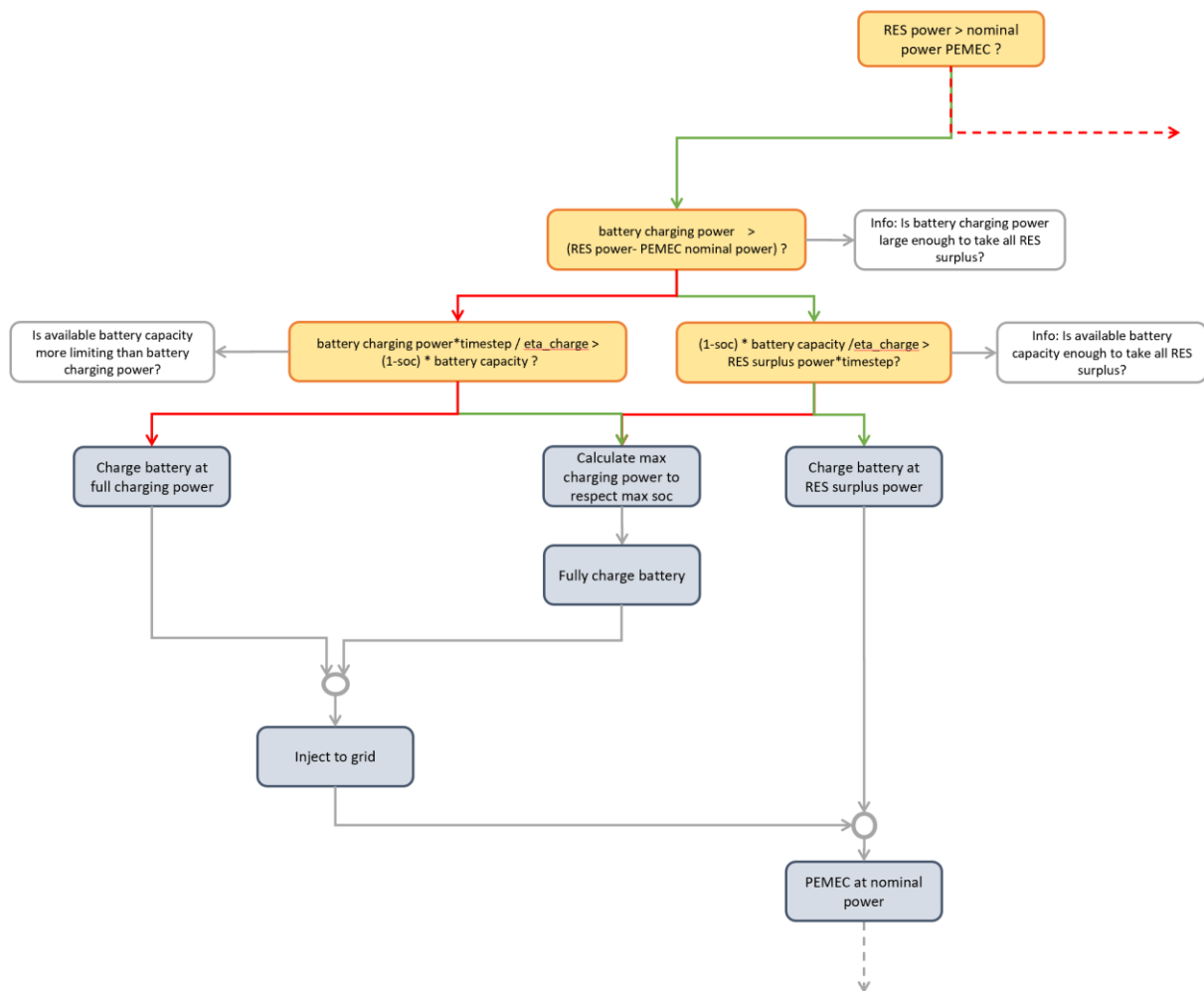


Figure 2.12: Control strategy upper part U1

In Case U2 not enough power from RES is available to operate the electrolyzer at nominal power. In this case the battery is charged considering limits to maximum discharge power and SOC. The resulting battery and RES power is converted to hydrogen in the electrolyzer. The current electrolyzer state is saved for later considerations in every case.

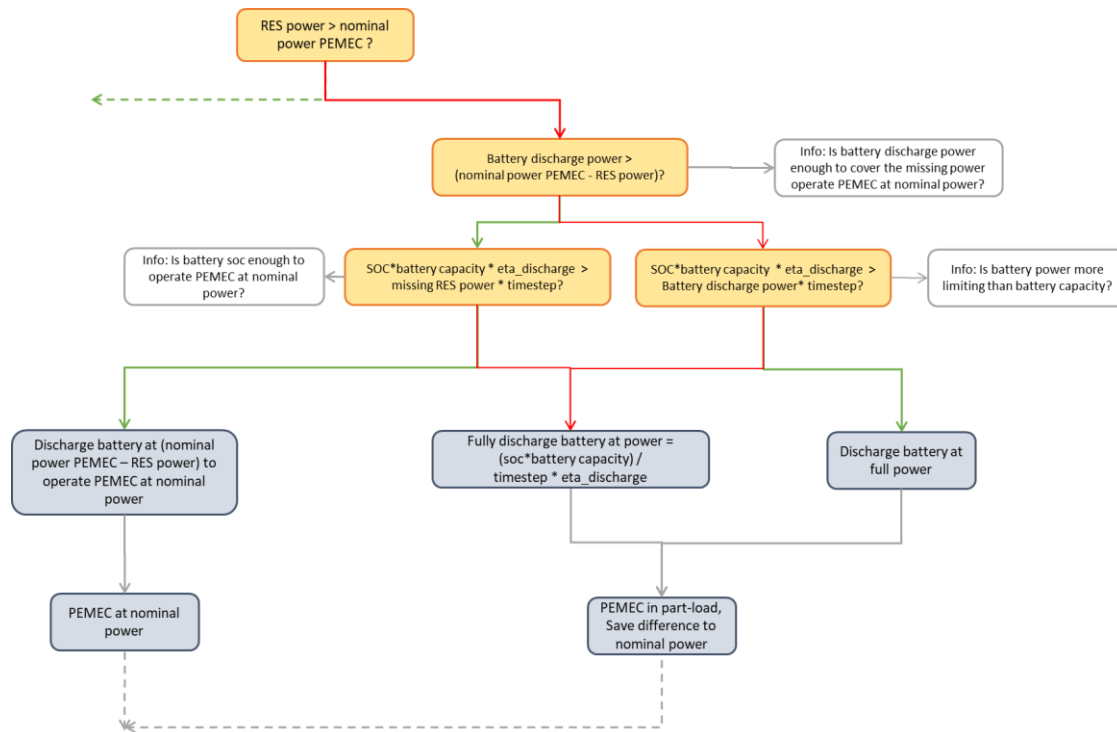


Figure 2.13: Control strategy upper part U2

Following the assessment of the upstream side of the model with RES supply, the hydrogen side involving the user demand is considered to eventually correct the upstream operation. The connection of the upper and lower modelling part is presented in Figure 2.14. In the **lower part** the hydrogen production determined by the upper part of the control logic is compared with the user demand to determine if the system is in a surplus or deficit case. Depending on the resulting case, the operation of the electrolyzer is optimized to follow the control system objectives. Again, two main cases exist:

- Case L1: The hydrogen production from RES is larger than the user demand. A surplus situation is present and the available storage options have to be investigated.
- Case L2: The hydrogen production calculated upstream is not enough to meet the user demand. Available storage capacity is checked and if this is not enough also electricity withdrawal from the grid.

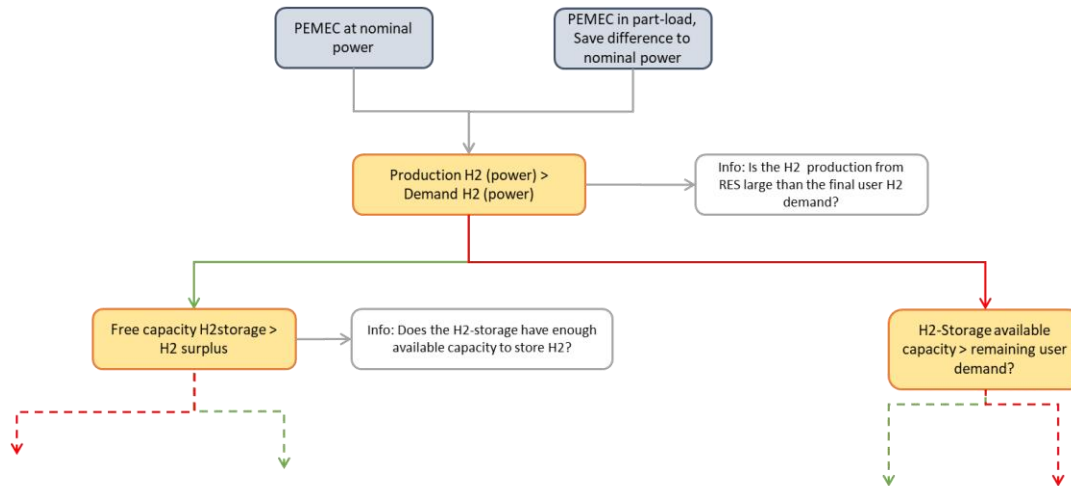


Figure 2.14: Control strategy, connection of upper and lower part

In Case L1 the hydrogen production exceeds the hydrogen demand. The system logic for this case is visually presented in Figure 2.15. The surplus must be stored in the hydrogen storage. Therefore, an initial check determines if the available hydrogen storage capacity is sufficient to accommodate the remaining surplus. In this case all the excess hydrogen is stored in the hydrogen storage, the user-demand is satisfied and the electrolyzer and battery are operated as determined in the upper control part.

If the H₂-storage does not have enough capacity to store all the excess hydrogen a reduction of production is necessary upstream to avoid unnecessary energy losses. This case is more complex as it involves a correction of the upstream production, reducing the electrolyzer output. First the maximum hydrogen production which can be handled by user-demand and storage is calculated. This is the production target of the electrolyzer. Due to the knowledge of the efficiency curve of the electrolyzer given a desired hydrogen output, the corresponding electricity input can be determined. The new electricity input implies a reduction to the previous input of RES and battery established upstream. The input reduction is then tried to achieve by discharging the battery less or charging it more, while respecting available battery charging power and free capacity. The idea is still to use all the possible PV power within the system and use the new electricity surplus to charge the battery rather than injecting excess electricity into the grid. If the electricity input of the electrolyzer through battery is insufficient, then the additional electricity is injected to the grid.

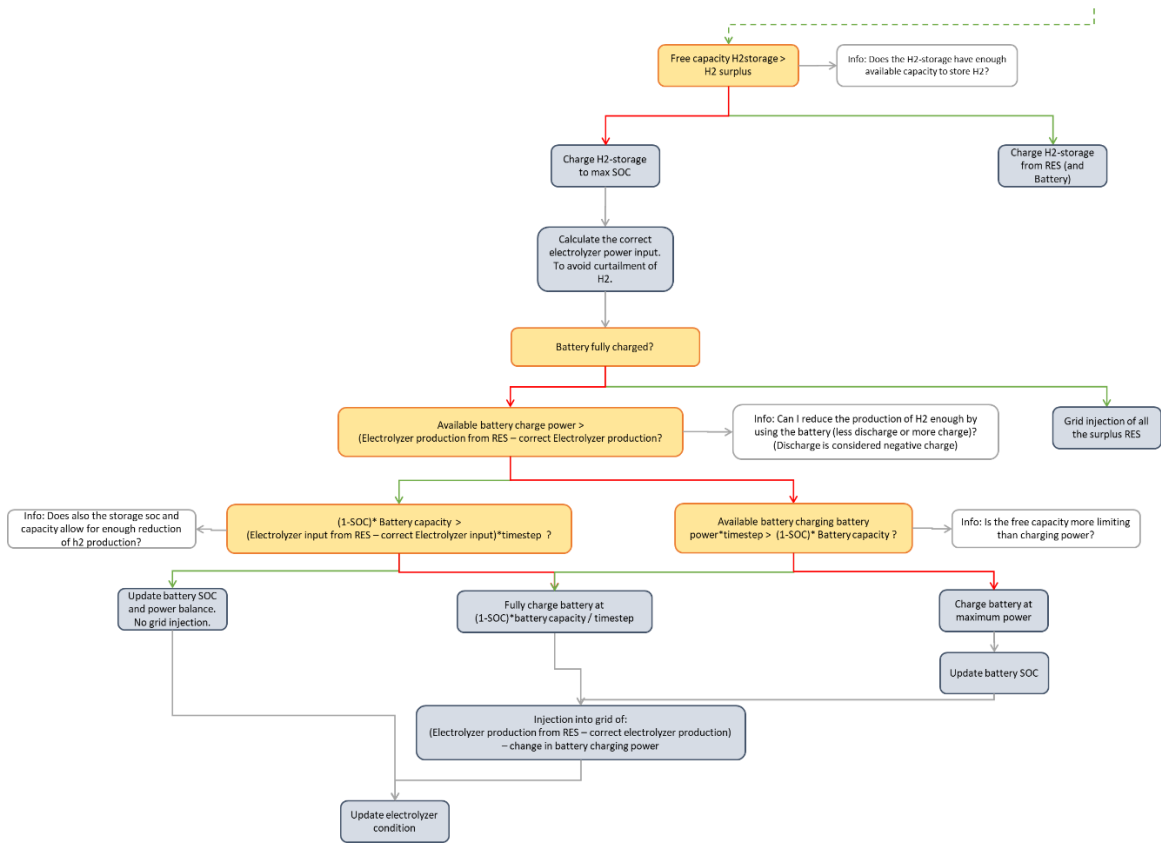


Figure 2.15: Control strategy lower part L1

In Case L2 of missing hydrogen supply the strategy is the opposite and it is presented in Figure 2.16. To satisfy the unmet user demand the first check is to see if the hydrogen storage can supply the rest of the demand. When the stored hydrogen is enough, the remaining demand is discharged and the upstream operation of electrolyzer and battery remains the same.

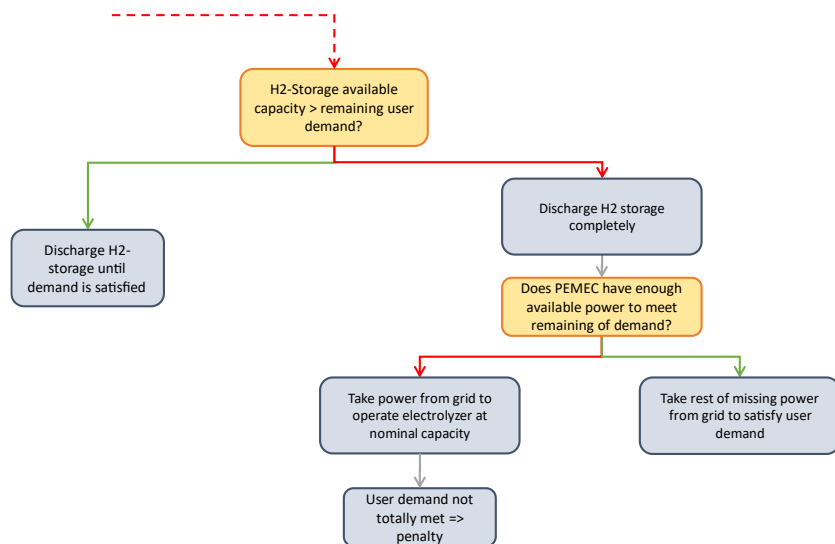


Figure 2.16: Control strategy lower part L2

The other case where the demand cannot be met only by discharging the hydrogen storage is more complicated. First the hydrogen storage is completely discharged, but still a part of the user demand is unmet. Then it has to be checked upstream if the H₂ production of the electrolyzer can be increased enough using grid electricity to meet the missing demand. Thereby the operation of the electrolyzer is changed. Due to the upstream logic all possible power from RES and the battery is already used in the electrolyzer. Thanks to this principle only the load condition of the electrolyzer has to be investigated. Thereby the electrolyzer is simulated at full load and checked if this hydrogen output is enough to satisfy the remaining user demand after discharging the hydrogen storage. Again, two subcases exist:

In the first subcase the user demand can be satisfied by using grid electricity to operate the electrolyzer at a higher capacity. This means that the increase in hydrogen production is equal to or larger than the remaining user demand. In this case the correct hydrogen production is calculated and using the electrolyzer efficiency curve the electricity input. Knowing the total RES production and battery discharge determined in the upper part, the correct electricity acquisition is computed.

In the second subcase the user demand cannot be satisfied, even with the use of grid electricity. In this case the electrolyzer works at nominal load, taking the missing electricity from the grid. The difference between the total production and hydrogen storage discharge on one side and the hydrogen demand on the other equates to the unmet demand. This unmet demand is also associated to a cost by multiplying it with a penalty of 5 €/kWh to incentivize the algorithm to select a different set of sizes which avoids this case. The selection of the penalty should be high enough to let the model avoid these kinds of situations but also not hindering the conversion of the algorithm by incentivizing it to choose over-dimensioned sizes.

The penalty is introduced to reduce the computational cost, while still assuring to meet the final user demand. When the yearly simulations for the particles are conducted the sizes of the components are already determined. Hence an adaptation of the sizes to avoid the occurrence of unmet demand would require restarting the simulation, escalating the computational time. An alternative approach is to introduce system reliability as a second optimization objective, with the drawback of creating a bilevel optimization problem.

In the case of an electrolyzer which sizing is smaller than the peak final user demand it can be useful to also to charge the hydrogen storage preventively with grid electricity, if the SOC is lower than a certain threshold value. Thereby the danger of not meeting the customer demand for peak hours is reduced. Hence the strategy with a variable threshold for grid supply is included but not active in a base case scenario and provides a future application strategy. Conditions to avoid overcharging of H₂-storage with grid electricity is that the H₂-storage has a much larger capacity than the maximum production by the electrolyzer. These safety constraints are introduced for cases with a large electrolyzer and small hydrogen storage, to avoid undesired behavior. An example of this additional part of the control strategy is presented in Figure 2.17.

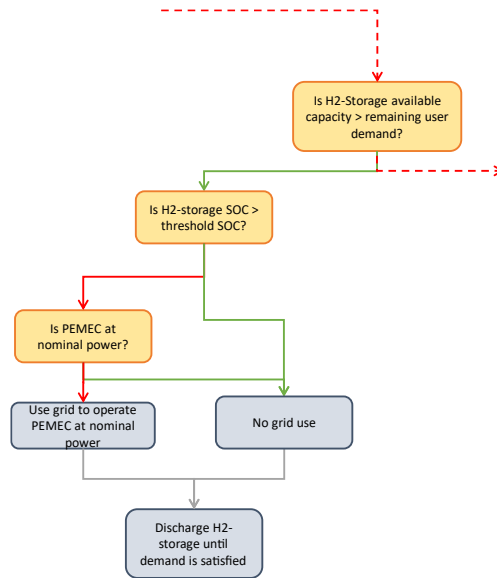


Figure 2.17: Example of preventive charging strategy to reduce supply loss probability.

Most of the modelling strategy is straightforward and clearly in line with the control objectives. However, some decisions must be critically discussed. For example, the case that the battery is discharged to charge the hydrogen storage even if the user demand is already met. This simplification is valid since both electrolyzer and hydrogen storage operate at the same pressure on the hydrogen side, meaning no additional compression work and associated losses are present. Charging the hydrogen storage does not lead to significant energy losses and the usage of the battery increases the supply security. If the hydrogen would be stored at higher pressure or liquified, this assumption is not valid anymore, meaning that the rule-based strategy would not obtain the optimal result.

2.4 Particle Swarm optimization

The present study explores the optimization of a complex model, characterized by numerous interdependencies and nonlinearities, wherein achieving the exact optimal solution becomes impractical. Consequently, the adoption of metaheuristic algorithms becomes imperative to tackle these intricate optimization challenges effectively. Within the domain of energetics Particle Swarm Optimization (PSO) is frequently employed algorithm and emerges as a prominent choice for addressing such complexities.[58]

Particle swarm optimization is inspired by the social behavior of bird flocking or fish schooling. PSO mimics a swarm by using multiple particles where each of these particles represent an individual of the swarm. In the context of birds, the idea is that each bird has its own idea of where to find food, but they also pay attention to the other birds in the swarm. If one bird finds a good source of food, the other birds will follow it. In PSO, each particle represents a possible solution to the problem. The particles are initialized with random positions and velocities. At each iteration, each particle updates its position and velocity based on its own best past position p_{best} and the

best position of the entire population g_{best} . The particles are attracted towards their own and global best position to achieve converge to the global optimum.[58],[59]

The particles positions X from one iteration to the next are updated according to the following equations, updating first the velocity V :

$$V_i^{k+1} = w * V_i^k + c_1 * r_1 * (p_{best}^k - X_i^k) + c_2 * r_2 * (g_{best}^k - X_i^k) \quad 2.11$$

Then the position is updated, summing the new velocity V_i^{k+1} to the previous particle position X_i^k .

$$X_i^{k+1} = X_i^k + V_i^{k+1} \quad 2.12$$

w is the inertia factor which describes how much of the previous velocity of the particle is kept. The acceleration factors c_1 and c_2 determine the magnitude of the pulling towards the personal best values of a particle p_{best} and globally best value of the swarm g_{best} . The parameters r_1 and r_2 are randomly generated numbers between 0 and 1. Other important parameters to be set are the number of iterations and the number of particles.

2.4.1 Setting the PSO algorithm

Given the intricate nature of the optimization problem at hand, a pivotal aspect of the study revolves around the selection of appropriate parameters (c , w , population, iterations) for the PSO algorithm. This crucial decision-making process aims to find an optimal trade-off between the quality of solutions obtained and the computational resources expended. This parameter-selection is not straight forward as the correct choice of parameters is highly problem specific and sensitive. The search space is not well known before running the model and it is only explored in detail when the algorithm is running. Hence it is also difficult to access the algorithms performance in depth.

However, the assignment of random positions during the initialization phase and the incorporation of the two random components when updating a particle provides validation possibilities. There is no knowledge of an optimal solution for many of the cases. Nevertheless, a validation of the performance is still possible.

One opportunity consists in running multiple simulations with the exact same setting the results will be different with every run. If the algorithm works well on this specific problem and finds results close to the global minimum, it must produce similar results each run. This still does not exclude the possibility that every of these runs gets trapped in a local minimum but gives an idea on how well the algorithm converges. Repeating the simulations multiple times and adapting systematically the hyperparameters to find the most economical and reproducible result is a useful strategy to optimize parameter setting.

A second validation strategy is the simulation of extreme cases where the optimal result can be obtained manually, allowing simple benchmarking. One of many examples is to set high specific electricity prices for renewable grid injection, expecting the optimizer to increase the size of the PV-plant.

Another idea of validation is the discretization of the search space and the calculation of all different size combinations in the discrete search space. The discrete optimal value could then be confronted to the PSO output in the continuous space. However, to get a reasonably exact result a discretization of must investigate a set of sizes per parameter. If the discretization is too rough minima could be in between the discretization steps and produce incorrect result. With the 5 optimization parameters the number of possible combinations is n^5 where n is the number of sizes for a single component. This number of combinations is easily out of a feasible range from regarding the computational cost.

Consequently, a trial-and-error approach involving multiple runs with a 24 h generation and consumption profile. Since in the model CAPEX are annualized and the summed to the OPEX for the calculation of the objective function, it has to be avoided to overestimate the CAPEX. Therefore, in the test runs with a 24-hour profile CAPEX were divided by 365 to simulate a setting close to the complete optimization problem with a whole year. Simulations were performed on a desktop computer with an Intel Xeon E3-1245 v5 of 3.4 GHz and with 32 GB RAM.

For each setting 5 runs were conducted to validate the runs against each other and evaluate the quality and stability of the algorithm with this hyperparameter setting. From literature c_1 and c_2 usually have the same value and this was kept for all the testing runs. It started with a high c value of $c_1 = c_2 = 2$ which was known from literature.[60] The value of c_1 and c_2 was reduced in 0.2 to determine the most suitable value until reaching 0.6. Also values of $c > 2$ were checked but as expected from the calculation of the velocity they lead to non-convergency using $w = 0.9$.

The tests found values from 1.4 to 1.8 to achieve the best results. Finer testing and many repetitions revealed a value around 1.7 to suit best. The other parameter to set is the inertia w . According to equation 2.12 the inertia says how much of the velocity of the previous iteration is kept. The velocity is then influenced by the correction toward c_1 and c_2 .

The inertia w is usually set between 0.4 and 1. Testing for various w rates was done taking $c = 1.7$. The simulations with $w = 0.9$ show the best results. Also, other combinations were tried, however over all the tests relatively high values performed because of the tendency to not get stuck in local minima.[59],[60]

Testing revealed the problem of getting trapped into local minima, showing the difficulty of dealing with a multimodal programming problem. This happened especially for the optimization parameters which were less significantly influencing the cost. While during the test runs the purchased electricity and PV-plants caused the highest cost these parameters were optimized reasonably well. The final parameter configuration was tested by repeating 15 simulations with the same setup.

Historically, it was commonly assumed that a swarm size of 20 to 50 particles represents the best choice for PSO algorithms [60]. The higher the dimensions the more complex the search space can become, meaning that more particles enhance the performance. Piotrowski et.al. found out that previous hypothesis on swarm size is not necessarily true and PSO performance can be significantly enhanced with a larger swarm size for some application. The correct swarm size depends on the variant of the algorithm and usually is best set over 70. The analysis was conducted

on optimization problems with 10 or more dimensions.[61] Considering practical constraints of available computational resources in this specific problem a swarm size larger than 25 is difficult to realize. The lower dimensions of the problems allow also to achieve reasonably stable results with a lower number of particles, accepting a lower conversion rate because of higher acceleration factors and inertia.

2.4.2 Improvements and variations to the standard algorithm

Currently numerous versions of PSO-Algorithms exist with the aim of performance improvement and applicability to specific problems. These involve for example, fully informed PSO where the target particle is affected by all its neighbors instead the single best success of the population. Other approaches involve the use of local best topology, allowing for parallel searches in different regions with equally promising optima, or dynamic topologies. In this study the general idea of a classic PSO algorithm was kept as benchmark different PSO algorithm is outside of the scope of this thesis. From the classical PSO algorithm as a basis small modifications were observed.

For example, Liu introduces an advanced PSO method, to optimize a standalone PV-plant including battery storage. The structure of their operational logic remotely resembles the one of this study using a rule-based logic too. In this context a standard PSO algorithm with the parameters $c = 2$, $w = 1$, population = 30, and iterations = 100 is compared to a leveraged version. The proposed optimization consists in the damping of the inertia with increasing iterations. This is thought to allow a good exploration of the search space in the beginning. At the later iterations with decreasing inertia the particles converge faster towards the current global and individual optima and improve the fine search. When the approximate area of the minima is identified a lower w suit for quick convergency and an efficient fine search[59].

The same strategy was tested also in work on a 24 h profile with 5 simulations for each hyperparameter setting. For a low number of particles, the results fell short of expectations and converged in local minima. It was hypothesized that the search space wasn't explored enough and in the discontinuous search space of the 24 h profile the algorithm then converged in a local minimum. Therefore, it was further modified reducing the inertia w linearly from 0.9 to 0.4 only after half of the iterations. For the first half of the iterations w is kept at 0.9. This modification significantly reduced the variation between simulations, resulting in a more stable algorithm and a lower LCOH. As a result, this adapted approach was retained for simulations based on the real yearly consumer profile, with ongoing monitoring to ensure that the number of particles and iterations are sufficient to reliably identify the global optima.

Additionally, a constraint was introduced regarding components sizes, to prevent the optimization from assigning negative sizes. Occasionally, the algorithm yielded negative sizes, which are not physically feasible. In such instances, the sizes were reset to a minimum value of 0.001 to avoid division by zero errors. It's important to note that when resetting the sizes, the velocity of the particle also needed to be updated. This adjustment was necessary because failing to correct the velocity would result in incorrect component sizes during the next iterations and a tendency of getting stuck in local minima. To address this, the position values from the previous iteration were saved and then subtracted from the updated corrected position of the particle.

An attempt was made to improve the algorithm by using two vectors of random numbers instead of the two single random numbers r_1 and r_2 , which are multiplied to the acceleration factors c_1 and c_2 to determine the new particle velocities. The idea behind using a vector of random numbers was to allow for individual weighting of the velocity of sizes for each component. This means that one component could have slow changes while another experienced rapid size changes, potentially leading to different exploration behaviors. However, after testing this strategy, it did not yield any considerable benefits, and as a result, this approach was abandoned.

2.5 Global modelling strategy

The PSO algorithm is incorporated in the general modelling strategy. The global strategy starts with an initial random selection of component sizes. These sizes are initialized within a reasonable range based on approximate knowledge of area constraints and model physics. If the optimal size of a component is larger than the initially selected area the PSO algorithm is still likely to find the optimum if the hyperparameters are set correctly and the function has no strong multimodal characteristics. However, in such cases, the convergence might take longer, with less exploration around the actual global minimum.

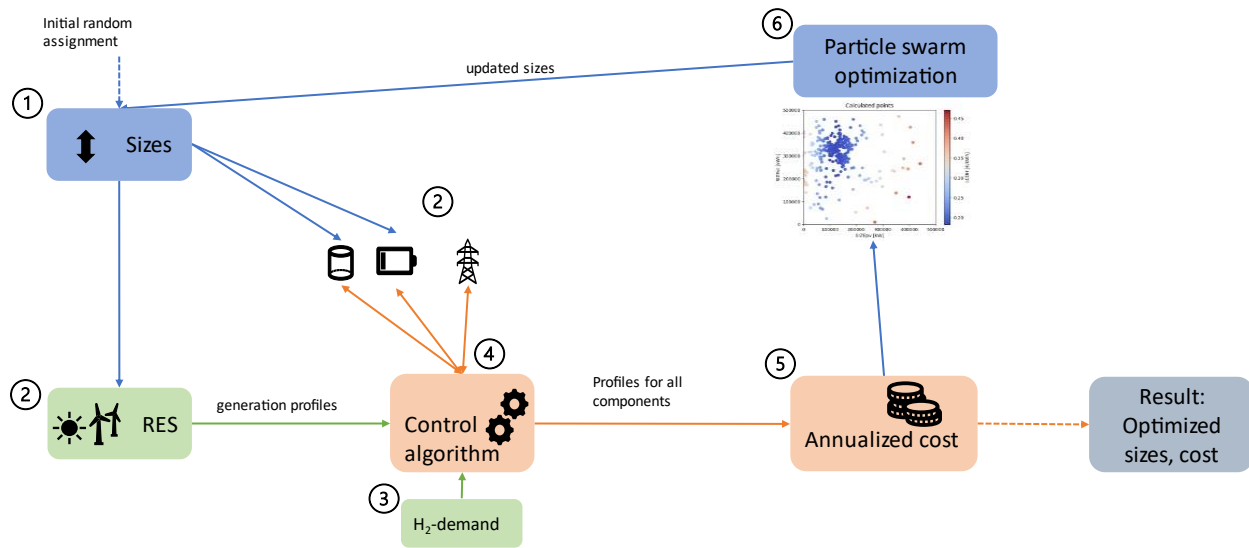


Figure 2.18: Global modelling strategy

From the component size the renewable **generation profiles are calculated** multiplying the specific generation profile with the size. This step involves the initialization of the storages with their sizes. The user demand is always the same profile and imported at this step.

Subsequently, the code utilizes the generation and determines the state of the system by running the control algorithm at every time step the control algorithm evaluates the current operational scenario, manages the charging and discharging of the storages, and records crucial operational parameters such as power balances and SOC. This iterative process continues for each time step throughout the simulated year, resulting in the creation of hourly system profiles.

The next step is to obtain the **levelized cost of hydrogen**. From the profiles the OPEX are calculated. Relevant for the operational expenditures are the grid withdrawal, the grid injection and profile of penalties in case the user demand was not entirely satisfied. Specifically, the hourly grid injection is multiplied by the corresponding hourly grid injection price, while the hourly grid withdrawal is multiplied by the hourly grid electricity price. Additionally, the hourly unmet demand profile is multiplied by the penalty rate. These multiplicative operations yield hourly cost profiles, which single cost values $cost_{tot_i}^t$ are then aggregated over the entire year.

$$OPEX_i = \sum_{t=0}^{8759} cost_{tot_i}^t \quad 2.13$$

The calculation of operational expenditures involves three components: purchased electricity, grid injection, and penalties for unmet demand. The total cost consists of both OPEX and annualized CAPEX. Capital Expenditures are obtained as described in chapter 2.2, considering the size of the particle. Finally, LCOH is calculated by dividing the sum of OPEX and annualized CAPEX by the final user demand.

Each particle is assigned a specific LCOH value, which serves as input for the Particle Swarm Algorithm. Based on the LCOH, the algorithm identifies the best position among the particles and calculates new velocities and positions (sizes) for the next iteration. With these updated positions, a new iteration begins, and the process continues until the maximum number of iterations is reached. The optimal solution corresponds to the global best position *gbest* across all particles and iterations.

The optimization algorithm and energy system model are implemented in Python using the open-source integrated development environment Spyder. Python's extensibility, versatility, and open-source nature make it a good choice for modelling energetic systems. Given the substantial volume of data involved, the pandas library provides a valuable framework for efficiently conducting the modelling process[62].

2.6 Scenario definition

The results are divided into two main parts. First in the base scenarios the main results are presented for 2023 and 2030 assumptions. Subsequently, specific cases are examined, with special focus on industrial needs involving hydrogen blending.

2.6.1 Base scenarios

In the **base scenario 2023**, the model utilizes current prices and component efficiencies as outlined in previous sections. No restrictive conditions were imposed on the size of the components, with the exemption of the PV field which is capped at a maximum of 500 MWp to prevent the installed power from reaching unrealistic levels. This limitation is necessary to avoid a situation where the installed power reaches infinity, which can be the theoretical optimum if the feed-in tariff is higher than the generation cost. In this case the additional PV power is sold to the grid operator and

generates enough revenues to compensate for its cost, lowering the LCOH. All base simulations are conducted with 25 particles and 120 iterations.

In the **base scenario 2030**, price and efficiency projections derived from the single components are used. In addition to the lower CAPEX of the components, the peak system efficiency of the electrolyzer is increased to 70 %, and the round-trip efficiency (RTE) of the LIB is set to 90 %, reflecting advances in battery technology.

Further a **sensitivity analysis** regarding **electricity prices** is conducted. As previously discussed, the electricity prices have a determining influence on the sizing. Since the grid injection at prices higher than the LCOE subsidizes heavily the LCOH, the optimizer maximizes the installed PV capacity. In this case most of the PV electricity is just injected to the grid. This study is not trying to analyze utility scale PV plants for grid injection, but the production of green hydrogen related to energy storage, this is not the scenario which should be analyzed. Therefore, the two base scenarios are conducted without considering revenue from grid injection. Nevertheless, generation revenue from grid injection is a reasonable assumption. Therefore, a sensitivity analysis is conducted with different purchase and selling prices. This is done for the 2023 as well as for the 2030 base scenario.

2.6.2 Case studies

Apart from the scenarios where the economic conditions of the system modify considerably, some sensitivity and special cases are looked at, starting from the base case. As for the industrial client a 100 % substitution is out of reach, **blending** scenarios are considered.

Most of the gas turbines currently in use are not designed for 100 % hydrogen combustion and typically can handle hydrogen blends ranging from 30 % to 60 % volume percent. To burn exclusively hydrogen, adaptations to the turbines are needed, or even full replacements, with the associated cost. Most project blending shares start with 5-10 % blending regarding the energy content. One challenge is the higher combustion temperature of hydrogen, especially for dry natural gas turbines. An alternative approach is to install a fuel cell, which can not only accommodate hydrogen but also improves overall efficiency. Moreover, the availability of green hydrogen is expected to remain limited in the coming years, and the capacity of pipelines to transport hydrogen is constrained.[33]

Furthermore, hydrogen is a versatile energy carrier and will be in high demand for the decarbonization of various industries, such as high-temperature industrial processes, aviation, and marine applications. Due to demand from these hard to abate sectors, prices will be high compared to direct renewable electricity use, while its availability will be limited. Consequently, today blending represents a convenient and more feasible scenario in many use cases. Therefore, scenarios with a fixed blending ratio of 5 %, 20 % and 50 % were investigated. For these cases the final user demand is multiplied by the blending factor.

Table 2.11: Hydrogen blending cases

	H₂ Blending (Related to HHV)	Other assumptions
Base scenario 2023	100 %	See base scenario 2023
Case 1	5 %	See base scenario 2023
Case 2	20 %	See base scenario 2023
Case 3	50 %	See base scenario 2023

Blending including PV-size constraints

Ground-mounted utility-scale PV installations require significant space, and in real-world applications, the available area is often limited. This limitation introduces a constraint to the PSO algorithm, potentially resulting in solutions that are far from theoretical economical optimum and leading to higher LCOH. The analysis of real installed 24MWp Mono-axis PV-plant in Sardegna shows a space demand of 2 ha/MWp.[63] To analyse the specific case of the industrial client a blending scenario of substituting 20 % of the energy content of hydrogen is taken as a reference. Then three cases are modelled with a maximum PV size of 2 MW, 5 MW and 10 MW.

Furthermore, it could be relevant and interesting for future work to analyse the effects of size limits on the other components. Looking at the space requirements of the other technologies also the electrolyzer with about 1000 m²/MWe has a significant space demand. Utility scale battery storages are usually containerized and require significantly less space compared to PV-plants for typical storage durations of a few hours. The space requirement for hydrogen storage depends on various factors, including storage pressure and configuration. However, considering the assumptions of a storage pressure of 30 bar and the vessels described in 2.1.4 for a storage to cover the entire user demand for a duration of less than 24 h, the space requirement is much inferior compared to the expected PV sizes. Hence, a sensitivity analysis with limited PV-size is the most relevant and is conducted in this thesis.

Table 2.12: Sensitivity analysis limited PV-size

	PV Size constraint	Blending	Other assumptions
Case 1	2 MWp	20 %	See base scenario 2023
Case 2	5 MWp	20 %	See base scenario 2023
Case 3	10 MWp	20 %	See base scenario 2023
Case 4	[-]	20 %	See base scenario 2023

Hybrid energy storage system including LIB

The results in chapter 3 indicate that the hydrogen storage is heavily favoured over the battery storage, resulting in system without battery storage. As the scope of this thesis is to investigate the possible application of hybrid energy storage, also a scenario is analysed where battery storage is present. A further motivation for this scenario is that the objective function does not consider the benefit of a renewable electricity utilization, also regarding incentives for green hydrogen which are not incorporated. The high capital costs prevent the battery from being utilized by the algorithm, meaning that changes in the modelling conditions are necessary to put a battery into place. This is achieved following approaches:

- 1) A minimum battery size is included as a constraint, which can cover the hydrogen demand of the electrolyzer for approximately 4 hours with an energy to power ratio of 4.
- 2) The electricity price from the grid is set at an extremely high price and simultaneously increasing the specific cost of the electrolyzer, that it becomes economically convenient to install a battery to reduce the grid consumption.

3. Results

In the section the results of the simulations are presented. These include the 2023 and 2030 scenarios, as well as more specific case analysis regarding blending and size constraints.

3.1 Base scenario 2023

The different scenarios are analysed with a population size of 25 particles and 120 iterations. An overview of the optimal sizes for the base scenario are given in Table 3.1. The results for the single components and the algorithm behaviour are discussed in detail in the following diagrams.

Table 3.1: Optimal sizes for the base scenario 2023

Component	Base scenario 2023
PV installed capacity [MW]	63,0
Electrolyzer [MW]	40,7
Battery Power [MW]	0
Battery Capacity [MWh]	0
Hydrogen Storage [MWh]	87,3
LCOH [€/kg _{H2}]	8,09

Figure 3.1 displays the PV size for each particle and every iteration in function of the levelized cost of hydrogen. The graph shows a conversion of the particle to an optimum of 63,0 MWp. Generally, a slow and steady conversion rate is observed, resulting in a broad exploration of the search space during the first iterations. Due to the decreasing inertia factor, as discussed in chapter 2.4.2, the fine search is fostered for the last iteration. The multidimensional nature of the problem causes some outliers with high costs, even within the optimal PV size range. It is important to note that an optimal PV size doesn't always guarantee an efficient solution. This is because each particle is characterized by sizes for all components, not just the photovoltaic power. As a result, some inefficient solutions may occur, such as having a very small electrolyzer size, which means that a significant portion of the PV electricity cannot be converted into hydrogen, ultimately failing to meet the final user demand.

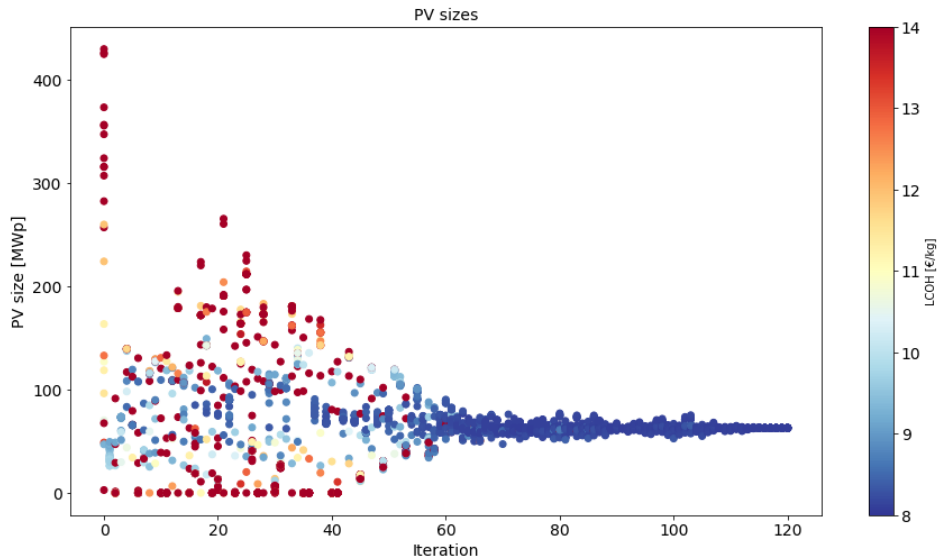


Figure 3.1: LCOH and PV sizes of all particles for every iteration

Similar to the optimization process for PV sizing, the exploration of electrolyzer sizes begins with a broad search, showing lower conversion progress until the 40th iteration. Subsequently, a rapid convergence is observed, leading to an optimal size of 40,6 MWe.

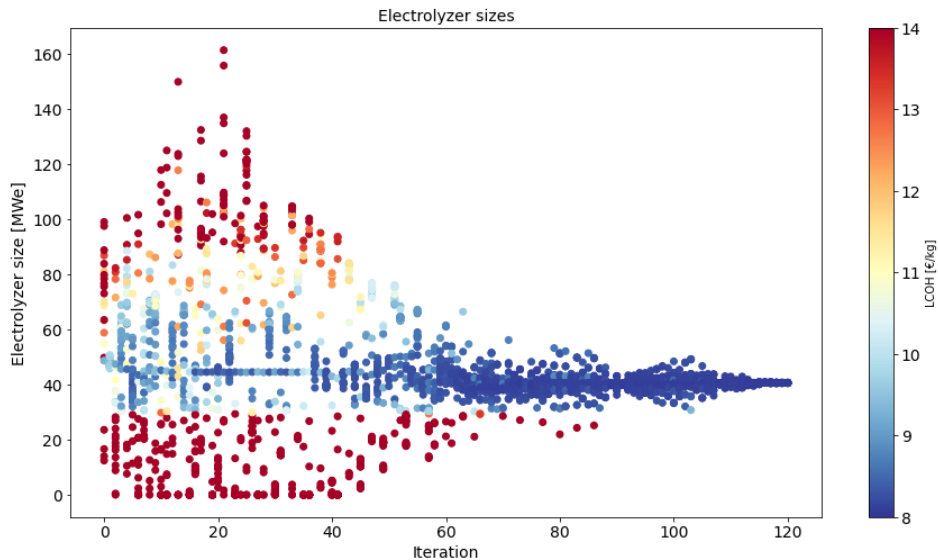


Figure 3.2: LCOH and Electrolyzer sizes of all particles for every iteration

The optimization of the battery storage capacity clearly shows that battery storage is economically not convenient and immediately avoided by the algorithm. After the 4th iteration all particles set the battery capacity to 0 MWh. This outcome is attributed to the substantial capital cost associated

with battery storage, which cannot be offset by reductions in the cost of acquired electricity. The economics of the battery storage are discussed in chapter 3.3.3.

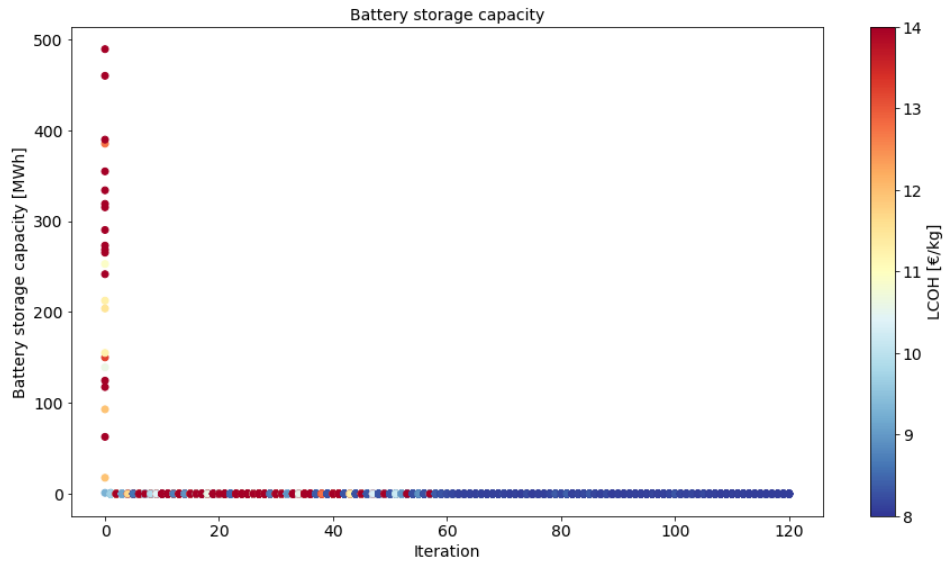


Figure 3.3: LCOH and Battery capacity of all particles for every iteration

Similar to the battery storage capacity, the optimization of storage power capacity also indicates an optimal value of 0 MW. However, it requires a longer time to reach this optimum compared to battery capacity. For all the iterations after the 4th, no benefit for a higher installed power is obtained as the installed capacity is 0 MW for all particles. Nevertheless, it takes the algorithm approximately 60 iterations to converge to the optimal size. The extended convergence period can be attributed to the lower importance of the power cost, which are less restrictive compared to energy related costs. This means that the algorithm does not experience a strong push towards lower installed power. It is worth noting that the initial particle sizes range from 0 to 100 MW for power capacity, whereas they extend from 0 to 500 MWh for battery capacity, resulting in a much higher importance of the battery capacity cost.

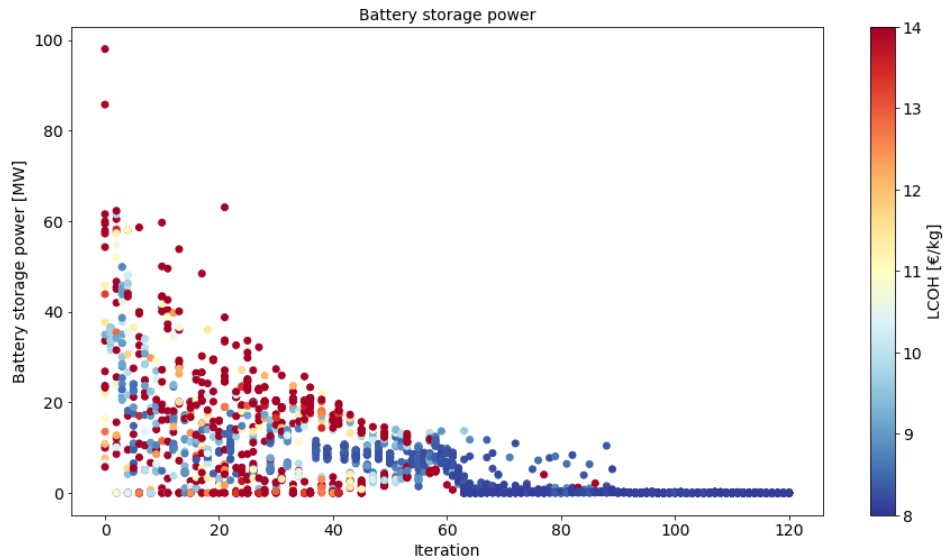


Figure 3.4: LCOH and Battery power of all particles for every iteration

The hydrogen storage capacity is initialized with sizes between 0 and 1.000 MWh. The algorithm even explores a broader range of sizes until 2.000 MWh in the beginning. Later a continuously converging behavior can be observed with an optimal size of 87,4 MWh of hydrogen, related to the HHV. This storage capacity equates to a storage solution capable of meeting the user's demand for a continuous 5-hour period.

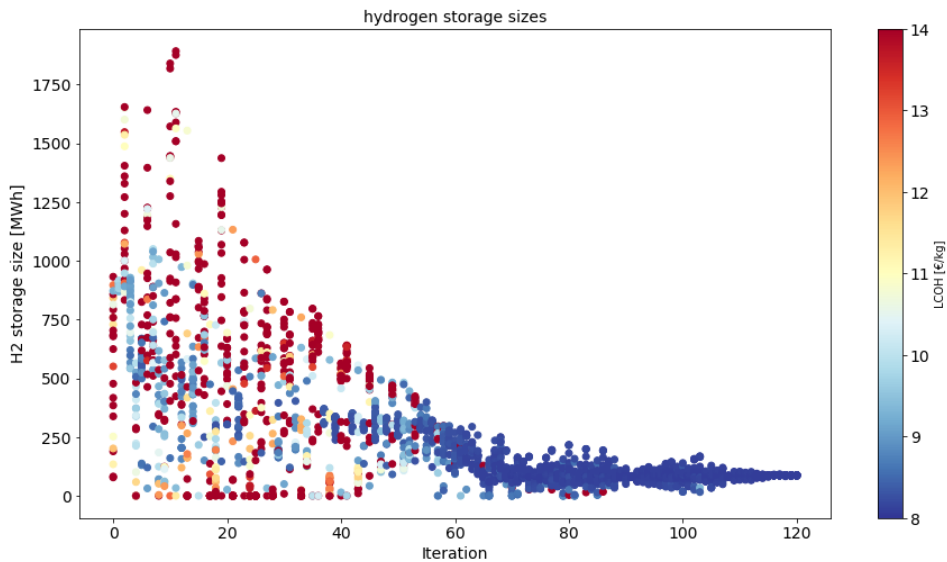


Figure 3.5: LCOH and hydrogen storage sizes of all particles for every iteration

In Figure 3.6 the best values regarding the LCOH are shown for each iteration. In the beginning a strong improvement of the solution can be observed, while the fine search during the last iterations has a lower impact on the final result.

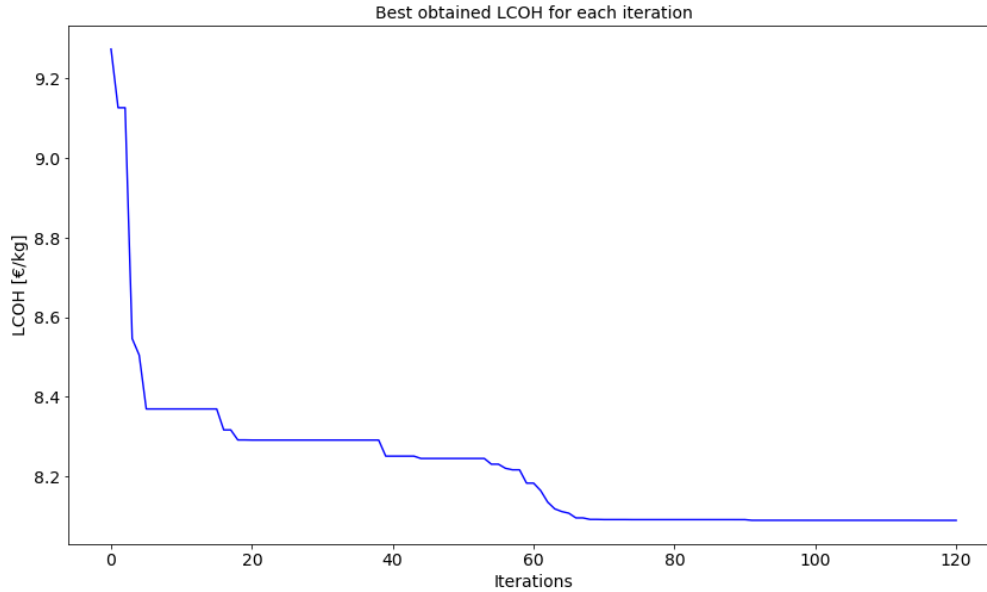


Figure 3.6: Development of the best global LCOH in function of the iteration

An analysis of the annualized cost for the optimal configuration in the base scenario reveals that the majority of the cost is attributed to purchased electricity. As the grid injection price is 0 €/MWh, no revenue is generated. The annualized PV costs are comparatively moderate because there is no incentive to install a larger PV capacity with increased grid injection. A small penalty is assigned for hours when the user demand is not satisfied. This occurs during two demand peaks in the user profile, one in autumn and the other in spring, each lasting for one hour. The algorithm accepts these two hours of penalty instead of significantly increasing the sizes of the electrolyzer or storage. In this scenario, Li-Ion battery storage is not economically viable, so only hydrogen storage is utilized. The hydrogen storage costs are not significant, partly due to the relatively low capital cost of hydrogen storage and the absence of the need for additional compressors. Additionally, the moderate share of PV generation does not justify the installation of large hydrogen storage volumes.

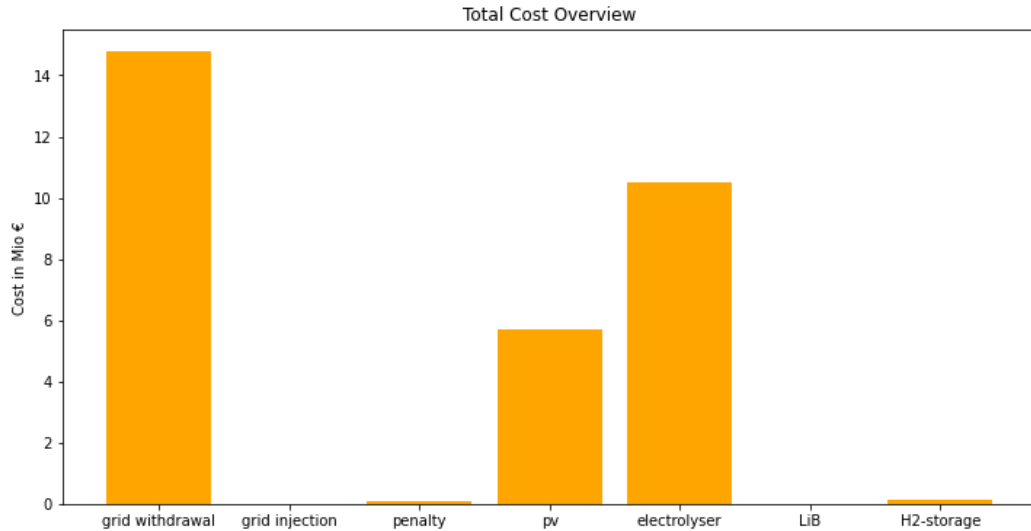


Figure 3.7: Overview on the total cost of the optimal solution of base scenario 2023

The analysis of the energy balance reveals that 50.4 % of the electricity input is sourced from the PV plant. A small part of the PV production is injected into the grid. This happens primarily when the hydrogen storage is fully charged and especially during two weeks in august when the client has no demand for hydrogen. Additionally, during peak hours, the PV production can surpass the electrolyzer nominal power, meaning that grid injection is necessary. The electrolyzer has an average efficiency of 65,5 % based on the HHV. Most of the produced hydrogen is directly consumed by the industrial client, while 8,8 % is stored in the hydrogen storage.

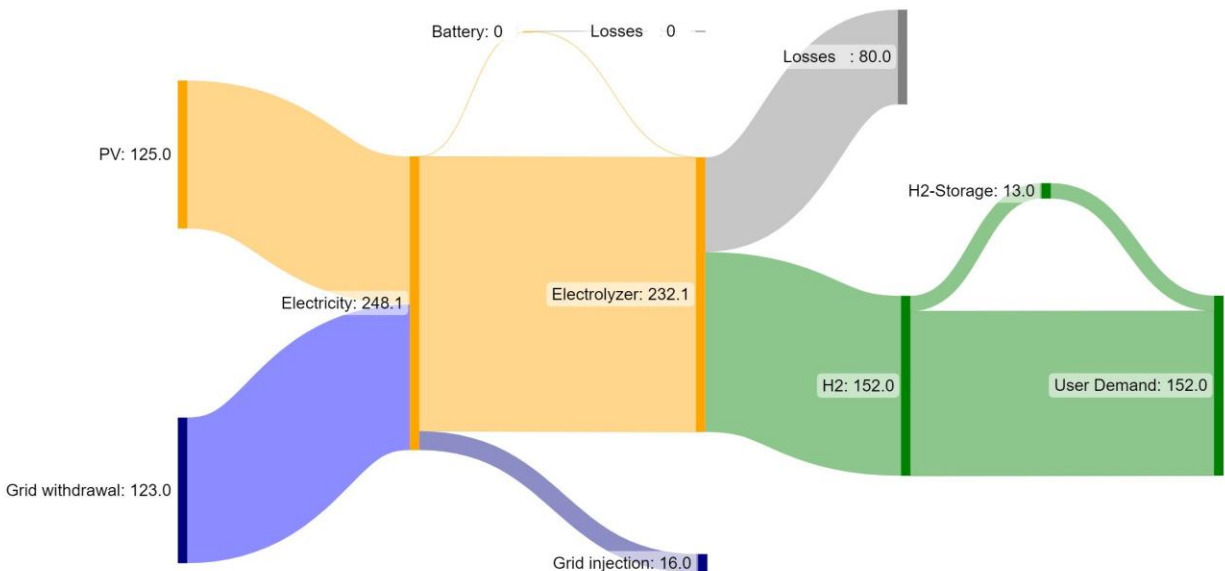


Figure 3.8: Sankey diagram of the energy flows in the optimal solution of base scenario 2023 [GWh] [64]

Examining the system's operation, two typical weeks are analyzed: one in early January and the other in July. These weeks offer insights into how varying levels of solar radiation impact system performance. In winter, there are instances where solar radiation exceeds demand, but only for a

few hours under favorable weather conditions. Grid injection of surplus electricity is infrequent but occurs on two days when PV production briefly surpasses the electrolyzer's nominal power. Notably, during off-peak hours, most of the electricity demand is covered by supply from the electrical grid.

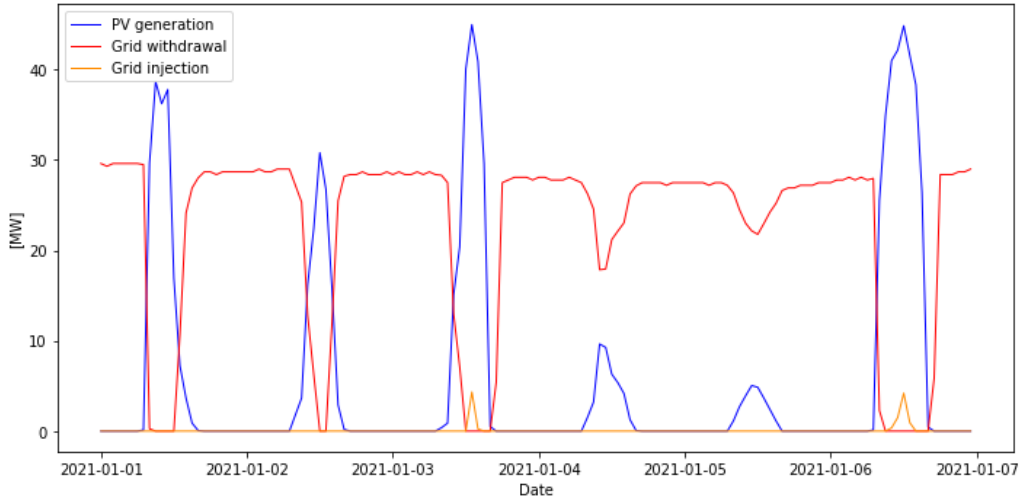


Figure 3.9: PV production, grid injection and grid withdrawal, week in January

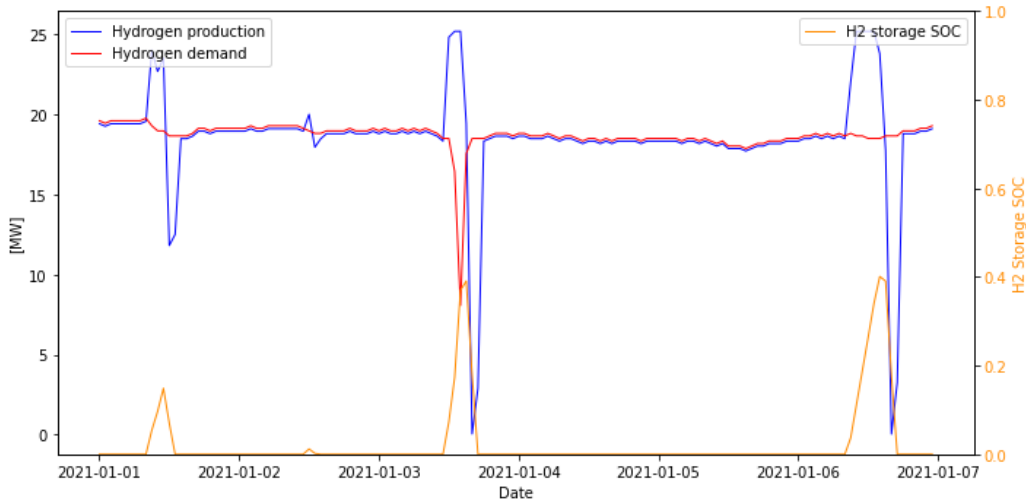


Figure 3.10: Hydrogen demand, production and storage, week in January

Looking at the hydrogen side in Figure 3.10, most of the time production follows the demand. Only when PV generation exceeds demand does the electrolyzer produce excess hydrogen, which is then stored for use when solar production decreases. This means that the electrolyzer operates at around 70% of its nominal hydrogen output for the majority of hours.

During a typical July week, the PV production is significantly higher and stretches over more hours of the day, further supported by the monoaxial tracking system. The grid withdrawal during this time is mostly limited to the later part of the night when the hydrogen storage is already empty.

The grid injection is still limited, as it is not associated to revenue, and the optimization algorithm has no incentive to increase this share.

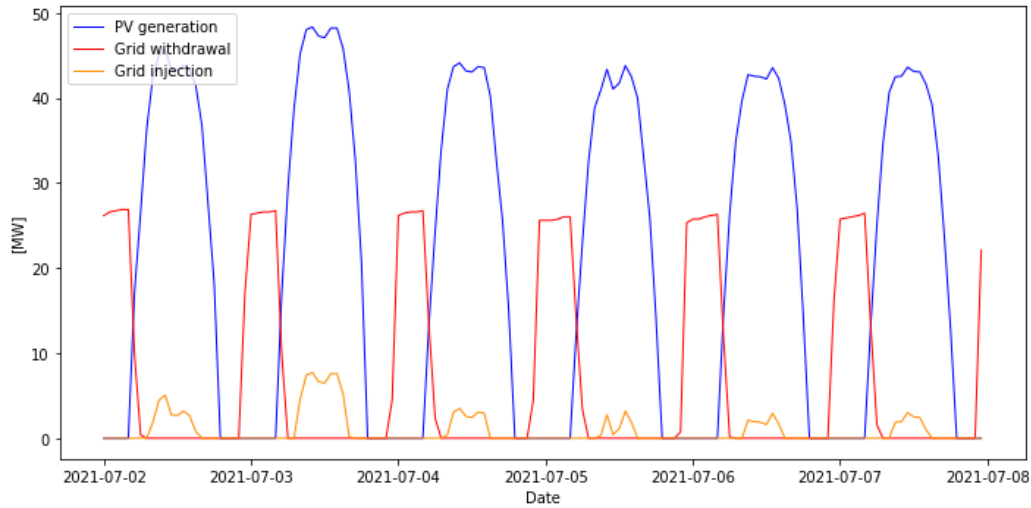


Figure 3.11: PV production, grid injection and grid withdrawal, week in July

During summer, hydrogen production deviates more from the demand profile. The system tends to produce excess hydrogen during peak sun hours, while in the evening hours, the stored hydrogen is used to cover the demand. When the hydrogen storage is discharged, the electrolyzer production drops until the storage cannot cover the demand.

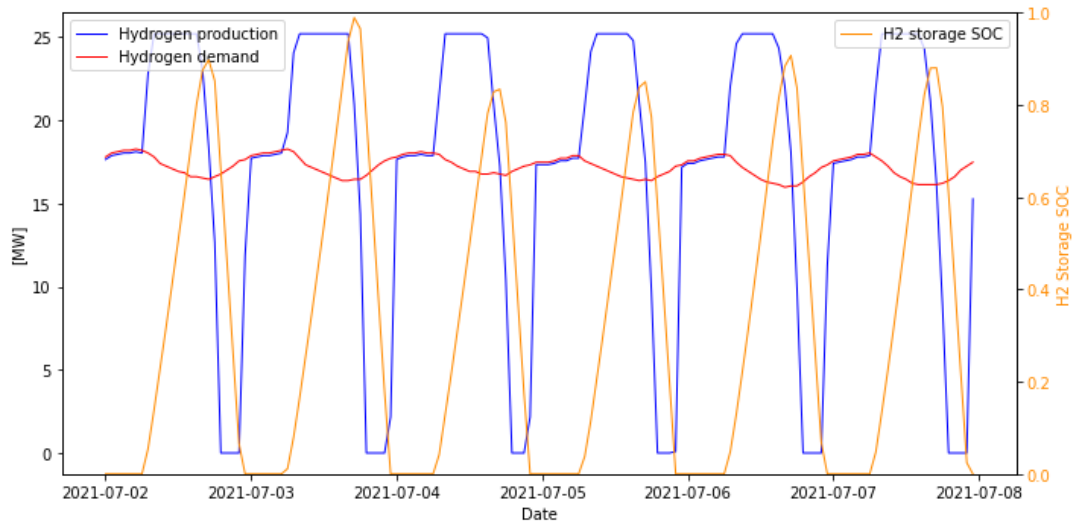


Figure 3.12: Hydrogen demand, production and storage, week in July

To achieve high system efficiency, it is important to operate the electrolyzer within the correct power range. Figure 3.13 illustrates the operational characteristics of the electrolyzer, with hourly operational powers arranged by size. Since the electrolyzer is of the PEM type, it performs well even in part-load conditions and exhibits good dynamic characteristics. The electrolyzer is in operation for more than 7.500 hours a year, resulting in 5.700 full load hours. This load

characteristic leads to a high overall efficiency and only 115 hours with a system efficiency of less than 40 %.

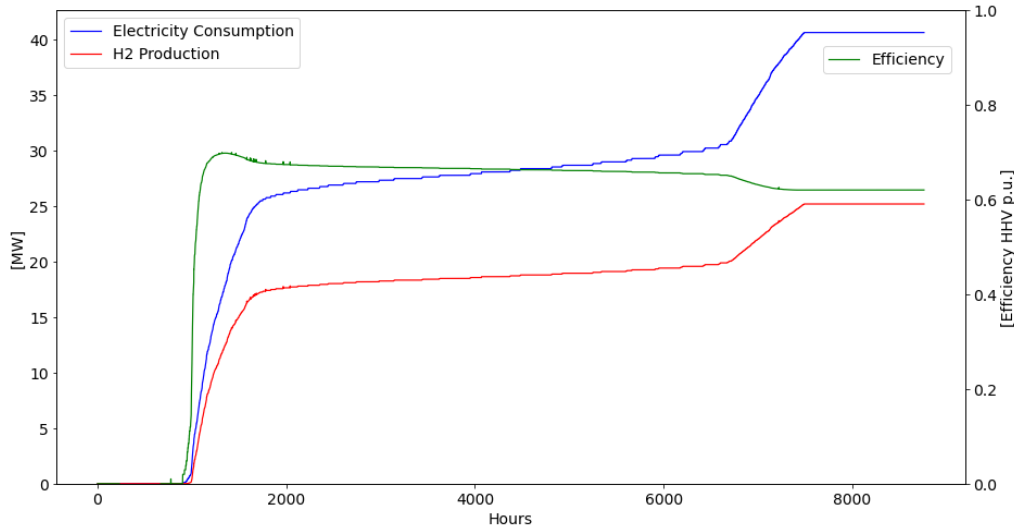


Figure 3.13: Electrolyzer operation profile, ordered by size

Additionally, the impact of changes in energy prices after installation is examined. Figure 3.14 displays the levelized cost of hydrogen using the fixed set of sizes determined in the base scenario for 2023. As expected, a higher grid injection price and a lower withdrawal price have a favorable effect on achieving lower costs. The influence of these two electricity prices is remarkably significant. Notably, the sensitivity regarding the grid injection price is lower than the sensitivity to the acquisition price, as more electricity is withdrawn than injected from the grid. The cases in the upper left part of the diagram are very unlikely to occur, as the acquisition price is typically higher than the selling price.

From this sensitivity analysis a realistic case can be analyzed, including remunerative grid feed-in without distorting the PV sizes. A realistic case could be grid injection remuneration at the zonal price of around 100 €/MWh. For the electricity purchased the base assumption of 120 €/MWh is kept. For this set of prices, a LCOH of 7,68 €/kg_{H2} is obtained, a reduction of 5 % compared to the base scenario 2023.

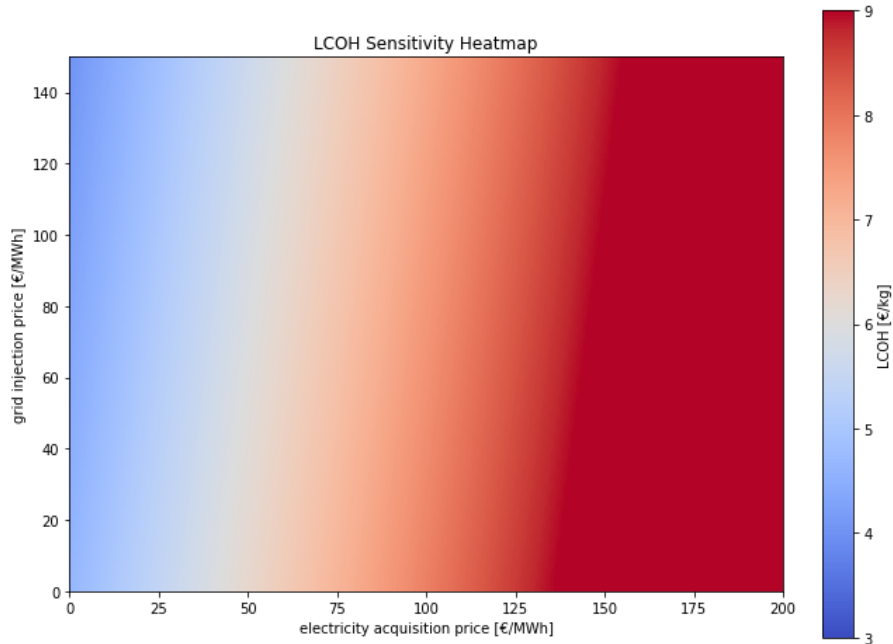


Figure 3.14: Sensitivity analysis electricity price of base scenario 2023

The following chapters deal with an optimization case of other input electricity prices, meaning that the system sizes are not fixed as in the figure above.

3.1.1 Sensitivity analysis electricity acquisition prices

Selecting the electricity acquisition price is nontrivial, as discussed in chapter 2.1.6, and has a large influence on component sizing and LCOH. In contrast to the previous sensitivity analysis, where component sizes were fixed, here the sizes of the components are optimized for different price assumptions. The analysis clearly demonstrates that an increase in electricity price makes it more advantageous to increase the share of solar energy and reduce purchased electricity. For instance, when the electricity price is increased from 120 to 150 €/MWh, the LCOH augments by 11 %, while the PV and hydrogen storage capacity increase by 30 % and 71 % respectively. This achieves a rise in the share of self-produced PV electricity from 50 % to 63 %. Even at a grid withdrawal price of 300 €/MWh, it is more cost-effective to increase the sizes of other components rather than including a battery storage.

Table 3.2: Sensitivity analysis of the optimal component sizes for different electricity acquisition prices 2023

Component	Electricity acquisition 100 €/MWh	Base scenario 2023 120 €/MWh	Electricity acquisition 150 €/MWh	Electricity acquisition 300 €/MWh
PV installed capacity [MW]	55,9	63,0	81,7	132,5
Electrolyzer [MW]	37,3	40,7	48,8	69,9
Battery Power [MW]	0	0	0	0
Battery Capacity [MWh]	0	0	0	0
Hydrogen Storage [MWh]	60,4	87,3	149,5	439,8
LCOH [€/kg _{H2}]	7,42	8,09	8,94	11,42

As expected, a higher electricity acquisition price causes an increase in the LCOH. This is driven by the need for larger PV capacity, electrolyzer, and hydrogen storage sizes to offset the higher cost of grid withdrawal. The detailed cost breakdown is illustrated in the following figure. The analysis clearly indicates that a higher electricity acquisition price results in a shift towards more significant investments in components to increase the proportion of hydrogen produced from PV electricity. It is notable that the total costs for grid supply are the lowest in the 300 €/MWh scenario, because of the drastic decline in electricity withdrawn from the grid.

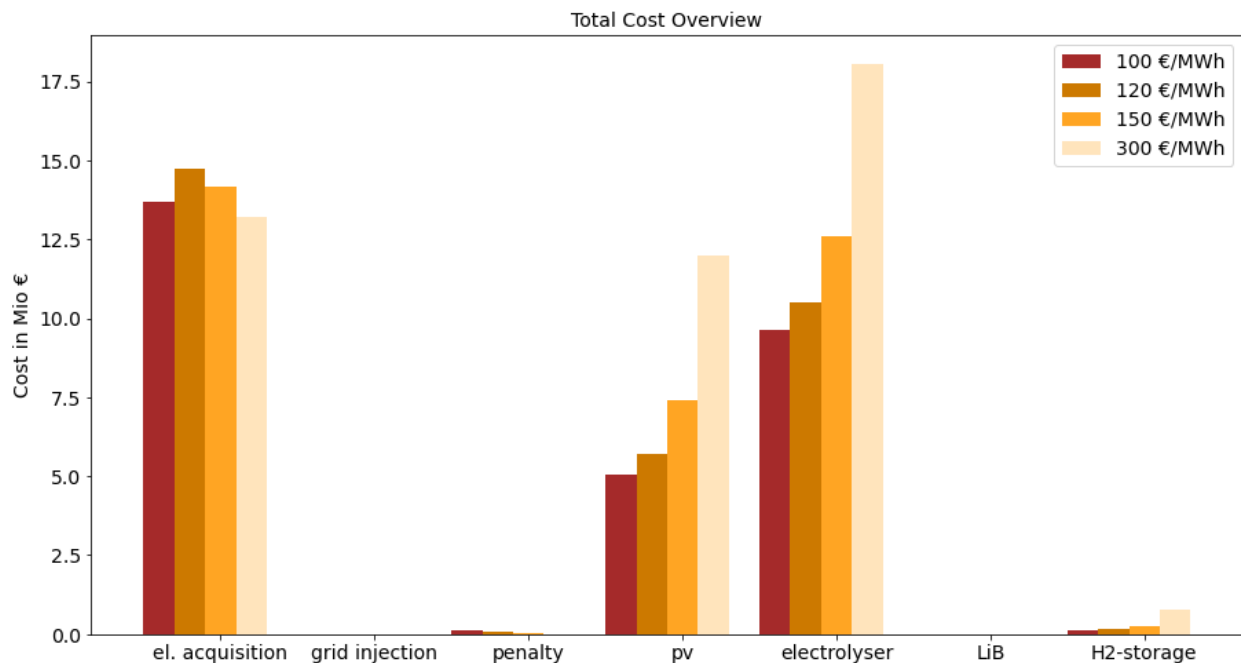


Figure 3.15: Cost overview of simulations with different electricity acquisition prices 2023

3.1.2 Sensitivity analysis electricity injection prices

The previous cases show the large influence of the electricity purchase. However, none of the simulations considers remunerative grid feed in. In this chapter the purchase price is fixed at 120 €/MWh as of the base scenario 2023, while the specific grid feed-in revenue is varied. The results show and motivate the base scenario setting, avoiding distortions caused by PV subsidization effect.

Table 3.3: Sensitivity analysis of the optimal component sizes for different grid injection prices 2023

Component	Base scenario 2023: 0 €/MWh	Grid injection 30 €/MWh	Grid injection 50 €/MWh
PV installed capacity [MW]	63,0	86,3	500,0
Electrolyzer [MW]	40,7	40,9	42,4
Battery Power [MW]	0	0	0
Battery Capacity [MWh]	0	0	0
Hydrogen Storage [MWh]	87,3	97,8	127,9
LCOH [€/kg _{H2}]	8,09	7,89	6,36

The introduction of a remuneration for grid injection changes drastically the optimal results. And especially the PV capacity. It is notable that for the 50 €/MWh grid injection price the electrolyzer capacity remains almost the same, meaning that PV production during peak hours surpasses the electrolyzer nominal power by a factor of more than 10. All this excess electricity is injected into the grid. As a result, the algorithm indirectly maximizes the share of electricity injected to the grid and not the share of self-consumption. The cost overview in Figure 3.16 shows how the 50 €/MWh grid injection profoundly shifts the cost structure and offsets a large portion of the costs with revenue generated from the grid.

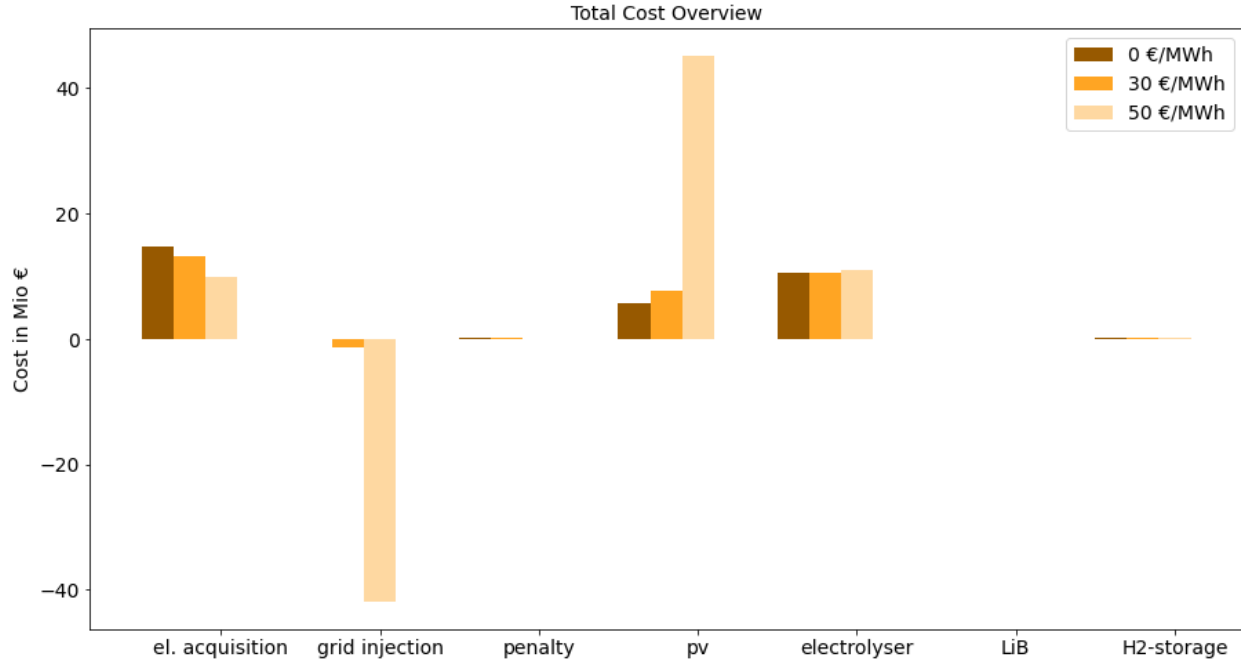


Figure 3.16: Cost overview of different electricity acquisition prices 2023

3.2 Base scenario 2030

In the 2030 scenario, cost and efficiencies are updated as described in component description chapter 2.1. Generally, the specific component costs are reduced compared to the 2023 base scenario, especially for the electrolyzer, battery storage and photovoltaic plant. The lower PV cost widens the gap between LCOE and grid withdrawal, making it more advantageous to increase solar electricity production. To convert this excess electricity, the system increases the electrolyzer size, which is further facilitated by the significantly lower electrolyzer cost. Even if the specific hydrogen storage cost does not change, the hydrogen storage size increases substantially and allows to satisfy approximately 13 h of the industrial user’s hydrogen demand. Overall, a cost reduction of 34 % is obtained, compared to 2023.

Component	Base scenario 2023	Base scenario 2030
PV installed capacity [MW]	63,0	93,8
Electrolyzer [MW]	40,7	59,0
Battery Power [MW]	0	0
Battery Capacity [MWh]	0	0
Hydrogen Storage [MWh]	87,3	237,7
LCOH [€/kg _{H2}]	8,09	5,32

Figure 3.17: Optimal component sizes for the base scenario 2023 and 2030

The analysis of the energy balances in Figure 3.18 shows that the share of solar energy on the total input increases from 50.4% in the 2023 scenario to 74.4% in 2030. Due to the increased electrolyzer efficiency there are fewer losses. Furthermore, the amount of hydrogen passing through the storage increases from 13 to 45 GWh per year, indicating that the utilization rate of the storage also rises to the equivalent of 187 full charge/discharge cycles.

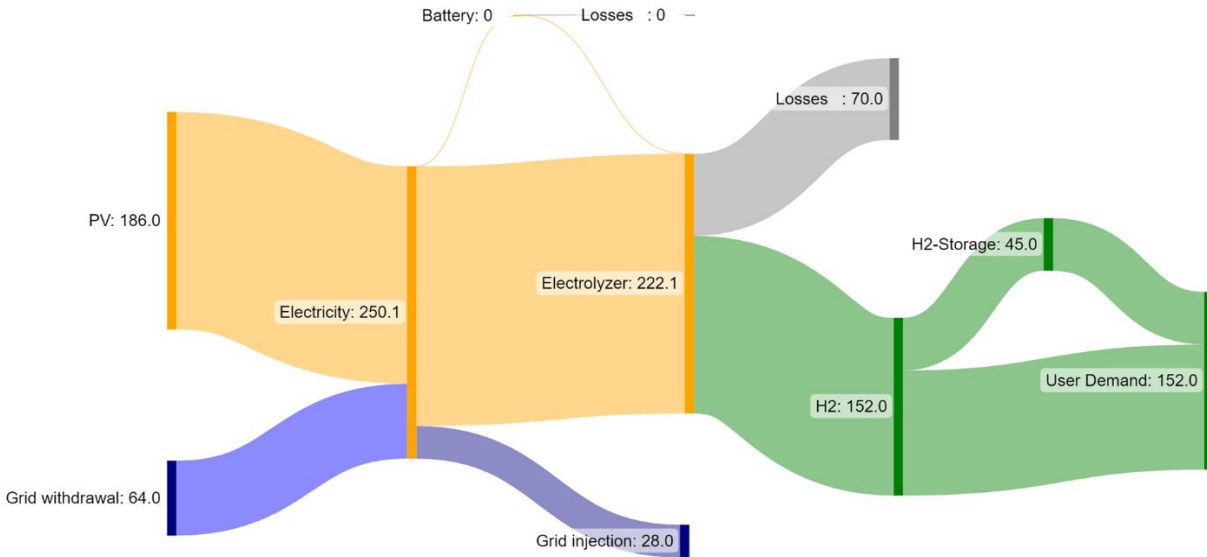


Figure 3.18: Sankey diagram of the energy flows in the optimal solution of base scenario 2030 [GWh] [62]

Like for the 2023 scenario a sensitivity analysis for changing electricity prices for a fixed set of sizes is conducted. Compared to 2023 the LCOH is significantly lower. Due to an increase in grid injection and decrease in prevailed electricity, the importance of the grid injection price is more significant, which results in the lines of same LCOH and consequently same color to turn clockwise in Figure 3.19 compared to the 2023 analysis. Again, the upper left triangle is very unlikely to occur, as the acquisition price is typically higher than the selling price.

From this sensitivity analysis also a more realistic case can be analyzed, without the distorting effect of grid injection revenue on the PV sizes. In this scenario, a grid injection remuneration of approximately 60 €/MWh in 2030 is considered, as the zonal price during hours of high PV production is expected to decrease. The electricity purchase price remains at the base assumption of 120 €/MWh, as the price is significantly higher during the night. Under these pricing conditions, a LCOH of 4.88 €/kgH₂ is achieved, representing an 8 % reduction compared to the base scenario 2030.

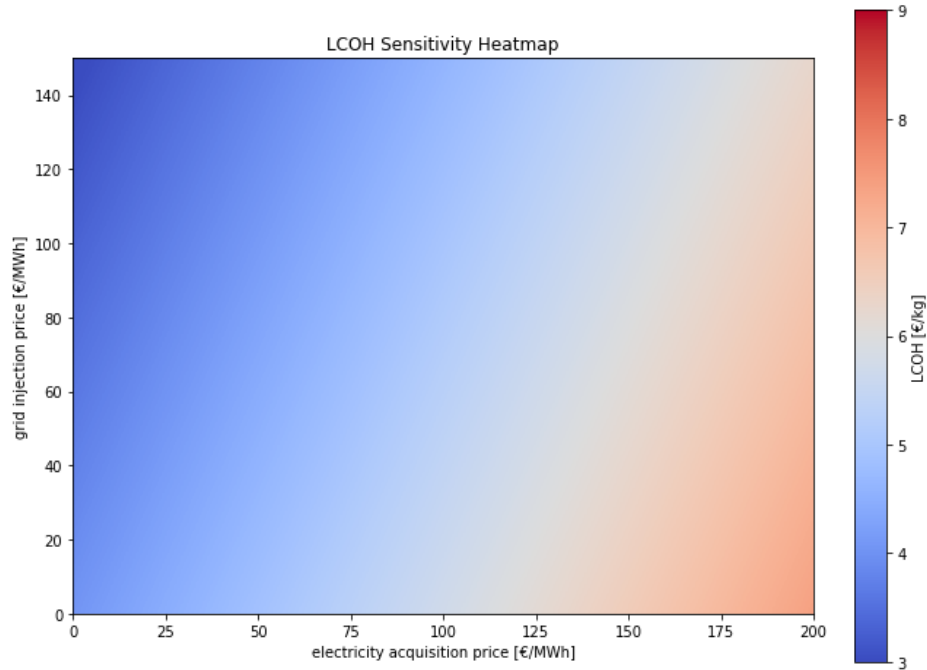


Figure 3.19: Sensitivity analysis electricity price base scenario 2030

3.2.1 Sensitivity analysis electricity acquisition prices

In reference to chapter 3.1.1, a sensitivity analysis is conducted for various assumptions regarding electricity prices with the component sizes not being fixed. The analysis clearly shows that increasing the electricity price, moves the optimal configuration to larger PV sizes, with a higher share of self-produced electricity and larger hydrogen storages. Interestingly, the battery is still not preferred by the optimizer, which instead tends to increase the sizes of other components in response to changing electricity prices.

Table 3.4: Sensitivity analysis of the optimal component sizes for different electricity acquisition prices 2030

Component	Electricity acquisition 100 €/MWh	Future scenario 2030: 120€/MWh	Electricity acquisition 150 €/MWh	Electricity acquisition 300 €/MWh
PV installed capacity [MW]	86,3	93,8	108,3	155,3
Electrolyzer [MW]	55,1	59,0	66,8	88,9
Battery Power [MW]	0	0	0	0
Battery Capacity [MWh]	0	0	0	0
Hydrogen Storage [MWh]	196,3	237,7	311,0	517,9
LCOH [€/kg _{H2}]	4,97	5,32	5,77	7.15

To analyse how the differences in LCOH occur, the costs of each simulation are split into the single contributions. Surprisingly, a higher electricity acquisition price does not lead to higher expenses for electricity. Instead, it drives the PSO algorithm to select solutions with larger PV production and storage capacity, which significantly reduces grid withdrawal. This reduction in grid withdrawal, however, comes at the cost of a larger photovoltaic plant and electrolyzer, both of which operate more frequently in part-load conditions and achieve fewer equivalent full load operation hours. Even for the highest analysed electricity price, with a resulting hydrogen storage capacity sufficient to cover approximately 29 hours of average user demand, the cost contribution of the hydrogen storage remains below 5 % of the total cost.

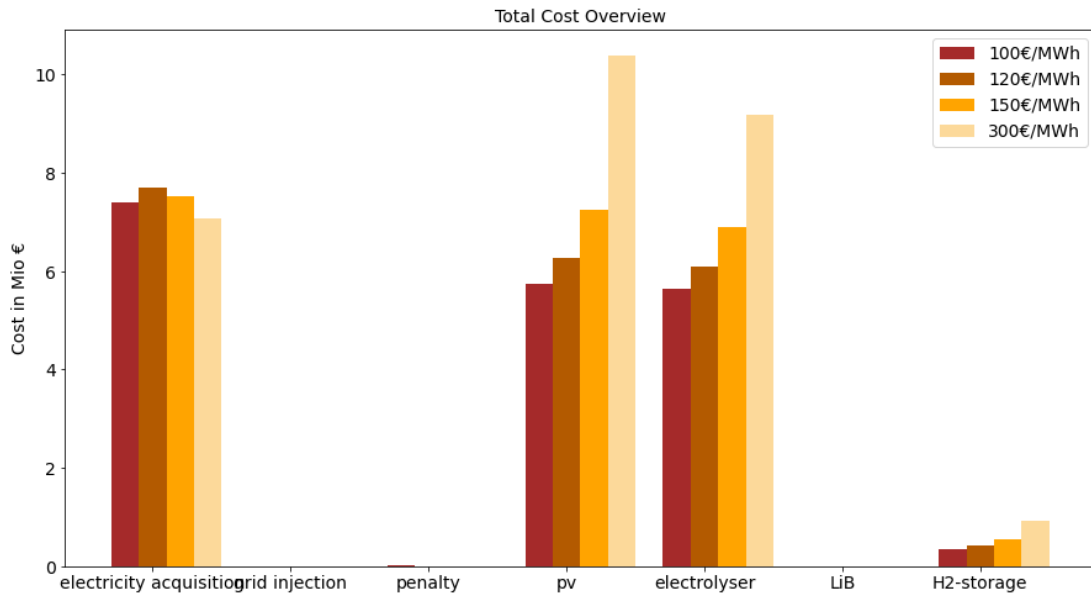


Figure 3.20: Cost overview of different electricity acquisition prices 2030

3.2.2 Sensitivity analysis electricity injection prices

As for the base scenario 2023, different revenues from grid injection are considered, with an initial electricity acquisition price of 120 €/MWh. Compared to 2023 the LCOE of solar energy drops considerably, meaning that even a low grid injection price has a large impact on the optimization and subsidizes the green hydrogen production. This effect pushes the optimizer to select a large PV capacity, leading to a substantial injection of surplus electricity into the grid. This outcome is evident in Table 3.5.

Table 3.5: Sensitivity analysis of the optimal component sizes for different grid injection prices 2030

Component	Future scenario 2030: 0 €/MWh	Grid injection 30 €/MWh	Grid injection 50 €/MWh
PV installed capacity [MW]	93,8	192,0	500,0
Electrolyzer [MW]	59,0	61,3	58,4
Battery Power [MW]	0	0	0
Battery Capacity [MWh]	0	0	0
Hydrogen Storage [MWh]	237,7	239,0	229,1
LCOH [€/kgH ₂]	5,32	4,80	1,05

The optimal sizes of the hydrogen storage and electrolyzer remain relatively stable with varying grid injection prices. However, there is a notable impact on the PV capacity. Even with a grid injection remuneration of 50 €/MWh, the PSO algorithm maximizes the PV sizes, generating substantial revenue that offsets other costs. As the optimal storage size does not increase for a higher grid remuneration, the grid withdrawal does not change considerably between the 30 and 50 €/MWh case. The increased PV capacity is mostly used for grid injection and not to increase PV-self consumption. This undesired effect again underscores the decision to assume no remuneration for grid injection in the base scenarios.

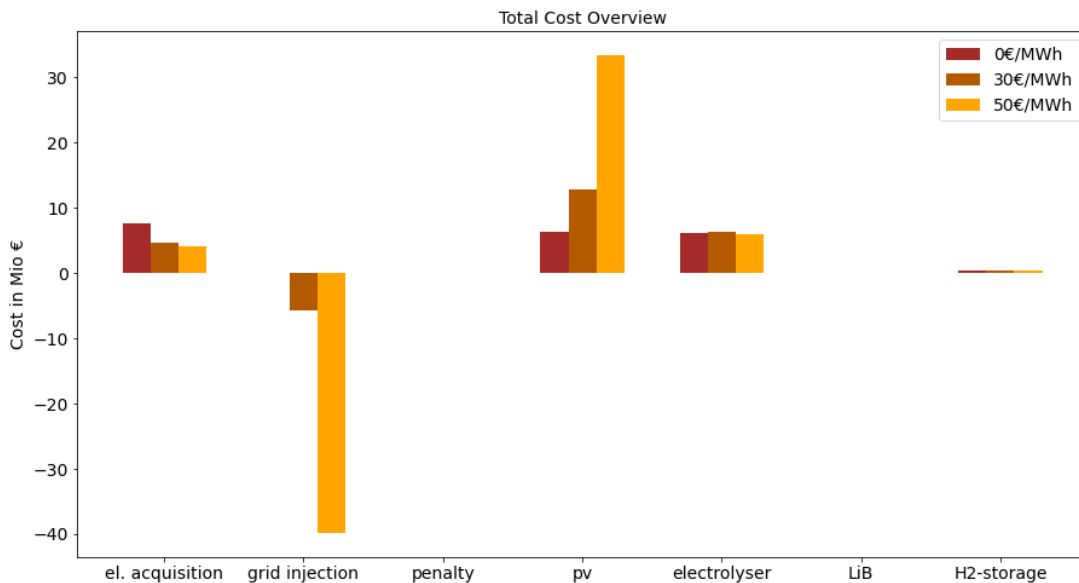


Figure 3.21: Cost overview of simulations with different grid injection prices 2030

3.3 Case studies

Starting from the base scenario 2023 different cases with a focus on industrial practicability are analysed. These involve hydrogen blending, constraints regarding the PV size and cases where a battery is present to analyse a hybrid storage configuration.

3.3.1 Blending without constraints

The table below summarizes three hydrogen blending cases. The sizes are obtained using an electricity acquisition price of 120 €/MWh and a selling price of 0 €/MWh, as in the base scenarios. In general, the sizes of the components scale with the blending factor, which aligns with the expected results. In the component cost and efficiency calculations, no size restrictions were imposed, and therefore, the blending share modelled in this thesis does not impact the system's operation. However, in reality, not all component sizes are commercially available, and some components even come in containerized forms. For a small blend the relative differences of available sizes and the optimal solution in the continuous search space can become significant, altering slightly the operation and LCOH.

Table 3.6: Case analysis H₂-blending, no size constraints on components

Component	100 % H ₂ supply	50 % H ₂ Blending	20 % H ₂ Blending	5 % H ₂ Blending
PV installed capacity [MW]	63,0	31,5	12,6	3,1
Electrolyzer [MW]	40,7	20,3	8,1	2,0
Battery Power [MW]	0	0	0	0
Battery Capacity [MWh]	0	0	0	0
Hydrogen Storage [MWh]	87,3	43,7	17,5	4,2
LCOH [€/kgH ₂]	8,09	8,09	8,09	8,09

3.3.2 Blending and area constraints

Following the request of the industrial client, the available area is limited. Hence different constraints are imposed on the maximum installable PV-size at 2, 5 and 10 MWp for a blending scenario of 20 % hydrogen. An overview of the optimal sizes obtained is given in Table 3.7. It is evident that limiting the PV size increases the LCOH, as more electricity has to be taken from the grid, which is at a cost higher than the LCOE of self-produced PV electricity. In all cases with constrained PV sizes, the algorithm identifies the optimal PV size directly at the size limit. The optimal hydrogen storage size depends strongly on the PV size, as it allows to storage excess solar production which is not present enough in the 2 MWp and 5 MWp cases. The electrolyzer capacity also shows a slight dependence on the installed photovoltaic power, allowing for the conversion of more solar energy into hydrogen with larger PV capacity.

Table 3.7: Case analysis 20 % H₂-blending, limited PV-size

Component	2 MWp	5 MWp	10 MWp	No PV limit
PV installed capacity [MW]	2	5	10	12,7
Electrolyzer [MW]	7,4	7,4	7,5	8,1
Battery Power [MW]	0	0	0	0
Battery Capacity [MWh]	0	0	0	0
Hydrogen Storage [MWh]	0	0	11,1	17,5
LCOH [€/kgH ₂]	9.42	8,91	8,19	8,09

An overview of the cost is given in Figure 3.22. There is a clear tradeoff between PV cost and the cost of electricity purchased from the grid. For all the constraint cases, the cost reduction achieved by installing a smaller PV plant is more than offset by the increased expenses for grid electricity. All the shown cases do not consider feed in remuneration. If feed-in is economically compensated, installing a larger PV plant is even more incentivized. The electrolyzer cost does not significantly decrease with stricter PV size constraints. The cost of the hydrogen storage is almost negligible, allowing an autonomy of only 3 hours in the 10 MW case. For smaller PV-plants the surplus production during peak times is not enough to provide an investment case to install battery storage. In general, installing a higher photovoltaic capacity reduces the importance of grid supply and decreases dependency on electricity prices.

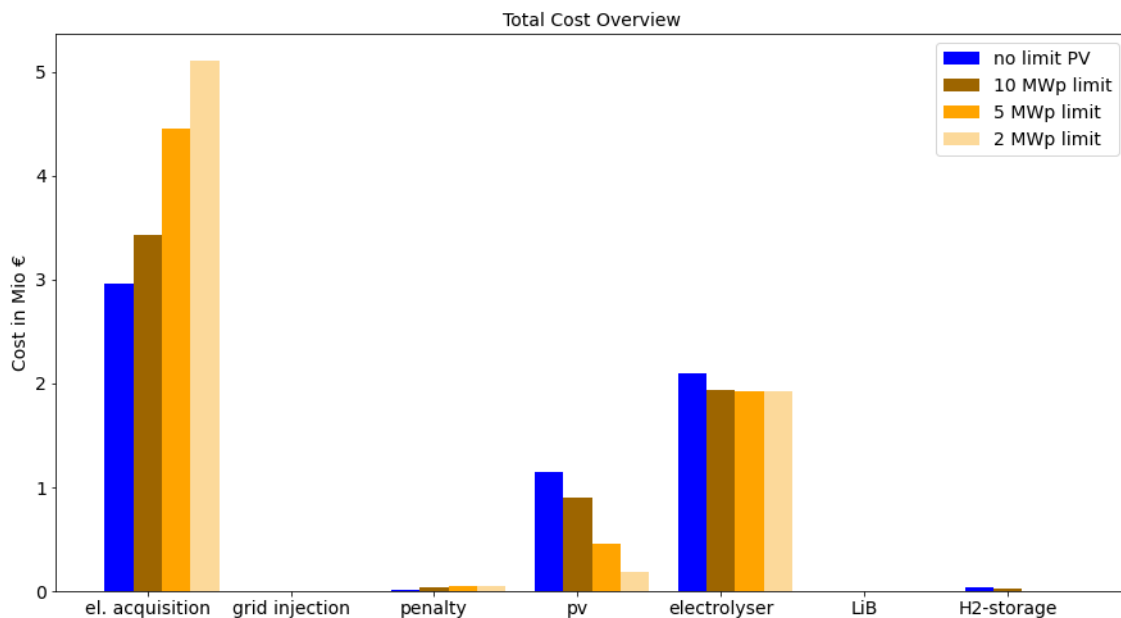


Figure 3.22: Cost overview for different PV constraints

Further the total area for these cases is calculated. As discussed in chapter 2.1.2, the required area for a utility scale PV plant with monoaxial tracker is approximately 20.000 m²/MWp considering the additional components needed for the plant. Electrolyzers are typically containerized, and 1 MW usually fits in a 40-foot container.[65] Additionally, there is the need for other components, connections, and spaces around the container, resulting in a space requirement of approximately 1.000 m²/MWe. For the hydrogen storage the largest vertical vessel for 30 bar storage found in the catalog is used, having a diameter of 4,5 m it can store 490 kg of hydrogen[40]. Further minimum distances to the other vessel for operation, maintainability, construction, and safety have to be considered. Taking this into account it is hypothesized that one vessel can be placed every 200 m².

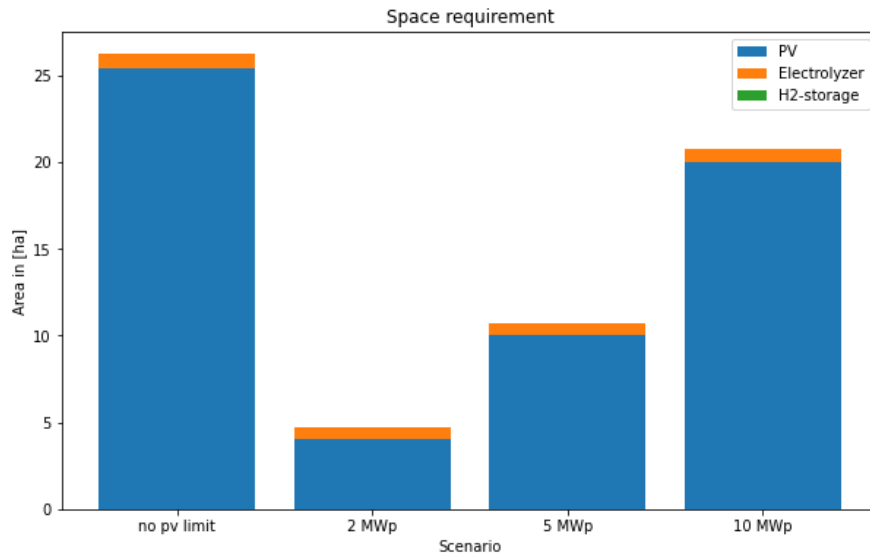


Figure 3.23: Analysis on the required area for the different PV-constraints

The analysis of space requirements highlights the dominance of photovoltaic space requirements over other contributions. The analysis reveals that the required area for the PV plant can be a significant constraint for an industrial user with a high energy demand, trying to produce its own green hydrogen even for a blending share of only 20 %. The electrolyzer space needs are much more manageable and do not pose a significant constraint, confirming that the case analysis with a limited PV area is the most relevant. The space demand for hydrogen storage which allows to satisfy the user demand for 5 hours, as in this case, can be neglected.

3.3.3 Cases including battery storage

As described in chapter 2.6.2 first a minimum battery size is included as a constraint, which can cover the hydrogen demand of the electrolyzer for approximately 4 hours. Thereby the effect on the LCOH can be seen. The results are shown in Table 3.8 and are confronted to the 20 % hydrogen blending case of 3.3.1. Apart from the 4-hour LIB all the other assumptions are kept the same and no further constraints are introduced.

Table 3.8: Case analysis, 20 % H₂ blending, 2023 cost, battery size forced

Component	20 % H ₂ blending case	Including 4-hour LIB 20 % H ₂ blending case
PV installed capacity [MW]	12,6	16,7
Electrolyzer [MW]	8,1	7,8
Battery Power [MW]	0	5,5
Battery Capacity [MWh]	0	22
Hydrogen Storage [MWh]	17,5	16,9
LCOH [€/kg _{H2}]	8,09	8,93

Forcing the algorithm to incorporate the 4-h battery storage increases the LCOH by approximately 10 %. The battery storage changes the behavior of the algorithm and plant as it favors a larger PV-plant to be able to have excess electricity which can be stored during high radiation hours and released at the end of the day. This increases the share of hydrogen produced from PV power, rather than the grid, which is advantageous to benefit from subsidies. The battery further allows to slightly decrease the electrolyzer and hydrogen storage size.

The energy flows of the system are shown in Figure 3.24. This time units are reported in MWh and not GWh to allow a detailed representation also for the smaller energy flows of the blending case. Comparing the shares to the base scenario 2023, it is evident that the grid withdrawal reduces, increasing the share of PV electricity in hydrogen production from 50,4 % to 63,7 %. This increase can be relevant to benefit from green hydrogen benefits of the EU.

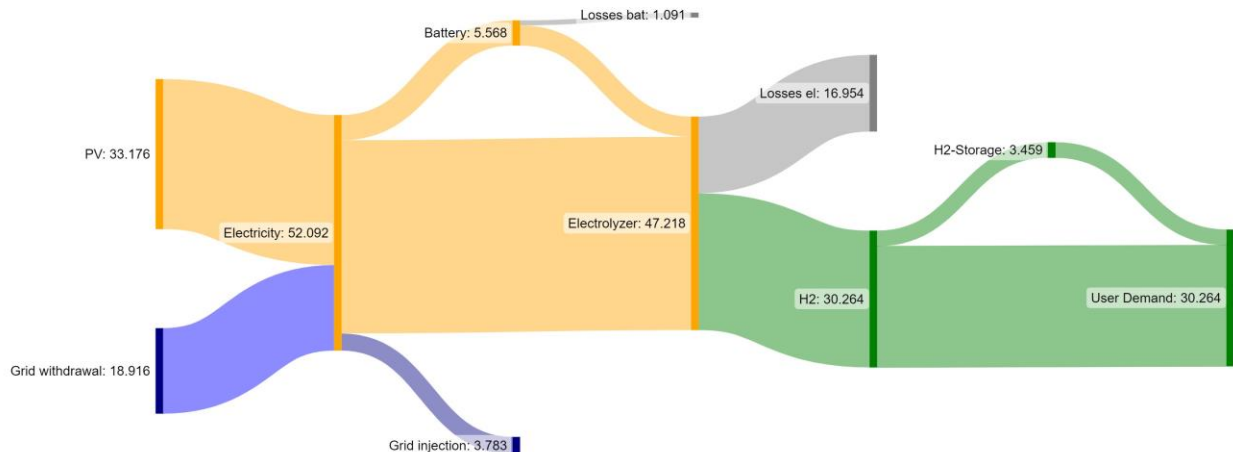


Figure 3.24: Sankey diagram of the energy flows in 4-hour LIB case [MWh] [63]

Figure 3.25 displays the system's operation over a typical day in July. It demonstrates the strategic cooperation between two energy storage systems, with a primary focus on hydrogen storage, as defined by the control strategy in Chapter 2.3. Immediately when enough hydrogen can be

produced from renewables and no grid supply is necessary, the hydrogen storage is charged. When the PV production exceeds nominal electrolyzer capacity, also the battery storage is charged. In the late afternoon, when PV electricity production cannot meet the hydrogen demand, there is a controlled discharge of the battery. Discharging the battery and converting this electricity into hydrogen satisfies the user demand over the next hours until also the hydrogen storage must be utilized. Notably, throughout these phases, no electricity is drawn from the grid. Grid electricity is only used when the hydrogen storage is empty, and there is no PV production, typically between 3 to 5 am, to meet user demand.

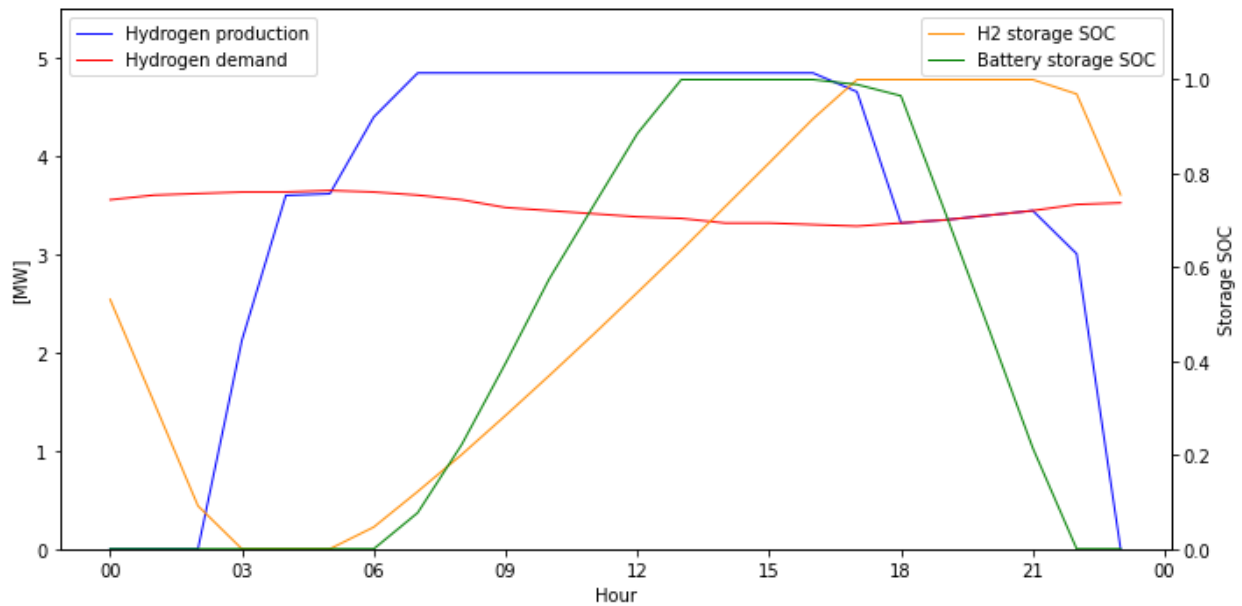


Figure 3.25: Hydrogen demand, production and SOC of the storages during a typical day in July

During the winter, solar resources are significantly reduced, leading to the system's increased dependence on grid electricity. Figure 3.26 illustrates the system's operation on a sunny day in January. This system behaves according to the same operational principles as in summer, although the periods during which PV production surpasses the electricity requirements for meeting hydrogen demand are limited. On most winter days, solar radiation levels are even lower, necessitating grid supply throughout the entire day.

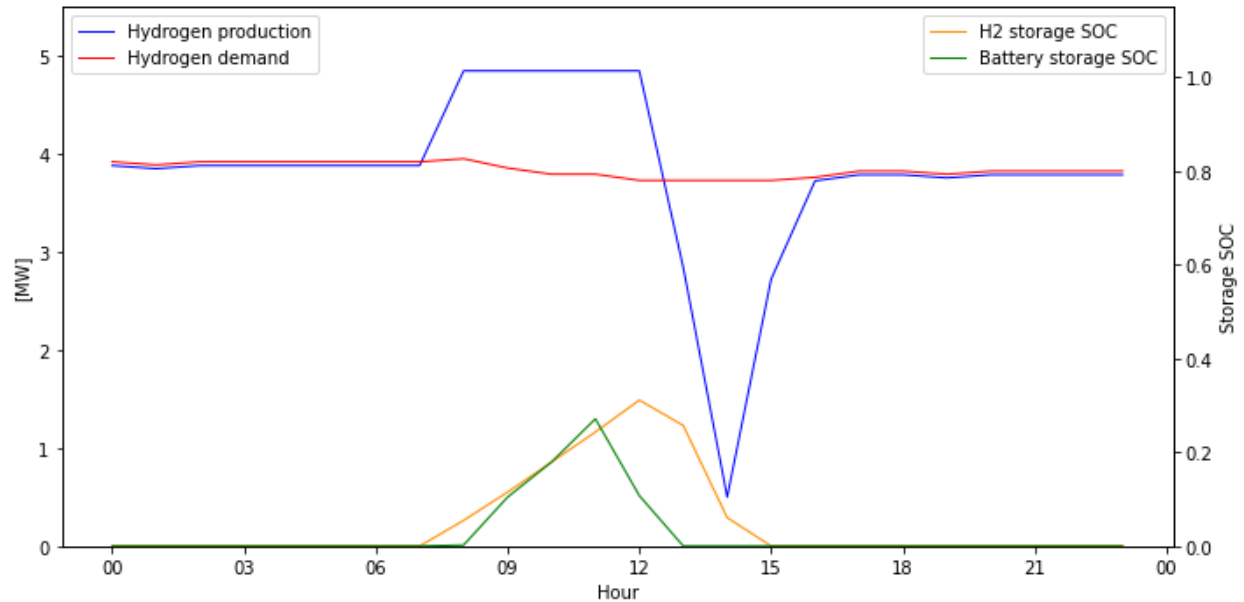


Figure 3.26: Hydrogen demand, production and SOC of the storages during a sunny day in January

In a second approach, a different strategy is employed to determine how the economic modelling indicators must be set to let the battery storage become relevant. Generally higher electricity acquisition price and increased electrolyzer cost are beneficial for the battery economics. Different setups were tested, which are all based on the 20 % H₂ blending case, using the base scenario 2023 settings.

This hypothetical case analyses the threshold electrolyzer cost for which a battery is convenient, considering an extreme electricity price of 500 €/MWh, which is in the range of the highest PUN values during the energetic crisis. Even for this case with a base case assumption for the electrolyzer the battery storage is not incorporated by the PSO algorithm. Only if the electrolyzer cost is increased to 2.000 €/kWe the algorithm selects a LIB with an installed power of 5,3 MW and a capacity of 26,8 MWh. Increasing the electrolyzer costs further to 3.000 €/kWe the battery size increases to 10,7 MW and 53,9 MWh.

4. Discussion

Generally, the modelled system is highly complex and depends on various parameters and assumptions. To draw general conclusion different sensitivity analysis were performed to understand the systems dynamic more in dept. This chapter intends to put the results in a context and discuss the outcomes as well as limitations.

4.1 Comparison to Methane

Generally, the modelling approach considered a favourable location and assumptions first to examine whether a green hydrogen production in combination with energy storage can be economically convenient in an optimistic scenario. From a purely monetary viewpoint the renewable scenarios cannot compete with a conventional natural gas-based system, given the natural gas prices as of August 2023. Natural gas price is subject to variation as the energetic crisis has shown, and therefore relying completely on natural gas poses a large geopolitical risk. In August 2022 the Dutch TTF Natural Gas Future peaked at 339 €/MWh compared to 36 €/MWh in August 2021, showing the enormous variability in prices[66]. This shows the risk of import dependencies and presents an additional motivation to diversify supply. On a yearly basis ARERA reports a price of 0,35 €/m³ for industrial clients with a consumption between 2,6 and 26 Mio m³/a in 2021. In 2023 the prices are again close to 2021 pre-crisis levels.[67],[53] In the Future Deloitte as well as Fitch Ratings project slight price increases in the last years before 2030 but significantly lower prices compared to 2022. These forecasts depend heavily on many exogenous factors, and it is unlikely that they will prove to be accurate. In a future price scenario, a slight increase of 10-20 % can be considered a reasonable assumption.[68],[69]

While the green hydrogen scenarios do not systematically emit CO₂ during the turbine usage, a methane-based supply does. The burning of natural gas causes 0.182 kg_{CO2}/kWh_{NG} based on the lower heating value. In a detailed assessment also the emissions due to leakage during transmission and extraction must be considered. Methane has a 25-time higher global warming potential than CO₂, meaning that leakages have a huge effect on global warming.[70] Hence to be in line with the national and European climate targets a reduction in natural gas consumption is necessary, and installing new infrastructure reliant on fossil fuels contains the risk to become a stranded asset.

An additional cost factor for the natural gas-based supply are Emission Trading System or carbon tax. On a European level there is the European Union Emissions Trading System (EU ETS) in place. Certificate prices are subject to a sharp increase since 2020 and currently range at approximately 90 €/t_{CO2}. [71] In many European countries there is also a carbon tax in place covering industries emitters which are not part of the ETS. Emitters which are already part of the ETS are excluded from the tax.[72] In Italy there is no additional carbon tax in place. For this study the certificate price of 90 €/t_{CO2} is considered and no carbon tax. The additional cost per kWh is obtained by multiplying the certificate price to the emission factor of natural gas and results in an additional price component of 1,6 c€/kWh. Together with the natural gas price of 3,2 c€/kWh a final levelized cost of methane of 4,8 c€/kWh is reached, which is significantly lower than in the base scenarios of green hydrogen production obtained in this thesis. Only if the remuneration of

grid feed in is set higher than the LCOE of PV production, as analyzed in chapter 3.2.2, the system cost can compete with natural gas. However, these cases must be critically evaluated, as explained in the dedicated chapter.

4.2 Context of green hydrogen production

To set the results into a context, green hydrogen production cost estimates are an interesting metric. A wide range of literature is available, and many studies also investigate future price developments. Volpe estimated the LCOH from hydrogen by wind electrolysis at 11 €/kg_{H2} in the best-case scenario. In their case hydrogen is produced for mobility application. Not taking into account the cost for refuelling stations and transport cost, LCOH is slightly below 8 €/kg_{H2}. [73] These findings are in line with IEA publications. In the Global Hydrogen Review cost of 4 to 8.5 €/kg_{H2} for water-electrolysis are reported for 2021. The wide cost range shows how the cost depend on various factors and are various case specific. The costs consist of two main components: CAPEX for the electrolyzer and the electricity cost. The CAPEX of the electrolyzer will significantly decrease, as discussed in chapter 2.1.3. The cost component of electricity depends on the efficiency of the electrolysis, the location and the CAPEX of the PV or other renewable plants. Both on the electrolyzer efficiency and renewable cost, improvements are projected. These advancements combined could reduce the cost of green hydrogen to 1 to 4.5 €/kg_{H2} in 2030, which on the lower end is comparable with the hydrogen production from natural gas by SMR and following CCUS to abate the emissions. [33]

The resulting LCOH of the base scenario 2030, do not achieve the same cost reductions and are slightly above the IEA projections. In this study the goal is not to produce as much hydrogen as possible from a given system configuration but satisfy the users hydrogen demand and its specific profile. Hence the plant could produce more hydrogen, which potentially lowers the LCOH. Most important no revenue from grid feed in is considered in the main scenario, meaning that excess solar production is wasted. The sensitivity analysis on this aspect shows the large impact of this assumption, explaining the deviation from the future LCOH estimates by the IEA.

4.3 Limitations

Selecting financial inputs is often a challenging task as the results and considerations depend highly on these factors. Especially due to the increased price volatility and drastic global developments the realistic choice of financial indicators is even more challenging. Due to the unpredictability of prices and other assumptions the scenarios can hardly simulate real conditions, especially in the future. However, the analysed sensitivities help to deeper understand some dynamics behind the results, how different factors influence the outcomes and allow to draw some general conclusions.

A main limitation of the model lays in the simplification of the component assumptions which are modelled as black boxes with only system efficiencies assigned. Actual physical modelling of each component is more precise and reveals losses and limitations much more precisely. However, the detailed modelling of each component again increases computational burden and programming

complexity, which are already a limiting factor. Hence in this context of the thesis the simplified approach is considered necessary. Still for future research some refinements of the model are possible adding additional detail to the modelling.

All the simulation were based on the available industrial user demand profile which comprises the year 2021. The year 2021 was still influenced by pandemic restrictions. Also due to other internal and external factors this year could not be representative for the whole lifetime of the components. Also, by simulating one year degradation of components is not included. Another problem of a one-year simulation lies in the fact that a final storage energy content at the end of the year is not economically accounted. Especially in scenarios where the optimized hydrogen storage size is large this could be relevant. The effect is minor as the starting SOC is 0, full storages are typically reached in summer while due to less radiation the SOC will be low towards the end of the year. The available data frequency of the of the user profile is another point of criticism. Potentially there could be short hidden demand fluctuations in the profile which cannot be determined on an hourly basis, making it harder to satisfy the user demand at all times. However, the demand profile in this study is relatively flat without major fluctuations during the day or seasonality, making this effect unlikely.

Furthermore, there are limitations regarding the optimization algorithm. PSO is a metaheuristic algorithm, and it does not necessarily find the exact best solution but rather a solution which is close. There is room for errors as particles can get trapped in a local minimum and it is hardly noticeable when this problem appears. The problem is multimodal being more challenging to optimize for algorithms. The setting of the hyperparameters is delicate and can lead to unstable solutions far from the global optimal solution. The hyperparameter setting is problem specific, but due to practical limits of available computational resources the parameter setting is done on base of short simulations (24h). The computational cost restricts the number of particles and iterations. Using a larger number of particles could stabilize the search of the minima as the algorithm already starts from a broader exploration base compared to using only few particles. Increased computational resources would mitigate this problem.

Further limitations lie in the missing prediction of future renewable energy generation. If the future demand and generation is approximately known, it allows for more advanced strategies. An example is to charge the hydrogen storage in advance of low renewable energy generation periods with grid electricity, which could reduce the needed electrolyzer size. Energy arbitrage ideas with the battery storage could be possible when free storage capacity is known to occur. Thereby additional revenues of the battery storage could be generated, improving its economics. If the system conditions change the previously defined rules in the operations strategy can be outdated, not leading to the optimal solution. Generally, an optimization-based control strategy including forecasting could achieve lower overall system cost, at the drawback of increased computational resources and programming complexity.

Another inaccuracy of this model is the scale effect on the cost regarding the component during the optimization. As in the modelling cases the scale is in a utility range and many components are containerized, the specific costs per installed capacity or power do not vary extremely, however in future work this effect should be included. Further, in the model the sizes of the components are

considered continuous, which improves the algorithms performance and facilitates the search of the global optima. In real world applications component sizes are discrete and for example for electrolyzers even containerized, meaning that large steps between the commercially available sizes exist. These considerations have a minor importance for a high blending share and large hydrogen demand, where even for largely discrete sizes the available solution is close to optimum. However, it can be important for low blending rates and considerably solutions where the available component sizes are far off the calculated optimum. In future work an additional modeling step could be added. This involves starting from a continuous optimization of the sizes, selecting fixed discrete sizes according to commercially available solutions and followingly simulating the operation again with a more advanced control strategy.

To benefit from subsidies for green hydrogen, it is crucial to meet the EU definitions to classify hydrogen as green. The exact incentives are case dependent and should be included in a further specific case analysis. In this case a storage on the electricity side could become more convenient as it increases the share of green electricity

The electricity withdrawn from the grid must origin mostly from renewables to meet the requirements discussed in chapter 1.5. This is important not only to profit from green hydrogen incentives, but also to avoid emitting considerable amounts of CO₂. Whether the grid supply during times of low PV production meets these requirements can be doubted. The exact incentives are highly case specific, considering also that the regulatory environment is currently evolving dynamically. Hence implementing the incentives on a case specific application is subject of future work. Generally modelling more precisely the share of green hydrogen could incentivize battery placement as it increases the share of renewable electricity in the electrolyzer, which is beneficial for incentives.

5. Conclusions and future research potentials

In the context of addressing greenhouse gas emissions from hard-to-abate industrial sectors, the replacement of natural gas by green hydrogen could be one of the main options to reduce greenhouse gas emissions. This thesis introduces a comprehensive system for the production of green hydrogen, tailored to meet the specific demand of an industrial client. The system includes a LIB and hydrogen storage to ensure a continuous supply of hydrogen according to the user's consumption profile. To achieve the lowest possible cost for hydrogen production, an optimization code using Particle Swarm Optimization is developed. The primary objective of the algorithm is to determine the optimal sizes for each of the system's components. The python code employs a rule-based strategy to obtain hourly profiles of each component and these profiles are then used to calculate the resulting cost. The costs become the crucial input parameter for the PSO algorithm to update the sizes for the next iteration. The output at the end of the simulation are an optimal set of sizes, production data and the cost composition. Different scenarios and sensitivities are analyzed to allow a deeper understanding of the systems behavior and economics.

The results of this thesis indicate that from a purely economic standpoint the substitution of methane by green hydrogen to satisfy an industrial user's demand today is economically not convenient, at least for cases similar to this study. Nevertheless, the projected cost reductions until 2030 are significant and when complemented by further incentives, they are poised to enable green hydrogen to competitively contend with fossil-based hydrogen production. Hybrid energy storage, while being a promising concept, does not yield favorable results. The high capital expenditures associated with battery storage, coupled with efficiency losses and the inability to directly consume self-produced renewable electricity, makes the placement of a battery economically unfavorable. An advantage of the battery to consider in future studies is the beneficial effect on self-produced electricity which is crucial to benefit from incentives and subsidies.

In contrast, hydrogen storage represents a cheaper storage option, with lower LCOS. Additionally it has the advantage of being on the hydrogen side and therefore is able to cover the user demand directly, without passing the electrolyzer in-between as for the battery. As a result, hydrogen storage is the preferred choice in all investigated scenarios, with storage durations ranging from a few hours to more than a day.

The sensitivity analyses regarding electricity prices of acquisition from and injection to the grid reveal the significance of these parameters. Higher electricity acquisition prices favor large PV plants, electrolyzers and hydrogen storages and lead to increased PV-electricity shares. If revenues from the grid injection are introduced, the algorithm increases the PV size. However, the study also highlights an unintended consequence of this effect: For grid injection remuneration above the LCOE of PV it is convenient to install as much PV as possible to maximize grid injection. Thereby the photovoltaic plant indirectly subsidizes the hydrogen production, which leads to unrealistic plant layouts and distorted LCOH results.

The analysis of the area requirements emphasizes that green hydrogen production causes a large footprint, dominated by the PV plant. For industrial clients, especially those with high blending shares or a complete substitution of methane, this could pose limitations. For practicability the

economically optimal PV sizes can be out of range of the available area for industrial clients. In such cases, alternative solutions for electricity supply must be explored. Conversely, the electrolyzer and hydrogen storage requires significantly less space, and do not represent a major constraint.

Based on this thesis, future work should validate the conclusions of this study with different user profiles, particularly those with variable hydrogen demand. Additionally, the integration of wind energy as a renewable electricity source could enhance availability and reduce grid withdrawal during periods of low solar production. This is also useful to increase the share of green electricity, aligning with EU definitions for green hydrogen. Moreover, exploring alternative energy storage options, such as Redox flow batteries, and benchmarking them against LIBs, could be valuable for future scenarios. Additionally, predictive modeling of renewable energy generation and demand enables more intelligent operation strategies, potentially leading to lower LCOH. Finally, future studies could benefit from testing different optimization algorithms, such as genetic algorithms, to determine their effectiveness in this specific application.

Bibliography

- [1] International Energy Agency, 'World Energy Outlook 2022', Oct. 2022. [Online]. Available: <https://www.iea.org/reports/world-energy-outlook-2022>
- [2] O. Schmidt, S. Melchior, A. Hawkes, and I. Staffell, 'Projecting the Future Levelized Cost of Electricity Storage Technologies', *Joule*, vol. 3, no. 1, pp. 81–100, Jan. 2019, doi: 10.1016/j.joule.2018.12.008.
- [3] Bloomberg, '2022 Energy Storage Market Outlook', Oct. 2022. Accessed: Aug. 05, 2023. [Online]. Available: <https://about.bnef.com/blog/global-energy-storage-market-to-grow-15-fold-by-2030/>
- [4] E. & I. S. UK Government Department for Business, 'Facilitating the deployment of large-scale and long-duration electricity storage Government Response', 2022.
- [5] LDES Council and McKinsey, 'The journey to net-zero', 2022. [Online]. Available: www.ldescouncil.com.
- [6] R. H. Hedayat Saboori, 'Emergence of hybrid energy storage systems in renewable energy and transport applications – A review | Elsevier Enhanced Reader'. Accessed: Mar. 21, 2023. [Online]. Available: <https://reader.elsevier.com/reader/sd/pii/S1364032116302374?token=E955F45D4E80822B1B9322639D6BDA708194E6E86AE89E0670FD78C2BB453B1316CA415206A2F529B530473D5FC4DBC7&originRegion=eu-west-1&originCreation=20230321094803>
- [7] X. Lin and R. Zamora, 'Controls of hybrid energy storage systems in microgrids: Critical review, case study and future trends', *J. Energy Storage*, vol. 47, Mar. 2022, doi: 10.1016/j.est.2021.103884.
- [8] S. Hajiaghahi, A. Salemnia, and M. Hamzeh, 'Hybrid energy storage system for microgrids applications: A review', *J. Energy Storage*, vol. 21, pp. 543–570, Feb. 2019, doi: 10.1016/j.est.2018.12.017.
- [9] P. Marocco, D. Ferrero, E. Martelli, M. Santarelli, and A. Lanzini, 'An MILP approach for the optimal design of renewable battery-hydrogen energy systems for off-grid insular communities', *Energy Convers. Manag.*, vol. 245, p. 114564, Oct. 2021, doi: 10.1016/j.enconman.2021.114564.
- [10] 'Global Hydrogen REVIEW 2021', International Energy Agency, 2021. [Online]. Available: <https://iea.blob.core.windows.net/assets/5bd46d7b-906a-4429-abda-e9c507a62341/GlobalHydrogenReview2021.pdf>
- [11] J. M. M. Arcos and D. M. F. Santos, 'The Hydrogen Color Spectrum: Techno-Economic Analysis of the Available Technologies for Hydrogen Production', *Gases*, vol. 3, no. 1, Art. no. 1, Mar. 2023, doi: 10.3390/gases3010002.
- [12] *Richtlinie (EU) 2018/2001 des Europäischen Parlaments und des Rates vom 11. Dezember 2018 zur Förderung der Nutzung von Energie aus erneuerbaren Quellen (Neufassung) (Text von Bedeutung für den EWR.)*, vol. 328. 2018. Accessed: Sep. 05, 2023. [Online]. Available: <http://data.europa.eu/eli/dir/2018/2001/oj/deu>
- [13] EU, *EUR-Lex - 32023R1184 - EN - EUR-Lex*. Accessed: Sep. 05, 2023. [Online]. Available: https://eur-lex.europa.eu/legal-content/EN/TXT/?toc=OJ%3AL%3A2023%3A157%3ATOC&uri=uriserv%3AOJ.L_.2023.157.01.0011.01.ENG

- [14] F. Zanellini, ‘Il vettore idrogeno Stato dell’arte e potenzialità dell’industria italiana’, ANIE, 2023. [Online]. Available: <https://anie.it/wp-content/uploads/2023/03/Quadro-normativo-UE-e-Italia-Zanellini.pdf>
- [15] *EUR-Lex - 32023R1185 - EN - EUR-Lex*. 2023. Accessed: Oct. 05, 2023. [Online]. Available: https://eur-lex.europa.eu/eli/reg_del/2023/1185/oj
- [16] *DECRETO-LEGGE 30 aprile 2022, n. 36 - Normattiva*. Accessed: Sep. 05, 2023. [Online]. Available: <https://www.normattiva.it/uri-res/N2Ls?urn:nir:stato:decreto.legge:2022;36~art9-com1>
- [17] *DECRETO LEGISLATIVO 8 novembre 2021, n. 199 - Normattiva*. Accessed: Sep. 05, 2023. [Online]. Available: <https://www.normattiva.it/uri-res/N2Ls?urn:nir:stato:decreto.legislativo:2021-11-08;199>
- [18] ‘Global Solar Atlas’. Accessed: Aug. 16, 2023. [Online]. Available: <https://globalsolaratlas.info/detail?c=37.425525,15.055046,11&s=37.485211,15.076332&m=site>
- [19] ‘JRC Photovoltaic Geographical Information System (PVGIS) - European Commission’, PVGIS. Accessed: Aug. 15, 2023. [Online]. Available: https://re.jrc.ec.europa.eu/pvg_tools/en/#TMY
- [20] ‘Polysun – Energiesysteme präzise simulieren und effizient Planen > POLYSUN’. Accessed: Sep. 01, 2023. [Online]. Available: <https://www.velasolaris.com/downloads/>
- [21] S. Alkaff, N. H. Shamdasani, G. Yun II, and Dr. V. Venkiteswaran, ‘A Study on Implementation of PV Tracking for Sites Proximate and Away from the Equator’, *Process Integr. Optim. Sustain.*, vol. 3, Sep. 2019, doi: 10.1007/s41660-019-00086-7.
- [22] D. S. Philipps, F. Ise, W. Warmuth, and P. P. GmbH, ‘Photovoltaics Report’, Fraunhofer Institute for Solar Energy Systems, ISE, 2023. [Online]. Available: <https://www.ise.fraunhofer.de/content/dam/ise/de/documents/publications/studies/Photovoltaics-Report.pdf>
- [23] A. Awasthi *et al.*, ‘Review on sun tracking technology in solar PV system’, *Energy Rep.*, vol. 6, pp. 392–405, Nov. 2020, doi: 10.1016/j.egy.2020.02.004.
- [24] ‘Projected Costs of Generating Electricity 2020 – Analysis’, International Renewable Energy Agency. Accessed: Aug. 23, 2023. [Online]. Available: <https://www.iea.org/reports/projected-costs-of-generating-electricity-2020>
- [25] ‘Renewable Energy Market Update - June 2023’, International Energy Agency, 2023.
- [26] ‘Global Market Outlook for Solar Power’, Solar Power Europe, 2023. [Online]. Available: https://api.solarpowereurope.org/uploads/Global_Market_Outlook_2023_2027_report_18b86a4568.pdf
- [27] ‘2030 Solar Cost Targets’, United States Department of Energy. Accessed: Aug. 31, 2023. [Online]. Available: <https://www.energy.gov/eere/solar/articles/2030-solar-cost-targets>
- [28] C. Kost, ‘Study: Levelized Cost of Electricity - Renewable Energy Technologies - Fraunhofer ISE’, Fraunhofer Institute for Solar Energy Systems ISE. Accessed: Aug. 31, 2023. [Online]. Available: <https://www.ise.fraunhofer.de/en/publications/studies/cost-of-electricity.html>
- [29] IRENA, ‘Future of Solar Photovoltaic – A Global Energy Transformation paper’, International Renewable Energy Agency, Nov. 2019. Accessed: Aug. 31, 2023. [Online]. Available: <https://www.irena.org/publications/2019/Nov/Future-of-Solar-Photovoltaic>

- [30] R. Wiser, M. Bolinger, and J. Seel, ‘Benchmarking Utility-Scale PV Operational Expenses and Project Lifetimes: Results from a Survey of U.S. Solar Industry Professionals’, 2020.
- [31] I. Guaita-Pradas and A. Blasco-Ruiz, ‘Analyzing Profitability and Discount Rates for Solar PV Plants. A Spanish Case’, *Sustainability*, vol. 12, no. 8, Art. no. 8, Jan. 2020, doi: 10.3390/su12083157.
- [32] H. Grimm, Gunter Marius, ‘Cost Forecast for Low-Temperature Electrolysis - Technology Driven Bottom-Up Prognosis for PEM and Alkaline Water Electrolysis Systems’, Fraunhofer Institute for Solar Energy Systems ISE, 2021.
- [33] ‘Global Hydrogen Review 2022’, 2022.
- [34] M. Kopp, D. Coleman, C. Stiller, K. Scheffer, J. Aichinger, and B. Scheppat, ‘Energiepark Mainz: Technical and economic analysis of the worldwide largest Power-to-Gas plant with PEM electrolysis’, *Int. J. Hydrog. Energy*, vol. 42, no. 19, pp. 13311–13320, May 2017, doi: 10.1016/j.ijhydene.2016.12.145.
- [35] O. Schmidt, A. Gambhir, I. Staffell, A. Hawkes, J. Nelson, and S. Few, ‘Future cost and performance of water electrolysis: An expert elicitation study’, *Int. J. Hydrog. Energy*, vol. 42, no. 52, pp. 30470–30492, Dec. 2017, doi: 10.1016/j.ijhydene.2017.10.045.
- [36] Lettenmeier, Philipp, ‘Efficiency – Electrolysis White paper’. Siemens energy, 2019. [Online]. Available: <https://assets.siemens-energy.com/siemens/assets/api/uuid:5342163d-2333-4c8d-ae85-2a0e8d45db56/white-paper-efficiency-en.pdf>
- [37] ‘LIFE 3.0 - LIFE Project Public Page’. Accessed: Aug. 23, 2023. [Online]. Available: <https://webgate.ec.europa.eu/life/publicWebsite/project/details/1306>
- [38] ‘STUDY ON EARLY BUSINESS CASES FOR H2 IN ENERGY STORAGE AND MORE BROADLY POWER TO H2 APPLICATIONS’, TRACTEBEL ENGINEERING S.A. and Hinicio, 2017.
- [39] J. Andersson and S. Grönkvist, ‘Large-scale storage of hydrogen’, *Int. J. Hydrog. Energy*, vol. 44, no. 23, pp. 11901–11919, May 2019, doi: 10.1016/j.ijhydene.2019.03.063.
- [40] BAGLIONI S.p.A., ‘CATALOGO SERBATOI STOCCAGGIO IDROGENO’. [Online]. Available: <https://baglionispa.com/idrogeno/>
- [41] E. G. Vera, C. Canizares, and M. Pirnia, ‘Renewable Energy Integration in Canadian Remote Community Microgrids: The Feasibility of Hydrogen and Gas Generation’, *IEEE Electrification Mag.*, vol. 8, no. 4, pp. 36–45, Dec. 2020, doi: 10.1109/MELE.2020.3026438.
- [42] R. R. Urs, A. Chadly, A. Al Sumaiti, and A. Mayyas, ‘Techno-economic analysis of green hydrogen as an energy-storage medium for commercial buildings’, *Clean Energy*, vol. 7, no. 1, pp. 84–98, Feb. 2023, doi: 10.1093/ce/zkac083.
- [43] P. Marocco, D. Ferrero, A. Lanzini, and M. Santarelli, ‘Optimal design of stand-alone solutions based on RES + hydrogen storage feeding off-grid communities’, *Energy Convers. Manag.*, vol. 238, p. 114147, Jun. 2021, doi: 10.1016/j.enconman.2021.114147.
- [44] C. Augustine and N. Blair, ‘Storage Futures Study: Storage Technology Modeling Input Data Report’, NREL/TP--5700-78694, 1785959, MainId:32611, May 2021. doi: 10.2172/1785959.
- [45] A. Grimaldi, F. D. Minuto, A. Perol, S. Casagrande, and A. Lanzini, ‘Ageing and energy performance analysis of a utility-scale lithium-ion battery for power grid applications through a data-driven empirical modelling approach’, *J. Energy Storage*, vol. 65, p. 107232, Aug. 2023, doi: 10.1016/j.est.2023.107232.

- [46] C. Betzin, H. Wolfschmidt, and M. Luther, ‘Electrical operation behavior and energy efficiency of battery systems in a virtual storage power plant for primary control reserve’, *Int. J. Electr. Power Energy Syst.*, vol. 97, pp. 138–145, Apr. 2018, doi: 10.1016/j.ijepes.2017.10.038.
- [47] W. Cole and A. Karmakar, ‘Cost Projections for Utility-Scale Battery Storage: 2023 Update’, National Renewable Energy Laboratory, 2023. [Online]. Available: <https://www.nrel.gov/docs/fy23osti/85332.pdf>
- [48] ‘Global Energy and Climate Model Documentation’, International Energy Agency, 2022. [Online]. Available: <https://iea.blob.core.windows.net/assets/2db1f4ab-85c0-4dd0-9a57-32e542556a49/GlobalEnergyandClimateModelDocumentation2022.pdf>
- [49] C. Bordin, H. O. Anuta, A. Crossland, I. L. Gutierrez, C. J. Dent, and D. Vigo, ‘A linear programming approach for battery degradation analysis and optimization in offgrid power systems with solar energy integration’, *Renew. Energy*, vol. 101, pp. 417–430, Feb. 2017, doi: 10.1016/j.renene.2016.08.066.
- [50] ‘ARERA - Prezzi finali dell’energia elettrica per i consumatori industriali - Ue a Area euro’. Accessed: Aug. 24, 2023. [Online]. Available: <https://www.arera.it/it/dati/eepcfr2.htm>
- [51] ‘Greenhouse gas emission intensity of electricity generation in Europe’, European Environment Agency. Accessed: Aug. 24, 2023. [Online]. Available: <https://www.eea.europa.eu/ims/greenhouse-gas-emission-intensity-of-1>
- [52] ‘Gestore Mercati Energetici Electricity Market statistics’. Accessed: Sep. 06, 2023. [Online]. Available: <https://www.mercatoelettrico.org/En/download/DatiStorici.aspx>
- [53] ‘ARERA - Prezzi finali del gas naturale per i consumatori industriali - UE e area Euro’. Accessed: Aug. 18, 2023. [Online]. Available: <https://www.arera.it/it/dati/gpcfr2.htm>
- [54] ‘Scenario National Trend Terna’, TERNA, 2021. [Online]. Available: https://download.terna.it/terna/National%20Trends%20Italia%202021_8d8c8fe48cb033f.pdf
- [55] J. C. L. Fish, *Engineering economics, first principles*. New York McGraw-Hill, 1923. Accessed: Aug. 13, 2023. [Online]. Available: <http://archive.org/details/engineeringecono00fishuoft>
- [56] T. Bocklisch, ‘Hybrid energy storage approach for renewable energy applications’, *J. Energy Storage*, vol. 8, pp. 311–319, Nov. 2016, doi: 10.1016/j.est.2016.01.004.
- [57] Y. He, S. Guo, P. Dong, C. Wang, J. Huang, and J. Zhou, ‘Techno-economic comparison of different hybrid energy storage systems for off-grid renewable energy applications based on a novel probabilistic reliability index’, *Appl. Energy*, vol. 328, Dec. 2022, doi: 10.1016/j.apenergy.2022.120225.
- [58] J. Kennedy and R. Eberhart, ‘Particle swarm optimization’, in *Proceedings of ICNN’95 - International Conference on Neural Networks*, Nov. 1995, pp. 1942–1948 vol.4. doi: 10.1109/ICNN.1995.488968.
- [59] H. Liu, B. Wu, A. Maleki, and F. Pourfayaz, ‘An improved particle swarm optimization for optimal configuration of standalone photovoltaic scheme components’, *Energy Sci. Eng.*, vol. 10, no. 3, pp. 772–789, 2022, doi: 10.1002/ese3.1052.
- [60] R. Poli, J. Kennedy, and T. Blackwell, ‘Particle Swarm Optimization: An Overview’, *Swarm Intell.*, vol. 1, Oct. 2007, doi: 10.1007/s11721-007-0002-0.
- [61] A. P. Piotrowski, J. J. Napiorkowski, and A. E. Piotrowska, ‘Population size in Particle Swarm Optimization’, *Swarm Evol. Comput.*, vol. 58, p. 100718, Nov. 2020, doi: 10.1016/j.swevo.2020.100718.

- [62] ‘pandas - Python Data Analysis Library’. Accessed: Aug. 05, 2023. [Online]. Available: <https://pandas.pydata.org/>
- [63] ng. S. F. – Arch. C. N. Arch.Cinzia Nieddu, ‘REALIZZAZIONE IMPIANTO FOTOVOLTAICO A TERRA DA 24,49 MW IN IMMISSIONE, TIPO AD INSEGUIMENTO MONOASSIALE “SAM-SE” COMUNI DI SAMASSI E SERRENTI (SU)’. ENERGYSAMSE SRL, 2022.
- [64] ‘SankeyMATIC: Build a Sankey Diagram’, SankeyMATIC.com. Accessed: Aug. 30, 2023. [Online]. Available: <https://sankeymatic.com/build/>
- [65] ‘PEM Electrolyzer ME450: H-TEC SYSTEMS products’. Accessed: Sep. 29, 2023. [Online]. Available: <https://www.h-tec.com/en/products/detail/h-tec-pem-electrolyser-me450/me450/>
- [66] ‘Dutch TTF Natural Gas Calendar (TTF=F) Interactive Stock Chart - Yahoo Finance’. Accessed: Aug. 18, 2023. [Online]. Available: <https://finance.yahoo.com/quote/TTF%3DF/chart/>
- [67] ‘Natural gas price statistics’, eurostat. Accessed: Aug. 18, 2023. [Online]. Available: https://ec.europa.eu/eurostat/statistics-explained/index.php?title=Natural_gas_price_statistics
- [68] FitchRatings, ‘Fitch Ratings Raises Mid-Term Oil and Cuts Near-Term Gas Price Assumptions’. Accessed: Aug. 18, 2023. [Online]. Available: <https://www.fitchratings.com/research/corporate-finance/fitch-ratings-raises-mid-term-oil-cuts-near-term-gas-price-assumptions-13-03-2023>
- [69] Botterill, Andrew, ‘Energy, oil, and gas price forecast - Energy costs are stretching price elasticity and energy affordability’, Deloitte, 2023. [Online]. Available: <https://www2.deloitte.com/content/dam/Deloitte/ca/Documents/REA/eo-g-price-forecast-q4-er-fy23-en-aoda.pdf>
- [70] ‘Greenhouse gas reporting: conversion factors 2022’, GOV.UK. Accessed: Aug. 18, 2023. [Online]. Available: <https://www.gov.uk/government/publications/greenhouse-gas-reporting-conversion-factors-2022>
- [71] ‘EU Carbon Permits - 2023 Data - 2005-2022 Historical - 2024 Forecast - Price - Quote’, TradingEconomics. Accessed: Sep. 05, 2023. [Online]. Available: <https://tradingeconomics.com/commodity/carbon>
- [72] M. Ferdinandusse, C. Nerlich, and M. D. T  llez, ‘Fiscal policies to mitigate climate change in the euro area’, Sep. 2022, Accessed: Sep. 05, 2023. [Online]. Available: https://www.ecb.europa.eu/pub/economic-bulletin/articles/2022/html/ecb.ebart202206_01~8324008da7.en.html
- [73] P. Marocco, M. Santarelli, and Volpe, Flaviano, ‘Evaluation of Levelized Cost of Hydrogen (LCOH) produced by wind electrolysis: Argentine and Italian production scenarios’, 2021. [Online]. Available: <https://webthesis.biblio.polito.it/17411/>